Canopy structure and the impact of drought on a *Quercus suber* L. woodland in Portugal

Dissertation

zur Erlangung des akademischen Grades doctor rerum naturalium
(Dr. rer. nat.)

vorgelegt dem Rat der Chemisch-Geowissenschaftlichen Fakultät der
Friedrich-Schiller-Universität Jena

von Arndt Gerald Piayda, Dipl.-Geoökol.
geboren am 07. Mai 1984 in Langenfeld (Rhld.) / Deutschland

Diese Dissertation ist während meiner Beschäftigung als wissenschaftlicher Mitarbeiter am Department für Hydrosystemmodellierung innerhalb des Helmholtz-Zentrums für Umweltforschung - UFZ in Leipzig in Kooperation mit der Abteilung für Agrar-Ökosystemforschung der Universität Bayreuth und dem Instituto Superior de Agronomia (Department of Forestry) der Technischen Universität Lissabon entstanden. Die Dissertation wurde finanziert durch die Deutsche Forschungsgemeinschaft (WATERFLUX Project: # WE 2681-61; # CU 173/2-1) und unterstützt von der Helmholtz Interdisciplinary Graduate School for Environmental Research (HIGRADE).

Gutachter:

Prof. Dr. Sabine Attinger
Friedrich-Schiller-Universität Jena
Gutachter

Prof. Dr. Christiane Werner
Universität Bayreuth
Gutachter

Die Dissertationsverteidigung fand am 27.01.2016 in Jena statt.

Email: arndt.piayda@ufz.de

Contents

Zusammenfassung

Die vorliegende Doktorarbeit behandelt zwei Hauptthemen. Das erste Thema stellt eine Evaluierung der Leistung mehrerer Messmethoden zur indirekten Bestimmung des Blattflächenindex L (Einseitige Blattfläche [m^2] pro Einheitsbodenfläche [m^2]) und der gap probability P_{gap} (Wahrscheinlichkeit für die ungestörte Passage eines direkten Lichtstrahls durch den Kronenraum [-]) dar. Der Fokus richtet sich hierbei auf die besonderen Probleme bei der Anwendung dieser Messmethoden in offenen, savannenartigen Kronendächern. Die erhaltenen Ergebnisse für L und P_{gap} sind im Zuge der Abhandlung des zweiten Hauptthemas notwendig. Hierbei werden der Einfluss von Dürren auf Wasser und Kohlenstoffflüsse als auch auf die Blattphysiologie eines typischen, mediterranen *montado* Ökosystems untersucht werden, welches von *Quercus suber* L. Bäumen dominiert wird.
Zwei der wichtigsten Parameter, welche die Struktur eines Kronendaches beschreiben sind Blattflächenindex L und gap probability P_{gap}. Sie sind unabdingbar um gemessene Massen- oder Energieflüsse von der Blattebene auf die Ökosystemebene zu skalieren und essenzielle Parameter von mathematischen Ökosystemmodellen. Trotz allem bleibt die indirekte Bestimmung dieser Parameter besonders in offenen, savannenartigen Ökosystemen eine große Herausforderung. Hier haben hohe Lichtintensitäten, heterogene räumliche Verteilung von Blättern und große Anteile von verholzten Pflanzenteilen im Sensorfeld Einfluss auf das Ergebnis. Des Weiteren ist ein größer werdender Bedarf von vertikal aufgelösten L und P_{gap} Messungen zu verzeichnen, da die Anzahl von elaborierten, vertikal aufgelösten Kronenmodellen ständig wächst. Diese Tatsache macht die Notwendigkeit einer schnellen und verlässlichen Messmethode für L und P_{gap} deutlich. Im Zuge dieser Doktorarbeit wird der etablierte, kommerziell vertriebene LAI-2000 Plant Canopy Analyzer mit der neueren und schnelleren Methode der Bedeckungsfotografie (DCP) im Hinblick auf die vorgenannten Probleme und Eigenschaften verglichen. Als Referenz werden Ergebnisse der direkten L Bestimmung aus Blattfallen verwendet. Während der Feldarbeiten zu dieser Doktorarbeit konnte die DCP Methode zum ersten Mal erfolgreich höhen- und winkelabhängig zum Einsatz gebracht werden. Die Ergebnisse der DCP Messung und der etablierten LAI-2000 Messung lieferten übereinstimmende Werte für gap probability P_{gap} und effektiven Blattflächenindex L_e. Um aus den winkelabhängigen Messungen der gap probability P_{gap} den tatsächlichen Blattflächenindex L zu berechnen ist Kenntnis des clumping index Ω notwendig, welcher das Maß der räumlichen Heterogenität des Blätterdaches darstellt. Der Erfolg dieser Doktorarbeit in der erstmaligen, winkelabhängigen Bestimmung von Ω mittels DCP war dafür entscheidend. Hierdurch konnte die Auswirkung der Heterogenität des *Q. suber* Blätterdaches bei der L Bestimmung berücksichtigt werden und führte so zu einem 30% höheren L

als bei der Messung durch den LAI-2000. Des Weiteren wurde zum ersten Mal die direkte Eliminierung des verholzten Pflanzenanteils aus den DCP Fotografien mittels objekt-orientierter Bildanalyse erreicht. Nach erfolgreicher Eliminierung verringerte sich der Blattflächenindex L im Mittel um 6.9% im Vergleich zur unkorrigierten Messung. Der objekt-orientierte Erkennungsalgorithmus wurde so gestaltet, das der Einfluss des verholzten Pflanzenanteils im Sensorfeld bei der Messung nicht überschätzt wird. Folglich kann die hier präsentierte Abschätzung des inhärenten Fehlers bei Messungen ohne Eliminierung des verholzten Pflanzenanteils als 'best-case' Abschätzung verstanden werden. Als Folge der Einbindung des clumping index und der Eliminierung des verholzten Anteils bei der DCP Methode konnte eine hohe Präzision bei der Herleitung von L erreicht werden, welches durch den Vergleich mit direkt gemessenen Werten aus Blattfallen bestätigt wurde und die Präzision des LAI-2000 bei Weitem übersteigt. Zuletzt wurde eine Messstrategie erfolgreich getestet, mit der die Herleitung einer höhenabhängigen L Verteilung innerhalb des Kronendaches ermöglicht wird und die ausschließlich auf boden-basierten Messung beruht und weder portable Stative noch Messungen im oder über dem Kronendach benötigt. Sie basiert auf der Messung simpler Kronenparameter und einer einzigen L Messung des gesamten Kronendaches.
Im ersten Hauptthema dieser Doktorarbeit konnte die herausragende Leistungsfähigkeit der DCP Methode im Umgang mit den großen Herausforderungen der Messung in offenen, heterogenen Kronendächern mit hohem Anteil verholztem Pflanzenanteil dargestellt werden. Durch den geringen Arbeits- und Zeitaufwand und die kostengünstige Verwendung von herkömmlichen Digitalkameras stellt DCP eine sehr effektive Methode dar, deren Verwendung in zukünftigen Forschungsarbeiten ausdrücklich zu empfehlen ist. Es ist jedoch anzustreben, den hier verwendeten Bildanalysealgorithmus von der kommerziellen eCognition Plattform auf eine Open Source Bildanalyse Plattform, wie zum Beispiel ImageJ, zu portieren um eine breite, Lizenz-unabhängige Nutzung zu ermöglichen.
Die Pfanzenarten des untersuchten *montado* Ökosystems haben große strukturelle und funktionelle Anpassungen zur Regulierung von Kohlenstoffbindung und Wasserverlust durch Transpiration entwickelt. Die hier dominierenden Korkeichen (*Q. suber*) besitzen tief dringende Wurzeln um das Grundwasser als permanenten Wasservorrat zu nutzen. Der Wasserverlust durch Transpiration wird unter Dürrebedingungen stark reduziert um einer kritischen Dehydrierung zu entgehen. Im zweiten Hauptthema der vorliegenden Doktorarbeit wird über den Einfluss der Dürre im sehr trockenen Jahr 2012 auf die Funktionen des Gesamtökosystems berichtet. Hierzu wurden mehrjährige Messungen des vorherrschenden Lokalklimas, der Bodeneigenschaften und der Massen- und Energieflüsse des Ökosystems durchgeführt, unter anderem mittels zwei Eddy Kovarianz Türmen.
Die Kombination von stomatärer Leitfähigkeits- und Photosynthese-Modellierung kann im Zuge der Messdatenanalyse verwendet werden, um Regulationsprozesse innerhalb des Blattes von Veränderungen im Lokal- oder Mikroklima zu trennen. In der Literatur finden sich dazu jedoch verschiedenste mathematische Beschreibungen der zugrunde liegenden Prozesse. Jüngste Studien zeigen das die Änderung lediglich eines

einzigen Modellparameters, zum Beispiel nur maximale Carboxylierungsrate oder nur die Sensitivität der stomatären Leitfähigkeit, nicht in der Lage ist beobachtete, simultane, dürre-bedingte Änderungen in Bruttoprimärproduktion und Transpiration zu erklären. Des Weiteren sind mehrere Beschreibungen für die Temperaturabhängigkeit der blattinternen Enzymprozesse in der Literatur vorhanden. Daraufhin wurde im Zuge der vorliegenden Arbeit ein stomatäre Leitfähigkeit-Photosynthese Modell anhand von Messdaten parametrisiert um blattinterne Reaktionen der vorherrschenden *Q. suber* Bäume auf eintretende Trockenheit abzubilden. Dabei wurden verschiedenste Prozessbeschreibungen getestet und die Modellleistung bei der Abbildung des beobachteten Verhaltens evaluiert. Die Ergebnisse zeigen im Trockenjahr 2012 einen stark erhöhten Effektivniederschlag ET/P von bis zu 122%, ermöglicht durch den Grundwasserzugang der *Q. suber* Bäume. Hierdurch konnte in diesem Jahr kein Wasser zur Grundwasserneubildung und Abflussbildung beitragen. Verringerte Bruttoprimärproduktion des Unterwuchses um 53% und der *Q. suber* Bäume um 28% waren die Folge des verzögerten Beginns der Herbstniederschläge und der schweren, zusätzlichen Winterdürre im Vergleich zum Vorjahr 2011. Bei der Anwendung des stomatäre Leitfähigkeit-Photosynthese Modells zur Beschreibung der Reaktion der *Q. suber* Bäume auf Trockenheit konnte die beste Modellleistung erreicht werden, wenn die Bäume in der Lage waren die maximale Carboxylierungsrate und die Sensitivität der stomatären Leitfähigkeit simultan den Bedingungen anzupassen. Die Steigung des stomären Leitfähigkeitsbeschreibung musste erhöht werden um die starke Abnahme der maximalen Carboxylierungsrate anteilig zu kompensieren. Des Weiteren wurde die Sensitivität der Stomata gegenüber dem Wasserdampfdefizit der blattnahen Atmosphäre verändert, da die vorgenannte Steigung des Modells hiermit stark korreliert ist. Die Modellleistung dieses Ansatzes (Leuning-Modell) war vergleichbar mit dem ebenfalls getesteten, einfacheren Ball-Berry-Modell. Zusätzlich zur gesunkenen maximalen Carboxylierungsrate wurde die Kohlenstoff-Assimilation durch eine verringerte Optimaltemperatur des Elektronentransportes im Photosyntheseapparat geschwächt. Dieser Effekt macht die Photosyntheserate der Blätter vermehrt anfällig gegenüber hohen Temperaturen während einer Dürre. Trotz allem war das Ökosystem in beiden Jahren (2011 und 2012) eine Kohlenstoff-Senke mit einer um 38% verminderten Senkenstärke in 2012. Folglich hatte die Bruttoprimärproduktion einen wesentlich stärkeren Einfluss auf die jährlichen Schwankungen in der Senkenstärke als die Ökosystemrespiration.

Im Zuge des Klimawandels sind verringerte jährliche Niederschläge und Veränderungen der saisonalen Niederschlagsverteilung auf der Iberischen Halbinsel in noch stärkerem Maße zu erwarten als bereits heute verzeichnet wird. Wenn Phasen der Dürre wie im Jahre 2012 vermehrt auftreten ist eine nachhaltige Verringerung der lokalen Grundwasservorräte und Staubecken zu erwarten. Dies würde großen Einfluss auf die örtliche Land- und Forstwirtschaft haben, da die Korkeichen den Grundwasserzugang nutzen und Bewässerungslandwirtschaft weit verbreitet ist. Langfristige Effekte auf den Pflanzenbestand, wie erhöhte Baumsterblichkeit oder eine Verschiebung in der Artenzusammensetzung der Unterwuchses werden vielleicht erst nach mehreren Dürrejahren wie 2012 sichtbar. Die gute Modellleistung des stomatäre

Leitfähigkeit-Photosynthese Modells unter simultanen Anpassung von maximaler Carboxylierungsrate und Sensitivität der stomatären Leitfähigkeit in diesem Ökosystem muss in anderen Ökosystemtypen noch bestätigt werden. Jedoch wird in jedem Fall eine erneute Evaluierung der Prozessbeschreibungen in weit verbreiteten globalen Klima- oder Landoberflächenmodellen empfohlen.

Abstract

This thesis covers two major topics. The first is a performance evaluation of indirect leaf area index L and gap probability P_{gap} observation techniques with special focus on the application in sparse, savannah-type canopies. L and P_{gap} estimates of the first part are used in the second part for the analysis of drought effects on water and carbon fluxes as well as on leaf physiology in a typical Mediterranean *montado* ecosystem dominated by *Quercus suber* L. trees.
Two of the most important parameters describing the structure of ecosystem canopies are leaf area index L and gap probability P_{gap}. They are mandatory for scaling of measured fluxes from leaf to canopy scale and are essential parameters for ecosystem models. However, their indirect measurement remains a challenging task, especially in open, savannah-type ecosystems where high light intensities, heterogeneous distribution of leaves and large amount of woody tissue in the sensor view field bias the observations. Further, a vertically resolved estimation of L and P_{gap} is needed for the growing community of vertically distributed models, increasing the demand for a fast and reliable estimation method. In the course of this thesis, the established commercial LAI-2000 device is compared to the rather new, fast digital cover photography (DCP) method with respect to the issues mentioned and to the precision of the results compared to a direct L determination. Firstly, DCP was successfully applied here for the first time height and angular dependent. Results show that gap probability P_{gap} and effective leaf area index L_e delivered by DCP were very similar to the established LAI-2000. Clumping index Ω is mandatory for deriving a correct leaf area index L from gap probability P_{gap} estimates at any view zenith angle θ accounting for the heterogeneity of natural canopies. Height and angular dependent Ω was successfully determined with DCP for the first time. Thus, the effect of leaf clumping on the total leaf area index L of the *Q. suber* canopy yielded a 30% higher leaf area index L compared to L approximated from LAI-2000. Further, the exclusion of woody tissue from DCP images was successfully conducted here for the first time. Using object-based image analysis, the exclusion yielded on average a 6.9% lower leaf area index L and improved the indirect estimation approach. This was a 'best case' approximation of the error introduced by woody tissue, because the algorithm was designed to not overestimate the effect. Consequently, when leaf clumping was included and woody tissue was excluded from DCP, L matched precisely with direct L determination using litter traps, exceeding the precision of the established LAI-2000 by far. Finally, when height dependent observations are not feasible, an observation strategy could been tested successfully using only ground-based observations of crown parameters to derive reasonable leaf area index L height distributions from a single, ground-based L observation.

It was shown in this thesis that DCP performed excellent handling the major challenges of open canopies, heterogeneous distribution of leaves and woody tissue influence. This encourages to use DCP in other ecosystems with different canopy structure in future research to benefit from the labor-effective application and low cost of off-the-shelf digital cameras. However, the developed algorithm for image separation of this thesis is based on the commercial eCognition image analysis platform. A desirable step for further development would be to port the algorithm to an open source image analysis platform like ImageJ to foster broader usability.
The plant species in the examined *montado* ecosystem have developed vast structural and functional adaptations to regulate carbon assimilation and respiratory water loss. The dominant Cork oak trees grow deep roots to tap the groundwater for a permanent water supply. They strongly reduce transpirational water loss by stomatal closure in response to drought to avoid a critical level of dehydration and hydraulic failure. In the context of the extreme drought year 2012, drought effects on the entire ecosystem functioning at the site in Portugal are reported in the second part of the thesis. Therefore, multi-year observations of climate forcing, soil properties as well as ecosystem flux observations with two Eddy Covariance towers were conducted.
Combined stomatal conductance-photosynthesis models can be used in order to disentangle regulatory processes in the leaves from effects of micro-climatic variations. However, different descriptions of the underlying processes exist in the literature. Recent studies could demonstrate that changes of one single parameter, e.g. only maximum carboxylation rate or only stomatal conductance sensitivity, do not explain drought-induced reductions in both, gross primary productivity and transpiration, simultaneously. Further, different temperature dependencies of leaf internal enzyme processes have been proposed in the literature. Here, a photosynthesis-stomatal conductance model was parametrized to match the observations in order to infer leaf physiological responses of the *Q. suber* trees in response to drought. Different model process descriptions have been tested with respect to model performance. The results show that precipitation effectiveness ET/P increased up to 122% in the dry year 2012, possible due to the ground water access of *Q. suber* trees leaving no water for groundwater replenishing and runoff generation. As a consequence, understorey gross primary productivity $\mathrm{GPP_u}$ and the overstorey gross primary productivity $\mathrm{GPP_o}$ were reduced by 53% and 28%, respectively, in 2012 compared to 2011 due to a late onset of 2011 autumn rains and an additional severe winter/spring drought.
When the combined photosynthesis and stomatal conductance model was used to describe the responses of *Q. suber* trees to drought, the best model-data fit could be achieved if the trees were allowed to adapt apparent maximum carboxylation rate $V_{\mathrm{c,max}}$ and stomatal conductance parameters simultaneously. The slope m of the stomatal conductance model had to be increased to compensate partly for the strong decrease in carboxylation rate. The model adjusted also the sensitivity of the stomata D_0 to vapour pressure deficit VPD in the Leuning model because both stomatal parameters, m and D_0 are strongly correlated. The model performance was similar to the Ball-Berry approach. Further, the optimum temperature of electron transport T_{opt} was adjusted to lower values. This decreased carbon sequestration under higher

temperatures in addition to the direct drought effect but makes the photosynthetic apparatus also more vulnerable to heat stress in dry years. However, the ecosystem was a carbon sink in both years with a 38% reduced sink strength in the dry year 2012 compared to 2011. Gross primary productivity GPP was thereby a much stronger driver of inter-annual variations of carbon sink strength than ecosystem respiration R_{eco}.

It is expected that the trend of decreasing total annual precipitation and alteration of precipitation patterns on the Iberian Peninsula will continue with proceeding climate change. If drought patterns similar to 2012 will occur more often, a sustainable depletion of local ground water reservoirs as well as water storage basins might be expected. This will affect strongly local agriculture that relies on ground water for the deep-rooted cork-oak trees and otherwise uses irrigation water from storage basins. Effects on plants such as tree mortality or a shift of understory species composition may only be evident in the long term after multiple, consecutive drought years. The performance of the photosynthesis-stomatal conductance model under simultaneous adaption of maximum carboxylation rate and stomatal conductivity clearly point to the necessity of similar investigations in other ecosystem types and the reevaluation of descriptions used in global climate or land surface models.

List of Figures

List of Tables

1 Introduction

1.1 Relevance of the project

Savannah-type ecosystems account for 26–30% of global gross primary productivity with water being one of the major driving factors. In the Mediterranean region of Europe, savannah-type woodlands cover an area of about 1.5 million ha. These woodlands are commonly two or three layered systems with a sparse overstorey layer of, e.g. *Quercus suber* L. (cork oak) or *Quercus ilex* L. (holm oak), a more or less distinct shrub layer of evergreen shrubs like species of the genus *Ulex* (gorse) or *Cistus* (rockrose) and a herbaceous understorey layer consisting of annual herbs and grasses like *Trifolium* species (clover), *Tuberaria guttata* L. (spotted rockrose), *Tolpis barbata* L. (european umbrella milkwort) or *Vulpia* species.
The Mediterranean climate is characterized by a moist and mild winter and a dry and hot summer. It shows an annual pattern of high winter precipitation and summer drought. The relevance of the winter precipitation to the hydrological cycle, biological productivity and survival is immense, since water availability is the limiting factor during large parts of the year. In particular on the Iberian Peninsula, the recent past has shown a significant decrease of precipitation in winter and spring as well as decrease of total annual precipitation. Strong effects on local water balance and carbon sink strength of ecosystems have thus been reported. These changes in precipitation regime are expected to increase with proceeding climate change.
The analysis of ecosystem behavior under changing conditions requires the measurement of ecosystem parameters and energy and mass fluxes. Two of the key structural ecosystem parameters are leaf area index (L) and canopy gap probability (P_{gap}), strongly influencing amounts of carbon uptake by photosynthesis and water loss by transpiration as well as energy distribution between plants and soil and ecosystem albedo. The precise estimation of L and P_{gap} remains a challenging task, especially in sparse, open canopies of Savannah-type woodlands. Multiple methods are still under development. Further, the precise determination of evaporation and transpiration is an important task in water-limited ecosystems since evapotranspiration is the largest water efflux. Disentangling both signals from a measured water flux is possible using stable δ^{18}O isotopes as tracer. For this purpose, the Craig & Gordon equation is commonly used (Craig and Gordon, 1965). However, general assumptions made in order to apply the equation to real observations and the sensitivity with respect to input measurements are objects of ongoing research.
In the course of the WATERFLUX project, a study site was established in a typical *montado* ecosystem dominated by *Quercus suber* trees and herbaceous understorey

vegetation in central Portugal to assess the canopy structure, understorey dynamics, evaporative water loss, important processes and water and carbon balances of a typical Mediterranean savannah-type woodland under regular and under drought conditions. A variety of observations and modeling have been conducted for about 3 years from 2010 to 2013, including the extreme dry year 2012 with a severe winter drought. In order to assess the *Q. suber* canopy structure and its properties for radiative transfer necessary for modelling and analysis purposes, the new digital cover photography method (DCP) was used. The DCP method was compared with other established indirect and direct methods to develop a labour efficient and precise observation strategy (Chap. 2, Piayda et al. (2015)). Further, the canopy cover data was used for the analysis of annual understorey development and community structure with respect to the spatial distribution of tree crown cover (App. **??**, Dubbert et al. (2014b)). The competition for water between over- and understorey and the altered microclimatic conditions are suspected to influence understorey species composition and thus, carbon sink strength.
The understorey and soil carbon and water fluxes were assessed with a sub-canopy Eddy Covariance tower for the entire period from 2010 to 2013 (Chap. 3, Piayda et al. (2014)) in order to characterise the annual pattern of carbon uptake and evapotranspiration and to quantify the impact of drought. The sub-canopy Eddy Covariance observations were complemented with open chamber measurements on trenching plots connected to an on-site cavity ring-down spectrometer. Obtained stable water isotope concentrations were used to separate water fluxes in evaporation and transpiration. On-site measured values were used to evaluate the performance of the frequently used Craig and Gordon model (App. **??**, Dubbert et al. (2013)). Further, the steady-state assumption of transpiration on the separation of evapotranspiration in its components (App. **??**, Dubbert et al. (2014a)) was tested and the impact of understorey evapotranspiration to ecosystem water fluxes (App. **??**, Dubbert et al. (2014c)) analysed using the stable water isotope approach.
The necessary water and carbon fluxes as well as climate forcing of the entire ecosystem were measured with an Eddy Covariance tower above the canopy top. These pure mass balance observations were extended by phenology measurements of tree growth and leaf and fruit setting (App. **??**, e Silva et al. (2015)) to characterize the impact of drought on the *Q. suber* trees during the extreme dry year 2012. Further, the drought impact on tree leaf physiology was modeled with a coupled photosynthesis-stomatal conductance model in a sunlit/shaded model scheme (Chap. 3, Piayda et al. (2014)). Changes in carboxylation efficiency and stomatal conductance during summer are evaluated as well as model performance with respect to a variety of different process descriptions.

1.2 Objective of the thesis

The thesis contains two major parts. The first part is a methodological treatment of indirect estimation of leaf area index and gap probability, with focus on the

application in open savannah-type ecosystems. The second part is an analysis of drought impact on ecosystem functioning and water and carbon balances. Even though the topics are very different, the results of the first part are mandatory to conduct the analysis of the second part.

Leaf area index L is an important structural parameter of plants, canopies and ecosystems and strongly influences amounts of carbon uptake by photosynthesis (e.g. Bunce, 1989) and transpiration (e.g. Monteith, 1965). The structural parameter quantifying the amount of light passing through the canopy is the gap probability P_{gap}, which depends on L, tree density and other stand attributes. It controls the energy distribution between plant surfaces and the soil surface as well as within the plant (Chen and Black, 1992; Nilson, 1971). P_{gap} and L are needed in soil-vegetation-atmosphere transfer modeling (De Pury and Farquhar, 1997; Sellers and Dorman, 1987; Sinclair et al., 1976). Because recent model development aims for high-resolution multi-layer models (Baldocchi, 1997), the demand for vertically resolved plant or ecosystem parameters is increasing.
Multiple techniques exist to measure leaf area index L and gap probability P_{gap}. Indirect techniques are based on the observation of P_{gap} and use the gap probability theory by Nilson (1971) to infer L. They include the commercially available LAI-2000 plant canopy analyzer (LI-COR, 1992; Cutini et al., 1998) and digital cover photography (DCP) (Ryu et al., 2010b; Macfarlane et al., 2007b). DCP offers the advantage of using off-the-shelf digital cameras and common image analysis software. Using methods based on P_{gap}, the influence of the spatially non-homogeneous distribution of leaves on P_{gap}, expressed as clumping index Ω, needs to be considered, especially in open canopies like savannahs, because the gap probability theory assumes randomly distributed light intercepting elements (Fassnacht et al., 1994; Nilson, 1971). The contribution of woody tissue (e.g., stems, branches, twigs) to observed gap probability P_{gap}, and thus inferred leaf area index L, is still an unsolved problem for indirect measurements. It is assumed to introduce substantial biases depending on the ecosystem type (Chen et al., 1997a,b; Deblonde et al., 1994; LI-COR, 1992).
In the face of the issues described above, the established LAI-2000 is compared against the DCP method with respect to leaf clumping effects, methodological biases and the influence of woody tissue. Height and angular dependent gap probability P_{gap} and height dependent leaf area index L are derived on the site in Portugal. Additionally, a ground-based approach to estimate height dependent L is tested when height distributed measurements are not feasible. The following research questions are addressed:

- How do gap probability P_{gap}, leaf area index L and clumping index Ω change with height and view zenith angle?
- How strong is the influence of non-homogeneous distributed leaves on both methods?

- How does the image size of DCP influence the accuracy of gap probability P_{gap} and leaf area index L observations?

- How strong is the influence of woody tissue on gap probability P_{gap} and leaf area index L estimates?

- How well can we derive height distributed leaf area index L with only ground-based observations?

Answering these questions will significantly contribute to the precision and feasibility of indirect canopy structure observations, in particular in sparse canopies, and will foster the use of the new low cost and efficient DCP method in future research.

Species in semi-arid environments have developed vast structural and functional adaptations to regulate carbon assimilation and respiratory water loss (e.g. Tenhunen et al., 1987; Werner et al., 1999). Cork oaks strongly reduce transpirational water loss by stomatal closure in response to drought to avoid a critical level of dehydration and hydraulic failure (Oliveira et al., 1992; Tenhunen et al., 1984, 1987; Werner and Correia, 1996; Kurz-Besson et al., 2006).
Common tools to disentangle biochemical processes in plant leaves from micro-climatic variations are combined stomatal conductance-photosynthesis models. However, a variety of process descriptions exist in the literature, e.g. for the temperature dependency of leaf internal enzyme processes (Medlyn et al., 2002; von Caemmerer, 2000; June et al., 2004). Further, a simultaneous change in both gross primary productivity and transpiration as response to drought could only be explained by a simultaneous change of multiple model parameters, e.g. maximum carboxylation rate and stomatal conductance sensitivity in recent studies (Egea et al., 2011; Reichstein et al., 2003; Zhou et al., 2013).
In view of context of the extreme drought year 2012, drought effects on the entire ecosystem functioning at the site in Portugal are reported in comparison with the rather wet year 2011 showing a regular drought pattern. Particularly, 2012 showed a severe additional winter/spring drought, characteristic for precipitation pattern changes in recent past on the Iberian Peninsula (2nd driest year since 1950, Costa et al., 2012; Santos et al., 2013; Trigo et al., 2013). The following research objectives are investigated:

- Quantifying the effects of drought on the local ecosystem water balance, overstorey and understorey gross primary productivity, as well as differences in net ecosystem carbon exchange between both years.

- Identifying physiological responses in the drought year 2012 of the *Q. suber* trees using a combined photosynthesis-stomatal conductance model.

- Testing the model performance with different process descriptions.

Investigating the objectives will assess the response of a typical Mediterranean ecosystem on possible climate change impacts. Additionally, the performance testing will improve model descriptions used in future climate impact research.

1.3 Outline

The thesis consist of five main chapters. The current chapter, Chap. 1, gives a general overview of the topic, how the WATERFLUX project is structured and which parts of the project are treated in this thesis. Chap. 2 compares three non-destructive leaf area index measurement techniques at the study site in central Portugal in order to derive vertically resolved L as well as vertically and angularly resolved P_{gap}. The established LAI-2000 device is compared with fast digital cover photography (DCP) and a purely ground-based approach. The influence of woody plant components is quantified and three different crown models are applied to describe the cumulative L distribution. The estimated L and angularly resolved P_{gap} are used in Chap. 3, where the impact of the extreme drought event on the Iberian Peninsula in 2012 on the water balance, gross primary productivity and carbon sink strength of the cork-oak ecosystem are quantified. Physiological responses of the *Quercus suber* (L.) trees are disentangled, employing combined photosynthesis and stomatal conductance modeling. Chap. 4 summarizes the results of the thesis and provides an overwiew on the results of the entire project. Chap. 5 gives an outlook on possible further development of the methods used and on long term development of the ecosystem.

2 Influence of woody tissue and leaf clumping on vertically resolved leaf area index and angular gap probability estimates

2.1 Introduction

Leaf area index L is defined as the one-sided leaf area per unit of ground area (Watson, 1947). It is an important structural parameter of plants, canopies and ecosystems and strongly influences amounts of carbon uptake by photosynthesis (e.g. Bunce, 1989) and transpiration (e.g. Monteith, 1965). It determines the radiative energy absorbed and reflected by the canopy (Monteith, 1959) as well as the maximum capacity of rainfall interception, and thus canopy evaporation (Rutter et al., 1971). The structural parameter quantifying the amount of light passing through the canopy is the gap probability P_{gap}, which depends on L, tree density and other stand attributes. It is the probability of a direct beam of radiation passing through the canopy without being intercepted by the foliage (Monsi and Saeki, 1953, 2005). It controls the energy distribution between plant surfaces and the soil surface as well as within the plant (Chen and Black, 1992; Nilson, 1971) and, thus, the ecosystem albedo.

P_{gap} and L are important ecosystem parameters that are needed in soil-vegetation-atmosphere transfer modeling (De Pury and Farquhar, 1997; Sellers and Dorman, 1987; Sinclair et al., 1976) or radiative transfer schemes (Jacquemoud et al., 2000; Haverd et al., 2012). Because recent model development aims for high-resolution multi-layer models (Baldocchi, 1997), the demand for vertically resolved plant or ecosystem parameters such as P_{gap} and L is increasing. Although vertically distributed observations in tree canopies are challenging (Meir et al., 2000), expensive and often not feasible, several observation approaches have been applied (Beadle et al., 1982; Hutchison et al., 1986; Parker et al., 1989; Strachan and McCaughey, 1996; Wang et al., 1992). Such approaches either required labor-intensive destructive sampling, heavy equipment, and 'above canopy readings' with a tower, or did not take into consideration important factors such as the leaf clumping index Ω.

Multiple techniques exist and have been widely used to measure leaf area index L

and gap probability P_{gap}. They can be classified into direct and indirect methods. Direct techniques include destructive sampling or litter traps (Jonckheere et al., 2004) and are not suitable for measuring P_{gap}. In general, they deliver the most precise results but are very labor intensive, and multiple observations during the year are often not feasible. Indirect techniques include the inclined point quadrat method (Warren Wilson, 1960, 1965), the commercially available LAI-2000 plant canopy analyzer (LI-COR, 1992; Cutini et al., 1998) or digital hemispherical (DHP) and digital cover photography (DCP) (Ryu et al., 2010b; Macfarlane et al., 2007b). DCP offers the advantage of using off-the-shelf digital cameras and providing a minimum of image distortion. Thus, common image analysis software can be used. Indirect techniques deliver P_{gap}, L and other structural parameters of the canopy, such as crown cover and porosity (Macfarlane et al., 2007c). They are less labor intensive than direct methods and allow repeat observations throughout the year (Ryu et al., 2012), but they are inferior in accuracy.

Most indirect techniques are based on the observation of P_{gap} and use the gap probability theory by Nilson (1971) to infer L. Some techniques need additional information about leaf inclination angles α to convert the projected leaf area observed by the sensors into actual leaf surface (Warren Wilson, 1960). Techniques such as the LAI-2000 instrument (LI-COR, 1992; Miller, 1967) or DCP applied at $\approx 57.3°$ (Macfarlane et al., 2007c; Pisek et al., 2011; Wit, 1965) circumvent this need. However, DCP applied at angles $0 < \theta < 90$ comes with a biased mean P_{gap} compared to DHP because a rectangular area is averaged but not a spherical sector. Still, when images represent only a small horizontal view span compared to 360°, the bias on mean P_{gap} is small.

Using methods based on P_{gap}, the influence of the spatially non-homogeneous distribution of leaves on P_{gap}, expressed as clumping index Ω, needs to be considered because the gap probability theory assumes random distributed light intercepting elements (Fassnacht et al., 1994; Nilson, 1971). This greatly influences L derivation in open, heterogeneous stands such as savannah-type ecosystems. However, estimating the spatial and angular distribution of Ω within a plant stand remains challenging (Leblanc et al., 2005; Ryu et al., 2010b).

The contribution of woody tissue (e.g., stems, branches, twigs) to observed gap probability P_{gap}, and thus inferred leaf area index L, is still an unsolved problem for indirect measurements. It is assumed to introduce substantial biases depending on the ecosystem type L (Chen et al., 1997a,b; Deblonde et al., 1994; LI-COR, 1992). Commonly, observations during leafless periods are used to estimate wood area index W and subtract it from L, which is only feasible in deciduous forests (Deblonde et al., 1994; Ryu et al., 2012) and assumes a random distribution of woody tissue with respect to the position of the leaves. Only a few approaches attempt to quantify this influence (Kucharik et al., 1998) and to our knowledge, it has not yet been included directly in computations.

The aim of the present study is to compare the performance of the established LAI-2000 against the DCP method with respect to leaf clumping effects, methodological biases and the influence of woody tissue. We derive height and angularly dependent

gap probability P_{gap} and height dependent leaf area index L in an open savannah-type woodland. Additionally, we test a ground-based approach to estimate height dependent L when height distributed measurements are not feasible. We address the following research questions: (1) How do gap probability P_{gap}, leaf area index L and clumping index Ω change with height and view zenith angle? (2) How strong is the influence of non-homogeneity on both methods? (3) How does the image size of DCP influence the accuracy of gap probability P_{gap} and leaf area index L observations? (4) How strong is the influence of woody tissue on gap probability P_{gap} and leaf area index L? (5) How well can we derive height distributed leaf area index L with only ground-based observations?

2.2 Material and methods

2.2.1 Theory

Gap probability theory

Beer's law for the absorption of light by particles (Bouguer, 1729; Beer, 1852) is used to relate leaf area index L to the gap probability P_{gap} of the canopy (Nilson, 1971):

$$P_{gap}(\theta) = \exp\left(\frac{-G(\theta)\, L\, \Omega(\theta)}{\cos(\theta)}\right) \tag{2.1}$$

where $P_{gap}(\theta)$ is the gap probability of the canopy, $G(\theta)$ is the leaf projection function, L $[\mathrm{m}^2_{\mathrm{leaf}}/\mathrm{m}^2_{\mathrm{ground}}]$ is the leaf area index (sometimes referred to as L_t), $\Omega(\theta)$ is the clumping index, and θ [°] is the view zenith angle. In fact, L refers to a foliage area index if it has not been corrected for the influence of woody tissue on $P_{gap}(\theta)$. By dividing by $\cos(\theta)$, the leaf area index is normalized to unity path length independent of the incidence angle. $G(\theta)$ was introduced in Eq. (2.1) by Monsi and Saeki (1953) to transform the projection of leaf area perpendicular to the view direction into actual leaf area index. The shape of $G(\theta)$ is dependent on the distribution of leaf angles $f(\alpha)$. Warren Wilson (1960, 1967) gave the solution as:

$$G(\theta) = \int_0^{\frac{\pi}{2}} \phi(\theta, \alpha) f(\alpha)\, \mathrm{d}\alpha \tag{2.2}$$

with

$$\phi(\theta, \alpha) = \begin{cases} \cos(\theta)\cos(\alpha) & \text{for } \alpha \leq \theta \\ \cos(\theta)\cos(\alpha)\left[1 + \left(\frac{2}{\pi}\right)(\tan(\vartheta) - \vartheta)\right] & \text{otherwise} \end{cases} \tag{2.3}$$

where $\vartheta = \cos^{-1}(\cos(\theta)\cos(\alpha))$. α [°] is the angle of the leaf's normal to the zenith. $\phi(\theta, \alpha)$ results from the scalar product of both the directional vector of the view direction and the directional vector of the leaf's normal. It is integrated over the azimuth angle assuming the same distribution of leaf inclination over the entire

azimuthal range. While Warren Wilson (1967) assumes a uniform distribution of leaf angles $f(\alpha)$, Goel and Strebel (1984) proposed a Beta-distribution with two parameters to represent the leaf inclinations of real plants.
The original formulation of Beer's law assumes the random distribution of light intercepting elements in the pathway of penetrating beams. Because leaf elements in natural canopies are seldom randomly distributed but instead clumped into crowns, Nilson (1971) introduced the clumping index $\Omega(\theta)$ in Eq. (2.1). It distributes the leaf area index from within the crowns to the entire canopy or region of measurement. It is one for randomly distributed leaf elements and decreases with increasing clumping.

LAI-2000

The internal software of the LAI-2000, as well as the FV2200 windows-software (LI-COR Biosciences, Inc., 2010) for post processing, calculates the gap probability $P_{gap}(\theta)$ for each reading from the ratio of above-canopy light intensity A and below-canopy light intensity B. This is used to calculate the contact frequency $K(\theta)$ for each view zenith angle θ of the instrument following Miller (1967, 1986):

$$K(\theta) = -\ln(P_{gap}(\theta))\cos(\theta) = G(\theta)L_e \tag{2.4}$$

$K(\theta)$ arises from the inclined point quadrat method (Warren Wilson, 1959, 1960) and is averaged over all readings for each angle to $\overline{K(\theta)}$ within each measurement. Because the clumping index $\Omega(\theta)$ is unknown here, only the effective leaf area index L_e can be described by Eq. (2.4) underestimating actual leaf area index L. Using the instrument software, the average gap probability $\overline{P_{gap}(\theta)}$ is reversely calculated via:

$$\overline{P_{gap}(\theta)} = \exp\left(\frac{-\overline{K(\theta)}}{\cos(\theta)}\right) \tag{2.5}$$

according to Eq. (2.4). Miller (1967) derived a solution to determine L_e directly from $\overline{K(\theta)}$ without knowledge of $G(\theta)$ under the condition that measurements of $\overline{K(\theta)}$ exist for different angles θ as:

$$L_e \int_0^{\frac{\pi}{2}} G(\theta)\sin(\theta)\,\mathrm{d}\theta = \int_0^{\frac{\pi}{2}} \overline{K(\theta)}\sin(\theta)\,\mathrm{d}\theta \tag{2.6}$$

and because $\int_0^{\frac{\pi}{2}} G(\theta)\sin(\theta)\,\mathrm{d}\theta = 0.5 \;\forall\; \mu,\nu \in \Re_+\backslash\{0\}$ of the leaf angle distribution function $f(\alpha)$, Eq. (2.6) reduces to:

$$L_e = 2\int_0^{\frac{\pi}{2}} \overline{K(\theta)}\sin(\theta)\,\mathrm{d}\theta \tag{2.7}$$

Recently, Ryu et al. (2010a) reported on the effects of averaging $K(\theta)$ instead of $P_{gap}(\theta)$ in Eq. (2.4) on the estimation of L_e by the LAI-2000 instrument software, which introduces an apparent clumping effect, partially compensating for the unknown

clumping index $\Omega(\theta)$ of Eq. (2.4). Therefore, the correct averaging method (averaging P_{gap} instead of $K(\theta)$), as well as the standard instrument software averaging, is applied throughout this work to compare the influence of apparent clumping of leaves on leaf area index estimation. With the correct averaging method, $\overline{P_{gap}(\theta)}$ is calculated directly from readings and Eq. (2.7) leads to the effective leaf area index L_e, assuming randomly distributed leaf elements making Eq. (2.5) obsolete.

Digital cover photography

The whole image must be separated into areas of gaps and plant tissue by some algorithm. If only the total number of pixels within gaps is known, the assumption must be made to face randomly distributed leaf elements resulting in effective leaf area index L_e (Leblanc, 2002, Eq. 7):

$$L_e = \frac{-\ln\left(\overline{P_{gap}(\theta)}\right)\cos(\theta)}{G(\theta)} \tag{2.8}$$

with mean gap probability $\overline{P_{gap}(\theta)} = \overline{gt}/A$ where $\overline{gt}$ [pxl] is the number of pixels in all gaps averaged over all images and A [pxl] is the total number of pixels in each image file, equal to Eq. 4 in Macfarlane et al. (2007a):

$$L_e = \frac{-\ln\left(\frac{\overline{gt}}{A}\right)\cos(\theta)}{G(\theta)} \tag{2.9}$$

DCP offers the advantage of determining different gaps in the canopy separately, i.e., between crowns as well as within crowns. Therefore, the clumping of leaf elements into crowns can be considered explicitly when calculating leaf area index L (Macfarlane et al., 2007a, Eq. 3):

$$L = -fc\frac{\ln\left(1-\frac{ff}{fc}\right)\cos(\theta)}{G(\theta)} \tag{2.10}$$

where crown cover $fc = 1 - \overline{gl}/A$ and foliage cover $ff = 1 - \overline{gt}/A$ with $\overline{gl}$ [pxl] is the average number of pixels in the largest gap of the image which is normally, but not always, the gap between adjacent crowns. This leads to:

$$L = \frac{-\left(1-\frac{\overline{gl}}{A}\right)\ln\left(\frac{\overline{gt}-\overline{gl}}{A-\overline{gl}}\right)\cos(\theta)}{G(\theta)} \tag{2.11}$$

where the expression $(\overline{gt} - \overline{gl})/(A - \overline{gl})$ calculates the gap probability within the crown envelopes. Because this gap probability is only valid within crowns, it needs to be scaled to the total canopy according to the ratio of the crown envelopes to the whole image area by $1 - \overline{gl}/A$ following Macfarlane et al. (2007c) and Leblanc (2002).

$\overline{gl}$, $\overline{gt}$ and A should further be understood as angularly dependent in this work, because the DCP method is applied for different angles. Hence, leaf area index L and effective leaf area index L_e can be calculated from observations at any θ because $G(\theta)$ is known.
The clumping index $\Omega(\theta) = L_e/L$ mentioned in section 2.2.1 can be calculated directly by dividing Eq. (2.9) by Eq. (2.11) (cf. Macfarlane et al., 2007c, Eq. 5):

$$\Omega(\theta) = \frac{\ln\left(\frac{\overline{gt}}{A}\right)}{\ln\left(\frac{\overline{gt}-\overline{gl}}{A-\overline{gl}}\right)} \left(\frac{1}{1-\frac{\overline{gl}}{A}}\right) \tag{2.12}$$

Additionally, the prior averaging of gap fractions avoids undefined leaf area index L and clumping index $\Omega(\theta)$ from images showing solely sky and prevents data loss.

2.2.2 Site description

The study was conducted in a Portuguese savannah-type cork oak forest located ca. 100 km north-east of Lisbon (39° 8′ 20.7″ N, 8° 20′ 3.0″ W, 162 m above mean sea level) which is part of the European integrated carbon observation system ICOS. The only tree species on the site is the evergreen *Quercus suber* (L.) with a tree density of 209 ha^{-1}. The understory vegetation consists of annual grasses and herbs that undergo annual die back at the onset of the summer drought (Dubbert et al., unpubl.). The site is managed by local farmers for the purpose of cork and cattle production.

2.2.3 Sampling design and measurements

In August 2011, a 100 m × 100 m regular transect grid close to the Eddy Covariance flux tower was established based on a semivariogram analysis of previous, ground-based leaf area index measurements with DCP (Fig. 2.1). On each point of the grid, a large but lightweight tripod of 8.5 m maximum height was set up and equipped with a LAI-2000 plant canopy analyzer sensor head (LI-COR Biosciences Inc., Lincoln, NE, USA) operated in *remote below mode* connected to the control unit on the ground. At heights of 3, 4, 5, 6, 7, 8, and 8.5 m, a sequence of 5 replicates was measured, taking into account all 5 rings of the sensor head (view zenith angle θ = 7°, 23°, 38°, 53°, and 68° respectively), each enclosing a view angle span θ_v of 10° to 13°. Simultaneously, on the nearby Eddy Covariance flux tower, a second plant canopy analyzer was operated in *remote above mode* with an automatic logging interval of 15 s. Both sensor heads were equipped with 180° view caps, calibrated against each other and aligned in the same azimuthal direction. All LAI-2000 measurements were conducted during dusk and dawn to avoid direct sunlight conditions. After the measurements, both control units were connected for data exchange.
During daylight conditions, the tripod was equipped with a Canon PowerShot D10 digital camera (Canon Inc., Tokyo, Japan) mounted on a tiltable rack that can be

inclined, pointing with the image center to zenith view angles θ of 0°, 10°, 23°, 38°, 53°, 68°, 71°, and 90° by a bowden cable and triggered by a custom built remote control. Images facing 0° North were taken at each height mentioned before avoiding back light conditions and assuring optimal image quality. The camera has a 1/2.3 inch (ca. 6.16 × 4.62 mm) CCD sensor and a focal length of 6.2 mm enclosing a horizontal and vertical view angle span θ_v of 53° and 41°, respectively. It was set to the maximum resolution of 4000 × 3000 pixel, fine compression ratio, automatic exposure and no zoom.
On 105 trees, the height of the crown top h_t and crown bottom h_b were determined from the ground using a digital hypsometer (Forestor Vertex, Haglöf Sweden). The crown radius r_c was measured with a measuring tape in 0°, 90°, 180° and 270° azimuthal directions and averaged for each tree.

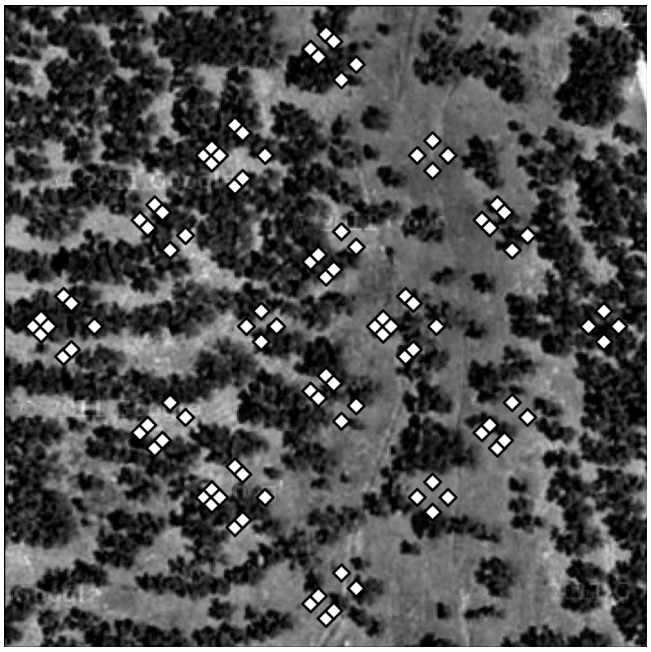

Figure 2.1: Rectangular transect grid (white squares) with 100 observation points of 100 × 100 m extend. Background: aerial photograph of the study site in central Portugal with *Q. suber* trees (Google, 2013).

2.2.4 Data processing and analysis

LAI-2000 and DCP

The readings of the LAI-2000 device were treated with the original and the correct averaging methods according to Section 2.2.1 for each height. Errors were estimated with bootstrapping (Efron and Tibshirani, 1993). Readings were thus randomly re-sampled ($n = 10\,000$) with replacement and averages and standard errors were

estimated from the bootstrap distribution of the mean. The digital cover images were analyzed separately in their original size representing a vertical view angle span θ_v of 41° and cropped rectangularly to 50%, 25%, and 12.5% of the original size around the image center representing θ_v spans of 20.5°, 10.25° and 5.625°, respectively.

The separation in gap, leaf and trunk area in the image was performed by object-based image analysis using the eCognition software (Trimble Germany GmbH). The images were segmented using multi-resolution segmentation with step-wise increased object sizes (Trimble, 2012). Gaps were classified by thresholds by an object's average brightness $\overline{bri}$, blue difference $\overline{bd}$ and blue ratio $\overline{br}$ (defined in Appendix A.2). The differences between neighboring objects were used to strengthen the discriminatory power on the edges of gap areas (Appendix A.2). Image objects were classified as woody tissue by thresholds based on shape features as well as rgb sums $\sum \overline{RGB}$ and green ratios $\overline{gr}$ (Appendix A.2). Objects are only classified as woody tissue when they did not obscure - or were not obscured by - leaves (Kucharik et al., 1998). If a woody tissue object obscures leaves behind itself, that cannot be determined directly from the image. However, if the relative number of sky objects in the direct surroundings of the woody object is dominant and above a certain threshold, the occurrence of leaves behind the object is considered to be unlikely.

The number of pixels in gaps between crowns gl and the number of pixels in all gaps gt were averaged, and standard errors were estimated using bootstrap (see above) and used according to Section 2.2.1 for each height. The 90° view zenith angle images were used to determine leaf angle distribution $f(\alpha)$ and leaf projection functions $G(\theta)$ utilizing the open source image processing package Fiji (Schindelin et al., 2012) measuring the angles of leaves whose lamina is aligned perpendicularly to the view direction (Ryu et al., 2010b). Measurements contained 281, 196, 234, 197, 147, 307, and 199 leaves at a height of 3, 4, 5, 6, 7, 8, and 8.5 m, respectively.

Auxiliary data

To infer the height distribution of the leaf area index L from purely ground-based observations, each set of crown top height h_t, crown bottom height h_b and crown radius r_c observations were used to determine a crown shape model representation. All representations of a specific crown shape model were averaged using bootstrap, normalized to unity and multiplied by the leaf area index L at a height of 3 m. This was performed for a symmetric ellipsoid crown shape model $S_e(h)$, an asymmetric ellipsoid crown shape model $S_{e\,9/10}(h)$ and a triangular crown shape model $S_t(h)$, as illustrated in Fig. 2.2. h [m] is the height above ground, r_c [m] is the horizontal semiaxis and $(h_t - h_b)/2$ [m] is the vertical semiaxis of the crown. The asymmetric crown shape model $S_{e\,9/10}(h)$ (with an ellipse center at 9/10th of the ellipse height) is estimated at the site to be the most representative crown shape. Additionally, the ellipsoidal $S_e(h)$ and triangular $S_t(h)$ crown shape models were used to estimate the influence of the model shape on L height distribution. For each model, the leaf density is assumed to be uniform over the entire height range.

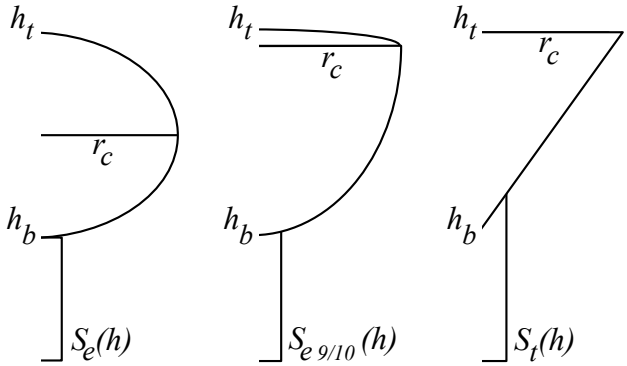

Figure 2.2: Sketches of crown models: ellipsoidal $S_e(h)$, asymmetric ellipsoidal $S_{e\,9/10}(h)$ and triangular model $S_t(h)$. h_t = crown top height, h_b = crown bottom height, r_c = crown radius.

2.3 Results and Discussion

In this section, an improvement of the LAI-2000 readings treatment is proposed and observed gap fraction distributions $P_{gap}(\theta)$ of LAI-2000 and DCP are compared. Accordingly, the leaf projection function $G(\theta)$ as well as the angular leaf clumping dependency $\Omega(\theta)$ are discussed with regard to leaf area index calculations. Then, the observed effective leaf area index L_e and the leaf area index L are compared for both methods. The influence of view the angle span on DCP uncertainty is shown and the bias on L due to the influence of woody foliage is quantified. Finally, a purely ground-based approach for estimating L height distribution is proposed.

2.3.1 LAI-2000 bad readings handling

The LAI-2000 device measures light intensity above and below the canopy to infer gap probability $P_{gap}(\theta)$. By default, the instrument software ignores transmittance readings, where at least one of the rings of the below canopy light intensity readings B returns a higher value than the respective above canopy light intensity reading A resulting in $P_{gap}(\theta)$ values > 1. It is assumed that these values are caused by operational errors, which is reasonable in canopies with higher leaf area index L (LI-COR, 1992). However, this introduces a large negative bias when used in open canopies; because light attenuation is generally small, A and B reading differences are small and normal measurement variations can lead to $P_{gap}(\theta) > 1$. This appears in approximately 50% of observations made for this work.
Inspecting the distribution of angularly averaged $P_{gap}(\theta) > 1$, the majority does not exceed 10% deviation (Fig. 2.3). Only few, distinct values apart from the main distribution exceed 10% deviation, indicating multiple $P_{gap}(\theta)$ values larger than unity due to operational errors. This can only be observed when plotting the angularly averaged P_{gap} instead of gap fractions from all rings individually,

because the magnitude of deviation depends on the view angle and multiple deviation distributions superpose each other making an error detection impossible. $\overline{P_{gap}(\theta)}$ values larger than 10% deviation were excluded from further calculations employing a median absolute difference filter (MAD) based on 2.5 standard deviations. The retained $P_{gap}(\theta)$ values were set to unity. The amount of bad readings could thus be reduced from 50% to 3% and by setting $P_{gap}(\theta)$ with deviations below 10% to unity instead of excluding them from calculation, resulting L is reduced by 26% at 3 m height and to 63% at 8.5 m height, respectively. $P_{gap}(\theta)$ and effective leaf area index L_e are then very comparable to DCP (Fig. 2.4, 2.7a), which is not subject to this source of error. Hence, this bad readings handling is considered to be appropriate to address the occurrence of large gaps in the canopy and is used in the further analysis.

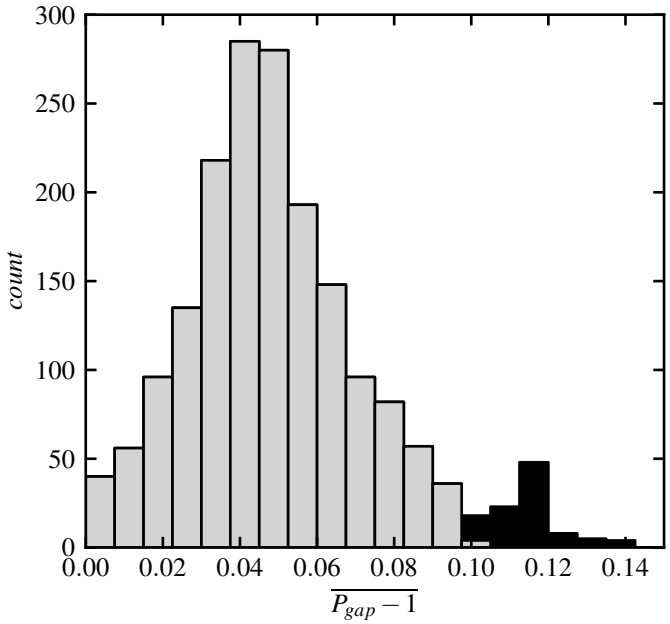

Figure 2.3: Histogram of angularly averaged transmittance deviations from unity $\overline{P_{gap}-1}$. Light grey: values set to 1 and kept for further analysis. Black: considered operational errors and excluded from further analysis with MAD filter based on 2.5 standard deviations.

2.3.2 Gap probability distribution

The height and angularly dependent gap probability $P_{gap}(\theta)$ was measured with the LAI-2000 and DCP, which is further used to calculate leaf area index L. At a height of 3 m, $P_{gap}(\theta)$ is nearly identical at all observed angles θ using both methods (Fig. 2.4), with a maximum difference of 6.5%. For all other heights, the differences do not exceed 10.6% (data not shown for the sake of clarity). In general, differences

may be caused by occasionally falling below the minimum distance from the sensors to the leaves, as defined in Lang (1986); LI-COR (1992, App. F). This is much more likely while measuring within tree crowns than below the canopy. However, both methods follow the same pattern of increasing $P_{gap}(\theta)$ with increasing height above the ground h and decreasing $P_{gap}(\theta)$ with increasing view zenith angle θ. DCP shows a more consistent picture of the height and angular dependence. The standard error of LAI-2000 is smaller than that of DCP because each LAI-2000 measurement integrates over a larger azimuthal angle range (see section 2.3.6). The close agreement of both methods substantiates the handling of bad readings as described in section 2.3.1. LAI-2000 $P_{gap}(\theta)$ calculated with the standard software, excluding all readings with $P_{gap}(\theta) > 1$, leads to up to 29.2% lower gap probabilities and never reaches values larger than 0.72, even at the highest height. The outer rings of the LAI-2000 sensor head are reported to be significant sources of error due to contamination by scattered light (Kobayashi et al., 2013; Comeau et al., 2006; Stenberg et al., 1994; Comeau et al., 1998; LI-COR, 1992) leading to an artificially higher P_{gap}. Compared with DCP, which is not subject to contamination, this effect was not observed in this study. In fact, LAI-2000 $P_{gap}(\theta)$ is rather lower than DCP $P_{gap}(\theta)$. Hence, to infer an effective leaf area index L_e and leaf area index L using the LAI-2000 method, all rings are considered in this work.

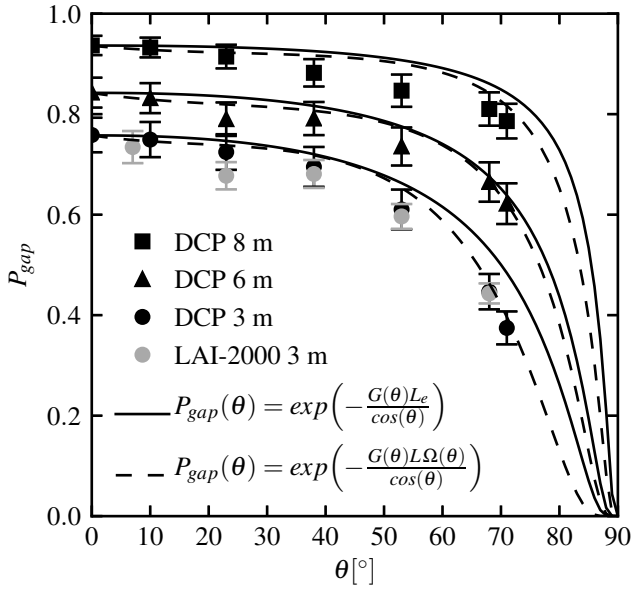

Figure 2.4: Dependency of gap probability P_{gap} on zenith view angle θ. Black symbols: DCP method at a height of 3, 6 and 8 m. Grey symbols: LAI-2000 method at a height of 3 m (6 and 8 m heights not shown). Solid lines: Beer's law with effective leaf area index L_e. Dashed lines: Beer's law with angular dependent leaf clumping $\Omega(\theta)$ of Fig. 2.6

Beer's law calculates effective leaf area index L_e and leaf area index L from $P_{gap}(\theta)$

observations (Eq. (2.1)). When the clumping index $\Omega(\theta)$ is incorporated in the calculation, the influence of non-homogeneous leaf distributions can be considered (Nilson, 1971) in DCP. Beer's law is plotted in Fig. 2.4, with the effective leaf area index L_e omitting the non-homogeneous leaf distribution and with a fit to the angular dependent clumping index $\Omega(\theta)$ in Fig. 2.6 (see section 2.3.4). When angularly dependent leaf clumping is taken into consideration, the angular dependence of Beer's law is improved, as it closely follows the measured angularly dependent gap probability $P_{gap}(\theta)$. Hence, the derivation of L from $P_{gap}(\theta)$ is improved, in particular for higher view zenith angles θ. This is of great importance for DCP when observations of leaf angle α are missing and L is derived from $P_{gap}(\theta = 57.3°)$ (see section 2.3.3). Clumping is taken into consideration in the calculation of L from $P_{gap}(\theta)$ in the further analysis shown in section 2.3.4.

2.3.3 Leaf projection function

The calculation of leaf area index L from gap probability $P_{gap}(\theta)$ requires information on the leaf projection function $G(\theta)$ and, therefore, on leaf inclination angle distribution $f(\alpha)$ (Eq. 2.1 and 2.2). To incorporate the empirical distribution of leaf angles into $G(\theta)$ calculations, a non-parametric kernel smooth (Härdle and Müller, 1997), considered to be the best approximation of the empirical distribution, and the two-parameter Beta-distribution of section 2.2.1 are used. The distributions are normalized to unity and plotted over $\alpha/90°$ in Fig. 2.5a. Both distributions lead to similar leaf projection functions $G(\theta)$ with comparable, narrow uncertainty bands (Fig. 2.5b). Hence, the beta distribution is considered appropriate for the *Q. suber* stand, concurring with results from Wang et al. (2007), and is used for the entire treatment due to lower computational expenses.

The majority of the leaves of the *Q. suber* trees are tilted at angles between 30° and 75° (Fig. 2.5a). Only a small amount of leaves is horizontally aligned, which is typical for trees adapted to high incoming radiation. Hence, the derived leaf projection function $G(\theta)$ shows very little change with view zenith angle and is 0.5 at 57.3° (Fig. 2.5b), according to theory (Pisek et al., 2011; Wit, 1965). Therefore, the influence on the transformation from gap probability $P_{gap}(\theta)$ to leaf area index L is nearly equal for all view zenith angles θ analyzed in this study. Additionally, $G(\theta)$ varies only slightly (0.05 on average for all angles) among the observation heights. This may be different in dense canopies, where a strong decrease in light intensity occurs, which would make height-dependent leaf angle distribution measurements essential to correctly estimate L. However, the need for leaf inclination angle information can generally be avoided for a single L estimation by choosing $\theta = 57.3°$ for observations of P_{gap} so that $G(\theta) = 0.5$ and is independent of $f(\alpha)$ (Macfarlane et al., 2007c).

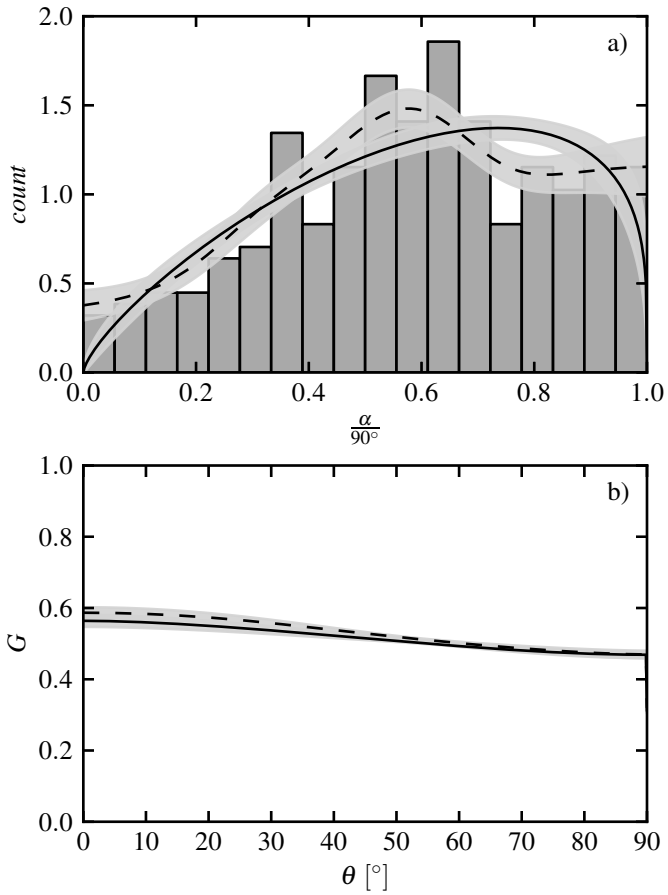

Figure 2.5: a) Empirical leaf inclination angle α distribution (bars, n= 281), non-parametric kernel smooth distribution function (dashed line), two-parameter Beta-distribution (solid line) at a height of 3 m. The abscissa displays angle of the leaf normal to zenith: 0 = horizontal aligned leaves, 1 = vertical aligned leaves. b) Leaf projection function $G(\theta)$ over view zenith angle θ derived from kernel smooth (dashed line) and Beta-distribution (solid line). Uncertainty bands present standard error.

2.3.4 Clumping index

The angular dependency of leaf clumping index $\Omega(\theta)$ is usually determined with the TRAC instrument based on gap size distribution, from digital hemispherical photographs (DHP) or inversely modeled from independent estimates of leaf area index L and effective leaf area index L_e (Ryu et al., 2010b; Leblanc et al., 2005; Leblanc, 2002; Kucharik et al., 1997; Chen and Cihlar, 1995; Chen and Black, 1992). Here, DCP is used to derive height and angularly distributed $\Omega(\theta)$ for the first time (Fig. 2.6).
$\Omega(\theta)$ decreases with increasing height above ground, theoretically, because the gaps within crowns $gt - gl$ observed by the sensor decrease and the gaps between crowns gl

increase. Theoretically, $\Omega(\theta)$ increases monotonically with increasing θ and approaches 1 at 90° because the camera's sensing pathway through the canopy approaches an infinite length and large gaps are successively decomposed into smaller ones (Haverd et al., 2012; Ryu et al., 2010b; Norman and Welles, 1983). This is only true for lower heights where the edges of the camera view angle span θ_v do not exceed the top canopy height. At upper heights, a certain amount of clear sky over the canopy top is always visible, even at low angles. Therefore, $\Omega(\theta) = 1$ is never reached.
However, observed $\Omega(\theta)$ shows a sigmoid behavior for all heights here with a decline at the mid view zenith angles at approximately 40°. This behavior, contrary to theory and model results, was observed in different studies with either TRAC or DHP methods. Leblanc et al. (2005) shows this behavior in a black spruce stand with DHP over a wide range of zenith view angles θ. Kucharik et al. (1997) observed

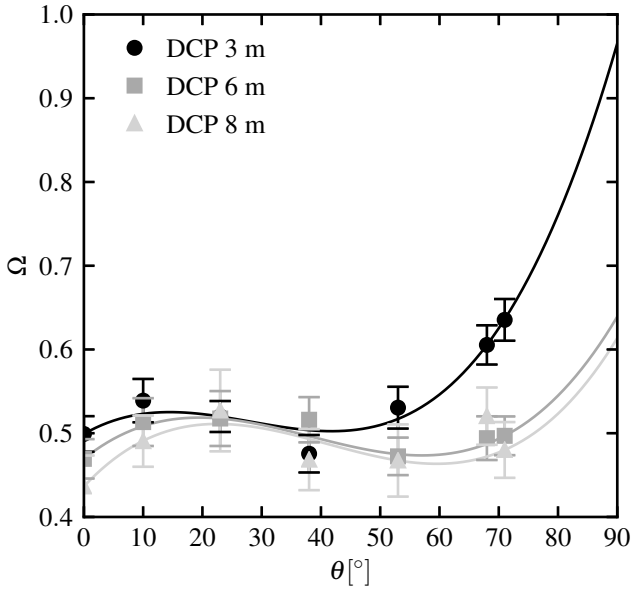

Figure 2.6: Change of clumping index Ω with zenith view angle θ at a height of 3, 6 and 8 m. Solid lines: fitted third degree polynomials.

it in an old aspen stand, and the mid view zenith decline could also be observed in a study by Ryu et al. (2010b); both studies used a TRAC system. In contrast, a study in which the angular behavior corresponds to theory is Macfarlane et al. (2007a), conducted with DHP in a eucalyptus stand. However, the monotonical increase of $\Omega(\theta)$ with θ seems to disappear with decreasing canopy density. The reasons for the sigmoid behavior are still unclear. Ryu et al. (2010b) proposed that heterogeneous ecosystem-scale tree distribution patterns cause different tree clustering at different zenith view angles θ. This could be a possible explanation here, because the western part of the experimental site is planted more densely than the eastern part (Fig. 2.1) and the *Q. suber* trees are planted in sparse tree rows along the contour lines of the sites, causing a stand-scale clumping effect.

Another possible cause for decreasing $\Omega(\theta)$ at mid view zenith angles could be the observation points that are located directly below or within a tree crown. Observations at the very center of the crown are impossible, because the trunk occupies that location. Hence, observations always take place at a certain distance to the horizontal crown center. When the instrument is tilted and faces *towards* the crown center, the path length through the crown increases with increasing θ, and thus leads to monotonically increasing $\Omega(\theta)$. If the instrument is tilted and faces *away* from the crown center, path length within the crown decreases with θ and leads to decreasing $\Omega(\theta)$ until the next adjacent tree crown interferes with the sensor's pathway. Even when the observation points are numerous, 50% of all observations below or within crowns are affected by decreasing path lengths with increasing θ, as is the canopy average. This effect should only occur when tree density is low and adjacent trees are interfering with the sensing pathway only at very high θ, such as in savannah-type ecosystems, and is also dependent on the crown shape. However, this effect should diminish with increasing height above ground, which cannot be observed here. Additionally, the clumping of leaves to shoots within crowns is not considered in DCP thus far. It may change with view zenith angle due to changing shoot angles projected to the view zenith angle, which results in different gap size distributions. This may counteract the mid view angle decline of $\Omega(\theta)$.
The influence on resulting leaf area index L remains unclear. The decreased $\Omega(\theta)$ may lead to an artificial overestimation of L or account for the shortened pathway at these particular observation positions leading to the correct L. This is of particular importance when L is inferred from $P_{gap}(\theta = 57.3°)$ because this effect occurs in the mid zenith view angles and therefore requires further study, e.g., with a radiative transfer model or investigations on the within crown gap size distribution. However, to represent the angular dependency of $\Omega(\theta)$ in Eq. (2.1) for further computations in section 2.3.2, a third degree polynomial fit is used.

2.3.5 Cumulative leaf area index height distribution

The effective leaf area index $\sum L_e$ is calculated from $\overline{P_{gap}}$ (with non-homogeneous leaf distribution omitted) for both methods and from $\theta = 53°$, taking into consideration the leaf projection function $G(\theta) = 0.5$ for DCP. The cumulative leaf area index $\sum L$ distribution (Fig. 2.7b) of LAI-2000 is calculated by $\overline{\ln(P_{gap})}$-averaging of the standard software introducing an apparent leaf clumping index (see section 2.2.1), whereas the cumulative DCP $\sum L$ distribution is calculated under explicit consideration of leaf clumping (Eq. (2.11) and section 2.3.4).
Both methods show very similar cumulative $\sum L_e$ height distributions and comparable uncertainties (Fig. 2.7a) as a result of well matching P_{gap} observations (Fig. 2.4). However, the distribution of total canopy leaf area index $\sum L$ shows considerable differences among both methods. Only the estimate by DCP (Fig. 2.7b) matches very well with direct litter trap based measurements of the same period with $\sum L$ of 1.15 to 1.05 m^2_{leaf}/m^2_{ground} (e Silva et al., 2015), and it is comparable to other savannah-type ecosystems (Ryu et al., 2010b; Pereira et al., 2007; Kim et al., 2006). At a height

of 3 meters, LAI-2000 L is 32% lower than DCP and underestimates $\sum L$ strongly compared to the litter trap measurements. This difference decreases with increasing height above the ground. Ryu et al. (2010a) showed that the apparent clumping of LAI-2000 overestimates $\Omega(\theta)$, leading to lower L, which can be confirmed in this study. Thus, with an independent estimation of clumping, LAI-2000 cannot be used to estimate L in this open canopy. Additionally, the decreasing difference between LAI-2000 and DCP with height above ground indicates a decrease in apparent clumping of LAI-2000 with decreasing canopy cover, proving the model results from Ryu et al. (2010a). This trend changes according to the order of canopy cover, and cannot be correlated to actual clumping.

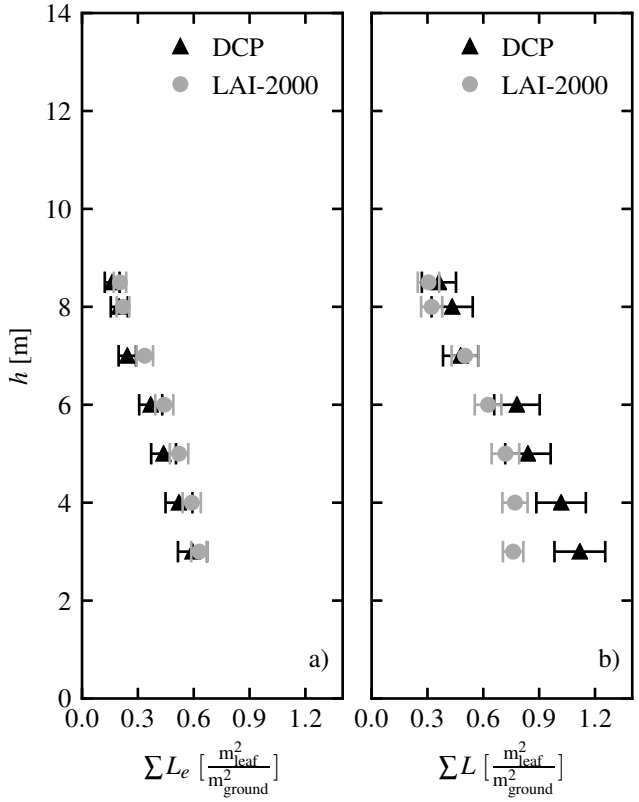

Figure 2.7: a) height distribution of cumulative effective leaf area index $\sum L_e$ for LAI-2000 and DCP derived from $P_{gap}(53°)$. b) same for cumulative leaf area index $\sum L$.

2.3.6 Influence of the view angle span on DCP results

The view angle span θ_v of the camera determines the amount of angular integration present in each image. Hence, the larger the θ_v, the smaller the standard error of the mean gap probability $\sigma_{\overline{P_{gap}}}$ and leaf area index $\sigma_{\overline{L}}$, as shown in Fig. 2.8b,d. The

standard error for the LAI-2000 device is generally smaller than for DCP, because each LAI-2000 measurement integrates over a 180° azimuth angle compared to a 53° to 6.625° angle (maximum sensor width to smallest image crop) in DCP.
However, the mean gap probability $\overline{P_{gap}}$ itself shows no change according to view angle span θ_v (Fig. 2.8a), illustrating the robustness of DCP to different image sizes. Nevertheless, the larger the θ_v, the larger the bias due to taking one leaf projection function $G(\theta)$ and $\cos(\theta)$ value for the whole image, leading to differences in the resulting mean leaf area index $\overline{L}$ (Fig. 2.8c), according to θ_v. Here, this bias is comparably small because $G(\theta)$ is rather flat (see Fig. 2.5). When $G(\theta)$ is strongly bent, e.g., with planophile leaves, the bias will be larger. Hence, the image needs to be cropped to an optimal size, minimizing the higher bias encountered with large image sizes and the higher uncertainty encountered with smaller image sizes. Throughout the rest of this study, $\overline{P_{gap}}$ and $\overline{L}$ values with $\theta_v = 10.25°$ are used to make comparisons with the LAI-2000 ring span.

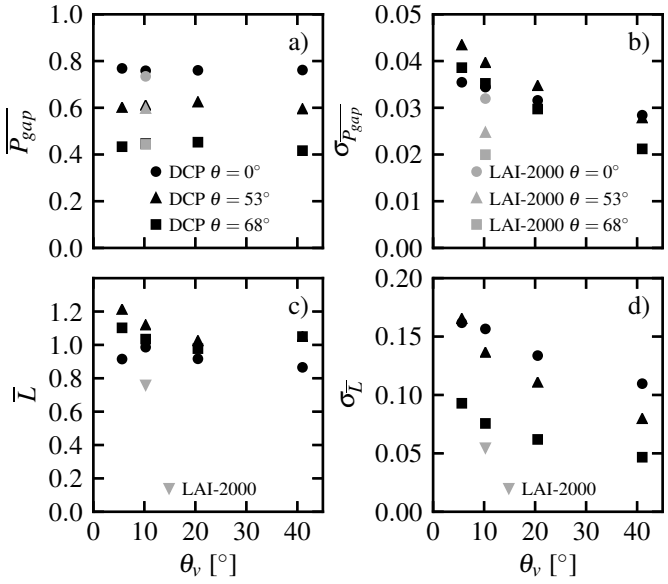

Figure 2.8: a, b) change of mean gap probability $\overline{P_{gap}}$ and standard error $\sigma_{\overline{P_{gap}}}$ with view angle span θ_v. c, d) change of mean leaf area index $\overline{L}$ and standard error $\sigma_{\overline{L}}$ with view angle span θ_v. All plots display observations at zenith view angles of 0°, 53°, 68° and at 3 m height above the ground for LAI-2000 and DCP.

Theoretically, observations of DCP gap probability $P_{gap}(\theta)$ at a certain height should lead to the same leaf area index L, independent from the chosen view zenith angle θ. However, average differences of 10.5% occurred with varying θ (Fig. 2.8c), most likely due to an insufficient estimation of the angular dependency of clumping index $\Omega(\theta)$ mentioned in section 2.3.4. According to Eq. 2.11, errors in $\Omega(\theta)$ or in the leaf projection function $G(\theta)$ linearly propagate to L. However, uncertainties associated

with $G(\theta)$ are comparably small (Fig. 2.5) with respect to uncertainties in $\Omega(\theta)$.

2.3.7 Exclusion of woody tissue

By excluding woody tissue, such as trunk and branch area in each image (see Sec. 2.2.4), the influence on gap probability P_{gap} and leaf area index L is quantified. The relative bias of not excluding the trunks and branches on gap probability $\varepsilon P_{gap}(\theta)$ is rather small and ranges up to -2.2%. The relative bias on the leaf area index εL is stronger, ranging from 3.1% to 20.9%. However, for angles and heights used here, the relative bias is on average 6.9%. An overview of the relative bias depending on view zenith angle is listed in Tab. 2.1. $\varepsilon P_{gap}(\theta)$ decreases with decreasing zenith view angle θ and with increasing height above the ground h because the amount of trunk area in the sensor view field is decreasing. In contrast, no height dependent behavior is evident for εL because woody tissue either occluded gaps between crowns or within crowns. Hence, the exclusion of woody tissue raises or diminishes the clumping index $\Omega(\theta)$ with no clear height dependency and superposes the influence of $\varepsilon P_{gap}(\theta)$ on εL. Throughout the entire treatment, $P_{gap}(\theta)$ and L values corrected for the influence of woody tissue are used. The woody tissue bias presented here can be understood as a

Table 2.1: Relative bias of gap probability P_{gap} and leaf area index L when woody tissue is not excluded. h = height above ground, $\varepsilon P_{gap}(\theta)$ = relative bias of gap probability at 0°, 53° and 71° view zenith angle, εL = relative bias of leaf area index L derived from $P_{gap}(53°)$.

h [m]	$\varepsilon P_{gap}(0°)$ [%]	$\varepsilon P_{gap}(53°)$ [%]	$\varepsilon P_{gap}(71°)$ [%]	εL [%]
8.5	0	−0.3	−0.4	8.5
8	−0.1	−0.4	−0.7	7.2
7	−0.4	−0.6	−0.8	7.6
6	−0.5	−0.6	−0.8	4.7
5	−0.5	−1.2	−1.2	8.0
4	−0.9	−1.0	−2.2	6.2
3	−0.6	−1.1	−2.2	5.8

"best-case" estimation because the classification algorithm is designed to rather fail at the detection of woody tissue than wrongly classifying leaves as woody tissue, to avoid an overestimation of the bias.
The whole image analysis process is fully automated by using object-based image analysis software to detect the number of pixels in all gaps gl automatically by object attributes. This avoids time consuming manual treatments, as required in previous studies (e.g. Ryu et al., 2010b; Macfarlane et al., 2007c,b) and contributes to a more standardized and less labor intensive processing of DCP images suitable for long term observations. Additionally, detection based on objects is less sensitive to thresholds

because the mean of the pixels contained in an object is used for classification, rather than using each pixel value separately. Furthermore, detection based on objects offers many more factors, such as geometry and neighborhood, to classify images than just pixel based approaches. Finally, the influence of woody tissue on gap probability $P_{gap}(\theta)$ and leaf area index L can be quantified even in evergreen canopies where no leafless period occurs, thus overcoming one of the disadvantages of indirect L estimation methods (e.g. Macfarlane et al., 2007c; Coops et al., 2004; Kucharik et al., 1998; Whitford et al., 1995).

However, the set-up of the algorithm and the adjustment of the thresholds, especially for the detection of woody tissue (see sec. 2.2.4), are site-specific and challenging. They require expert knowledge in object-based image analysis and to our knowledge, currently no open-source software is available for this purpose. Additionally, the presented algorithm is computationally expensive when compared to common image processing software. Furthermore, it would be desirable to improve the algorithm with more transferable thresholds, allowing for a fast application in different ecosystems.

2.3.8 Auxiliary data derived height distributions

Estimating vertical leaf area index L distributions in tall canopies is challenging because observations at different heights throughout the entire canopy are often not feasible. Therefore, an approach demanding only ground-based observations is tested here. In Fig. 2.9a, the height distribution of leaf area index L derived from the observed crown top height h_t, crown bottom height h_b, crown radius r_c, and bottom leaf area index L at a height of 3 m is shown for each crown model (see Section 2.2.4). The shape as well as the height of maximum L varies according to the model chosen. The higher the center of gravity of the crown model, the higher is the maximum L location in the crown. The integrated, cumulative $\sum L$ distributions are plotted in Fig. 2.9b together with the measured cumulative $\sum L$ height distribution of DCP. The ground-based crown model estimates fit very well with the distributions observed ($R^2_e = 0.96$, $R^2_{e\,9/10} = 0.95$, $R^2_t = 0.91$), even when each crown model assumes a uniform leaf density distribution with height, which is rather unlikely at the site in Portugal. The ellipsoidal and triangular crown model $S_e(h)$ and $S_t(h)$ are considered as to be the most extreme assumptions on the natural crown shape. However, they do not significantly exceed the observation's uncertainties. The relative error of the model-based distribution to the observed distribution is 3% for the ellipsoidal and asymmetric ellipsoidal crown model and 16% for the triangular crown model. Hence, if an appropriate crown model is chosen, it has a minor influence on the resulting distribution compared to other sources of error, such as the influence of woody tissue or neglecting leaf clumping. The assessment of L height distributions via ground-based observations of crown parameters and a single, ground-based L observation is feasible and a great opportunity for application in tall canopies where height-dependent gap probability P_{gap} observations are challenging.

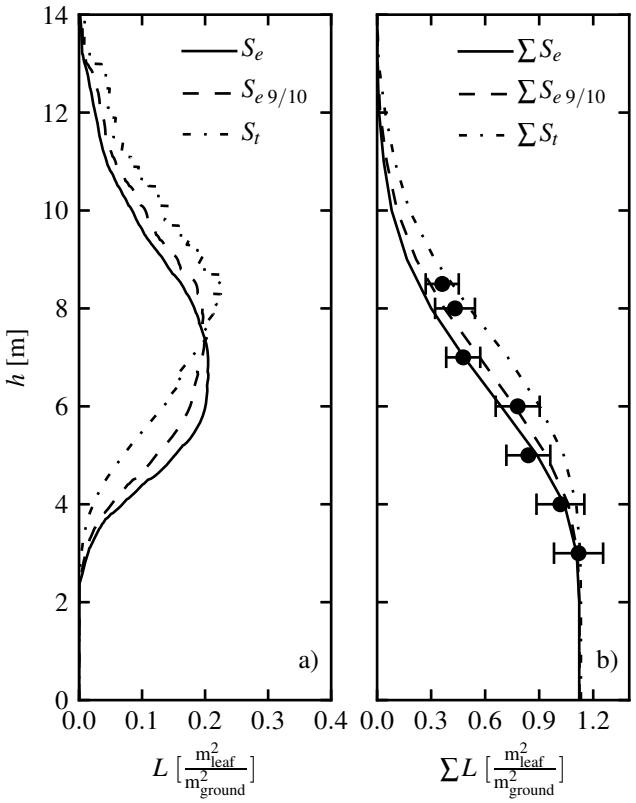

Figure 2.9: a) height distribution of leaf area index L estimated with the ellipsoidal (S_e, solid line), asymmetric ellipsoidal ($S_{e\,9/10}$, dashed line) and triangular (S_t, dotted-dashed line) crown model from crown parameters and leaf area index L derived from $P_{gap}(53°)$ at 3 m height. b) height distribution of cumulative leaf area index $\sum L$. Dots: measured cumulative height distribution with DCP. Lines: estimated cumulative height distribution by integration of S_e, $S_{e\,9/10}$ and S_t from a).

2.4 Conclusion

In this study, we employed vertically and angularly distributed gap probability P_{gap} observations and derived vertical leaf area index L and effective leaf area index L_e distributions for LAI-2000 and digital cover photography DCP in an open *Q. suber* forest. Additionally, we estimated vertical L distributions with ground-based observations of crown parameters and a single ground-based L observation.

We observed the following results: (1) Height and angularly dependent digital cover photography (DCP) was successfully applied here for the first time. It delivers gap probability $P_{gap}(\theta)$ and effective leaf area index L_e that is very similar to the established LAI-2000. (2) Height and angularly dependent leaf clumping index Ω was successfully determined with DCP and is mandatory for deriving a correct leaf area index L from gap probability $P_{gap}(\theta)$ at any view zenith angle θ. (3) The

effect of leaf clumping index Ω on the total leaf area index L yields a 30% higher L compared to L approximated from LAI-2000 observations. This difference decreases with increasing height above the ground. (4) The exclusion of woody tissue from DCP by object-based image analysis yielded on average a 6.9% lower leaf area index L values. This is a 'best case' approximation because the algorithm is designed to not overestimate the effect. (5) When clumping index Ω is included and woody tissue is excluded from DCP, L of DCP matched precisely with direct measurements using litter traps. (6) When LAI-2000 is used in open canopies, we recommend a treatment of the bad readings to avoid strong biases on gap probability P_{gap}, effective leaf area index L_e and leaf area index L due to small variations in light intensities. (7) When height dependent observations are not feasible, ground-based observations of crown parameters can be used to derive reasonable leaf area index L height distributions from a single, ground-based L observation.
For an efficient estimation of leaf area index height profiles of a forest canopy we recommend the following steps:

- Use below canopy digital cover photography DCP at a view zenith angle $\theta = 57.3°$ because no information on leaf projection function $G(\theta)$ is needed.
- Exclude woody tissue from the images with object-based image analysis.
- Infer total leaf area index L of the canopy explicitly, including leaf clumping $\Omega(\theta)$.
- Use a digital hypsometer to measure crown top height h_t, crown bottom height h_b, and crown radius r_c from the ground.
- Use the crown parameters and a suitable crown model to extrapolate total leaf area index L along heights above the ground.

3 Drought impact on carbon and water cycling during the extreme drought event in 2012

3.1 Introduction

One of the typical semi-arid ecosystem in Europe is a savannah-type woodland (*montado*), consisting of a sparse overstorey tree layer and a herbaceous understorey layer. During the biomass peak of the herbaceous plants in spring, the understorey layer can provide a large contribution to the whole ecosystem water and carbon balance and thus, can play a significant role in the annual carbon and water budgets (Unger et al., 2009; Paco et al., 2009; Dubbert et al., 2014c). However, each layer responds differently to changes in precipitation depending on their life form (chamaephyte or therophyte) and access to different water reservoirs throughout the year (Paco et al., 2009) including deep soil or ground water (David et al., 2004).
Montado ecosystems (span.: *dehesa*) cover an area of about 1.5 million ha in Europe (Bugalho et al., 2011) and contribute together with savannah-type ecosystems on other continents about 30 % to global gross primary productivity GPP (Beer et al., 2010; Grace et al., 2006). The major driving factor of GPP in *montado* ecosystems is water (Vargas et al., 2013; Pereira et al., 2007; David et al., 2004), since annual precipitation patterns show periodical summer droughts and evapotranspiration losses are high (Krishnan et al., 2012; Huxman et al., 2005).
In the recent past, precipitation shows a significant decrease of rain amount in February and March as well as a decrease of total annual rainfall on the Iberian Peninsula (Guerreiro et al., 2013; García-Barrón et al., 2013; Mourato et al., 2010; Paredes et al., 2006). A trend towards extreme events in the form of droughts is observed due to a more heterogeneous distribution of precipitation throughout the year (García-Barrón et al., 2013). These type of changes in precipitation regime have been reported to strongly affect local water balance (Rodrigues et al., 2011; Vaz et al., 2010; Grant et al., 2010) and carbon sink strength (Pérez-Ramos et al., 2013; Pereira et al., 2007; Granier et al., 2007; Ciais et al., 2005) of ecosystems in semi-arid regions and are expected to increase with proceeding climate change (Bussotti et al., 2013; Guerreiro et al., 2013).
Species in semi-arid environments have developed vast structural and functional adaptations to regulate carbon assimilation and respiratory water loss (e.g. Tenhunen et al., 1987; Werner et al., 1999). Considerable knowledge has been acquired on leaf-

level physiological processes in the last three decades (e.g. Beyschlag et al., 1986; Sala and Tenhunen, 1996; Tenhunen et al., 1985, 1990; Werner et al., 2001), emphasizing the role of ecophysiological adaptations to seasonality and summer drought in Mediterranean climate conditions. In these environments lack of precipitation often interacts with excessive irradiance and high temperature further constraining leaf carbon fixation through photoinhibition during drought (Werner et al., 2001, 2002). Cork oaks strongly reduce transpirational water loss by stomatal closure in response to drought to avoid a critical level of dehydration and hydraulic failure (Oliveira et al., 1992; Tenhunen et al., 1984, 1987; Werner and Correia, 1996; Kurz-Besson et al., 2006).

To investigate the influence of drought on carbon sink strength at the ecosystem level, combined stomatal conductance-photosynthesis models can be used in order to disentangle regulatory processes from effects of micro-climatic variations. Different descriptions of the underlying processes exist in the literature, though. For example, stomatal conductance can be modelled either reacting to relative humidity (Ball et al., 1987) or to vapour pressure deficit (Leuning, 1995). Also the determination of parameters in individual descriptions is different among different authors. The sensitivity of stomatal conductance to vapor pressure, for example, is often taken as a fixed value while determining only the other parameters in the coupled stomatal conductance-photosynthesis model time-variant, although the sensitivities of stomatal conductance to photosynthesis and to vapour pressure are highly correlated. Recent studies could consequently demonstrate that changes of one single parameter, e.g. only maximum carboxylation rate or only stomatal conductance sensitivity, does not explain drought-induced reductions in both GPP and T simultaneously (Egea et al., 2011; Reichstein et al., 2003; Zhou et al., 2013). Further, different temperature dependencies of e.g. maximum carboxylation or electron transport rate have been proposed (Medlyn et al., 2002; von Caemmerer, 2000; June et al., 2004).

In the present study, we report on drought effects on a Portuguese *montado* ecosystem using the unique opportunity of two consecutive years of very contrasting hydrological conditions. 2011 being a wet year with regular drought pattern occurring in summer, and 2012 being an extremely dry year with strongly reduced precipitation amount. Particularly, 2012 showed a severe additional winter/spring drought characteristic for precipitation pattern changes in recent past on the Iberian Peninsula (2nd driest year since 1950, Costa et al., 2012; Santos et al., 2013; Trigo et al., 2013). This study is focussing on: (1) quantifying the effects of drought on the local ecosystem water balance, overstorey and understorey GPP, as well as differences in net ecosystem carbon exchange NEE between both years. (2) Identifying physiological responses in the drought year 2012 of the *Q. suber* trees using a combined photosynthesis-stomatal conductance model and testing the model performance with different process descriptions.

3.2 Material and methods

3.2.1 Site description

The study was conducted at the savannah-type flux observation site "PT-Cor" (Fig. 3.1) of the European Integrated Carbon Observation System (ICOS) ca. 100 [km] north-east of Lisbon, Portugal (latitude: 39°8′20.7″ N, longitude: 8°20′3.0″ W, altitude: 162 [m a.s.l.]). The site is planted with evergreen *Quercus suber* (L.) trees of 209 individuals $[\mathrm{ha}^{-1}]$ on a Luvisol soil (Jongen et al., 2011). The tree canopy has a leaf area index LAI of 1.05 ± 0.07 $\left[\mathrm{m}^2_{\mathrm{leaf}}\,\mathrm{m}^{-2}_{\mathrm{ground}}\right]$, a midday gap probability $P_{\mathrm{gap}}(0)$ of 0.76 ± 0.03 and an average tree canopy height of 9.7 [m] (Piayda et al., 2015). The *Q. suber* trees likely have deep soil water and ground water access. Native annual grasses and herbs build the understorey vegetation (Jongen et al., 2013b; Dubbert et al., 2014b), which emerges after the first rains in autumn, has a peak stand height in spring (March–April) and becomes senescent at the beginning of the summer period (late May) with a maximum LAI of 0.70 ± 0.05 $\left[\mathrm{m}^2_{\mathrm{leaf}}\,\mathrm{m}^{-2}_{\mathrm{ground}}\right]$. The understorey vegetation density and LAI are spatially highly variable due to the heterogeneous topography and hence, differences in soil moisture regime. The whole region is under forest management.

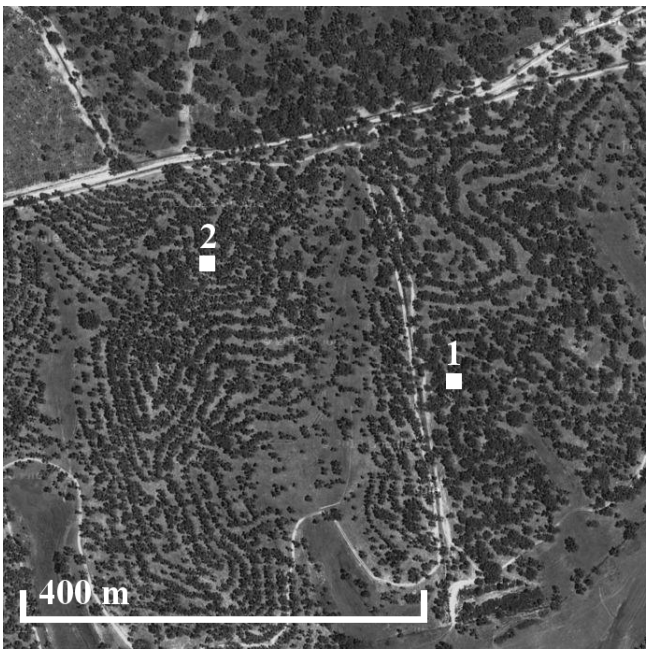

Figure 3.1: Satellite image of the study site (©Google Maps, 2013). 1: position of the overstorey tower. 2: position of the understorey tower.

3.2.2 Climate conditions

The site is characterised by a Mediterranean climate with moist and mild winters and dry and hot summers. The long term mean annual temperature is about 15.9 °C and the annual sum of precipitation is about 680 [mm] (Jongen et al., 2013b), with a characteristic annual pattern of high winter precipitation (November to January) and summer drought during June to September (Paredes et al., 2006). The relevance of the winter precipitation for the Portuguese hydrological cycle can be easily explained by the prevailing Mediterranean-type climate that concentrates most of precipitation during the winter half of the year, with little to no precipitation in summer. Hence, the following data treatment is based on the hydrological year beginning with first autumn precipitation (October to September).

Overstorey eddy covariance measurements

The overstorey tower (Fig. 3.1, point 1) is set up with a Gill R3A-50 ultrasonic anemometer (Gill Instruments Ltd., Lymington, UK) in combination with a LI-7000 closed path CO_2/H_2O analyzer (LI-COR, Lincoln, USA). The inlet tube has a length of 8.5 [m], is attached to one of the anemometer arms and operated with an average flow rate of ca. 8 [$L\,min^{-1}$]. The reference cell is flushed with N_2. The measurement height is about 23.5 [m] above ground. Data is continuously acquired and processed live on a field laptop with the eddy covariance data acquisition and processing software package EddyMeas (meteotools, Jena, Germany; Kolle and Rebmann, 2007). At a height of 20 [m] above ground, two up- and downward facing LI-190 Quantum sensors (LI-COR, Lincoln, USA) and a NR-LITE net radiometer (Kipp and Zonen, Delft, the Netherlands) are attached. A radiation shielded HMP 155 probe measures air temperature T_a and relative humidity rH (Vaisala, Helsinki, Finland). Precipitation P is measured with an ARG100 aerodynamic rain gauge (Environmental Measurements Ltd., North Shields, UK) at the tower top. The meteorological parameters are logged on a CR10X datalogger (Campbell Scientific, Logan, USA).

Understorey eddy covariance measurements

The understorey tower was located about 286 [m] north-west of the overstorey tower (Fig. 3.1, point 2). It was equipped with a Gill R3-50 ultrasonic anemometer (Gill Instruments Ltd., Lymington, UK) in combination with a LI-7500A open path CO_2/H_2O analyzer (LI-COR, Lincoln, USA). The gas analyzer was tilted 45° from the vertical and the sensor separation was about 30 [cm]. The measurement height of both sensors was 3.15 [m] above ground. EddyMeas was used for data acquisition here as well.
At 2 [m] height above ground, two PAR LITE quantum sensors facing up- and downward were attached to a CNR1 net radiometer (Kipp and Zonen, Delft, the Netherlands). Air temperature T_a and relative humidity rH were measured with a HMP 155 probe covered by a radiation shield and atmospheric pressure p was

measured with a PTB 110 barometer at 1.5 [m] above ground (Vaisala, Helsinki, Finland). The meteorological parameters were logged on a CR1000 datalogger (Campbell Scientific, Logan, USA).
A third eddy covariance system consisting of an Gill R3-50 ultrasonic anemometer in combination with a LI-7500A open path CO_2/H_2O analyzer was used to test comparability of over- and understorey tower systems. For a period of one week each it was mounted on the overstorey and the understorey tower and measured in parallel. Both systems showed high Bravais–Pearson correlation coefficients of 0.78 to 0.91 as well as small normalized root mean squared errors of 0.01 to 0.06 for water and carbon fluxes in comparison with the portable eddy system.

Soil temperature and moisture

Soil temperature T_s and soil moisture θ were measured at open and tree-shaded locations between the two towers. T_s was measured with PT100 PRT temperature probes (Campbell Scientific, Logan, USA) in 2, 4, 8, 16, 30, and 60 [cm] depth, with two replicates at the open and two replicates at the shaded location. θ was measured with 10hs sensors (Decagon Devices, Inc., Washington, USA) at 5, 15, 30 and 60 [cm] depth, with four replicates at the open and four replicates at the shaded location. The meteorological parameters were logged on CR1000 dataloggers (Campbell Scientific, Logan, USA).

Data treatment

Eddy flux data were post-processed using EddySoft and Python 2.7. Half-hourly means were calculated by block-averaging the 20 [Hz] data, time lags between CO_2/H_2O signals and vertical wind velocity were determined via cross correlation analysis following Aubinet et al. (1999). Whenever the cross correlation failed for the closed path analyzer signals of the overstorey tower, the dependency on rH was used to determine the lag for the H_2O signal according to Ibrom et al. (2007). High frequency losses were compensated with the use of inductances derived from co-spectral analysis (Eugster and Senn, 1995). The sectorial planar fit method was used for the coordinate rotation of wind vectors (Rebmann et al., 2012; Wilczak et al., 2001). For both towers, the moisture and cross wind correction according to Schotanus et al. (1983) was applied and the WPL correction for flux density fluctuations was used for the CO_2/H_2O signals of the open path understorey sensor only (Leuning, 2007; Webb et al., 1980). The storage term of CO_2 was calculated after Hollinger et al. (1994) and added to the turbulent CO_2 flux.
For the purpose of quality control, flags were determined for every half-hourly flux value including the following tests: the 20 [Hz] data were scanned for exceeded physical limits, change rates and variances. The stationary test of Foken and Wichura (1996) was applied to the high frequency data based upon a 50 % deviation criterion. On a half-hourly basis, the integral turbulence characteristics (ITC) were calculated following Thomas and Foken (2002) with a 30 % deviation criterion. For the un-

derstorey tower, the parametrisation of the ITC was recalculated according to the observations. A spike detection routine was used on the half-hourly data based on the absolute median deviation (Papale et al., 2006). All quality control tests were summed up in a simplified flag system referring to Mauder and Foken (2011).
The partitioning of the net CO_2 fluxes NEE into gross primary productivity GPP and ecosystem respiration R_{eco} followed Lasslop et al. (2010) and the flux gap-filling was made according to Reichstein et al. (2005). Gaps were only filled up to a maximum gap length of 6 days.
The measured wind speed was used to calculate aerodynamic conductance $g_a = u_*^2/u$ with the measured friction velocity u_*^2 and horizontal wind speed u. Leaf temperature is estimated using measured air temperature T_a and measured sensible heat flux H via $T_l = T_a + H/(g_a \rho_a c_p)$ with ρ_a being the density and c_p the heat capacity of the air.
T_{s} and θ were integrated over the respective depths and the replicates of each site (open and shaded) are averaged. To calculate ecosystem representative T_{s} and θ, the open and the shaded site were weighted using time-dependent P_{gap}, modelled from the daily course of sun inclination angle and the view zenith angle distribution of P_{gap} (Piayda et al., 2015).
The soil heat flux G was calculated from the averaged T_{s} profiles. To estimate the energy balance closure of the towers, the storage terms due to changes in T_{a} and rH were added to the energy balance equation and plotted against the turbulent energy fluxes for daytime values with global radiation $R_{\mathrm{g}} > 20\,[\mathrm{W\,m^{-2}}]$ (Mauder et al., 2013; Foken, 2008; Twine et al., 2000). The ratio was used to correct sensible heat H, latent heat λE and evapotranspiration ET flux with the bowen ratio being preserved.

Photosynthesis and stomatal conductance modelling

The Farquhar model for photosynthesis (Farquhar et al., 1980) combined with the Leuning model for stomatal conductance (Leuning, 1995) was used in a two-leaf scheme to model gross primary productivity and evapotranspiration $\mathrm{GPP_o}$ and $\mathrm{ET_o}$ measured at the overstorey tower for the summer months May to September of 2011 and 2012. The separation into sunlit and shaded leaves follows De Pury and Farquhar (1997) and could directly derived by measured leaf projection function and LAI from (Piayda et al., 2015). For model comparison, stomatal conductance was modelled as well with the approach of Ball et al. (1987). The model was fitted to a 31 day long moving window of $\mathrm{GPP_o}$ and $\mathrm{ET_o}$ to gain stable median daily cycles. These were cropped to the time from sunrise to 15:00. Model fitting was done using a Nelder–Mead simplex algorithm (Nelder and Mead, 1965) with a higher order multi objective cost function for $\mathrm{GPP_o}$ and $\mathrm{ET_o}$ according to Duckstein (1981) under varying apparent maximum carboxylation rate $V_{\mathrm{c,max}}$ (no separate modelling of mesophyll conductance), assimilation sensitivity m, vapour pressure deficit sensitivity D_0 of stomatal conductance g_{s} and optimum temperature T_{opt} of maximum electron transport rate J_{max}. Three different T_{opt} descriptions were used for model comparison.

The uncertainty of inferred parameters was estimated using bootstrap. See Appendix B.2 for detailed model equations.

3.3 Results and discussion

Ecosystem fluxes for the hydrological years 2011 and 2012 (October 2010 to September 2012) are discussed in the following. Flux time series are only compared when data availability is given for both hydrological years, but not on an annual sum basis. The dominant wind direction changes during the season. Absolute values of flux measurements of the overstorey tower are thus not directly comparable to the absolute values of the understorey tower due to changing footprint area and the heterogeneity of the ecosystem. However, comparisons of the intra-annual pattern of ecosystem fluxes between both towers and inter-annual changes between both years 2011 and 2012 are possible and conducted in the following.

3.3.1 Meteorological and environmental conditions

Water scarcity is the most important factor for ecosystem productivity in savannah-type ecosystems (Pereira et al., 2007). Drought severity and impact on vegetation depends on timing and amount of precipitation P (Peñuelas et al., 2004). The hydrological years 2011 and 2012 mark, therefore, exceptional years on the Iberian Peninsula. Precipitation P was 34 % higher in 2011 and 39 % lower in 2012 compared to the long term average precipitation of about 680 [mm] (Jongen et al., 2013a) (Fig. 3.2a and b). In particular, the winter 2011/2012 was very dry over Soutwestern Iberia, with only about 20 % of the long term precipitation (Santos et al., 2013; Trigo et al., 2013). 2012 was the second driest year since 1950. The last negative P anomaly of comparable severity occurred in the drought year 2004/2005 (Paredes et al., 2006; Santos et al., 2007).
The intra-annual pattern of precipitation has especially changed in 2012. Total annual reduction to the previous year 2011 was 495 [mm] of which 68 % occurred during a long drought event in winter and early spring (December–March). The beginning of autumn precipitation was also delayed by almost a month in 2012. Winter precipitation is the most important for replenishing the soil and ground water reservoirs after the summer drought. But the winter precipitation period was shortened and interrupted for about four months in the hydrological year 2012. These phenomena, i.e. reduced annual P, additional winter/spring drought, and prolonged summer drought, are characteristic for observed P extremes in the last decades (e.g. Guerreiro et al., 2013; Paredes et al., 2006).
We address first the question of changes in environmental and climatic components between both years, which may have caused significant changes in ecosystem functioning. The distributions of most relevant climatic and environmental variables for plant functioning are therefore analysed in quantile-quantile (Q-Q) plots in Fig. 3.3. Air temperature T_a (Fig. 3.3a) and incoming photosynthetically active radiation

PAR (data not shown) showed only minor changes between the two years so that plant available energy in both years was comparably high. In contrast, moisture related variables showed large deviations from the on-to-one line in the Q-Q plots (Fig. 3.3b–d). All precipitation P intensities of 2012 stayed well below the ones in 2011 (Fig. 3.3b). Air vapour pressure deficit vpd was considerably increased at high deficits in 2012 compared to 2011 (Fig. 3.3c). This comes from lower absolute humidity because air temperature T_a did not change substantially. Possible reasons are either diminished local ecosystem evopotranspiration ET due to diminished soil moisture (Fig. 3.3d) and plant transpiration or less air moisture input by incoming air masses from the ocean. Soil moisture was significantly decreased in 2012 compared to 2011 (Fig. 3.3d), which is exhibited especially in the missing medium soil moisture amounts. The contribution of local ET to the observed reduction in vpd was estimated by approximating the average contribution of local ET to absolute humidity of the atmospheric boundary layer. 50 % of absolute humidity reduction in 2012 compared to 2011 could be explained by a reduced contribution of local ET. This illustrates the strong influence of ET on local hydrological conditions and the reinforcement of plant drought stress due to increased vpd.
The ecosystem, therefore, faced increased transpirational demand from higher atmospheric vpd combined with strongly decreased soil water availability, which resulted in high water stress for the trees but also for understorey vegetation in 2012 compared to 2011. In the following, the effect of decreased water availability on the ecosystem water budget is discussed.

3.3.2 Drought influence on ecosystem water balance

Evapotranspiration ET is the major component of total water efflux in Mediterranean ecosystems on annual basis (Huxman et al., 2005). A comparably small amount of precipitation is left for ground water recharge and runoff. ET usually peaks in May before the onset of drought in the beginning of June in Mediterranean ecosystems (Vargas et al., 2013). But ecosystem evapotranspiration measured here at the overstorey tower ET_o (Fig. 3.4b) peaked within the summer drought period in June to July in 2011. This behaviour is typical for *montado* ecosystems with ground water access of the trees (Paco et al., 2009; Pereira et al., 2007; David et al., 2007, 2004). ET_o showed a slight peak shift towards spring in 2012 and was diminished by 26 % compared to 2011. The major decrease occurred in late spring and summer (March to September) although the major reduction in precipitation P occurred in winter and early spring (December to March) (Fig. 3.2b). When atmospheric demand (Fig. 3.4a) and energy input into the system increased in spring 2012, the *Q. suber* trees were not able to maintain transpiration T as high as in 2011. This indicates, that most likely the deep soil and/or ground water reservoirs were not refilled after summer 2011 due to the dry winter as displayed by soil moisture observations in 60 [cm] depth (Fig. 3.5b). However, the strongly diminished transpiration T led to a non-significant increase in maximum daily leaf temperature $T_{l,max}$ of only 1.7 °C during the summer period of 2012. The small influence of the reduced transpirational

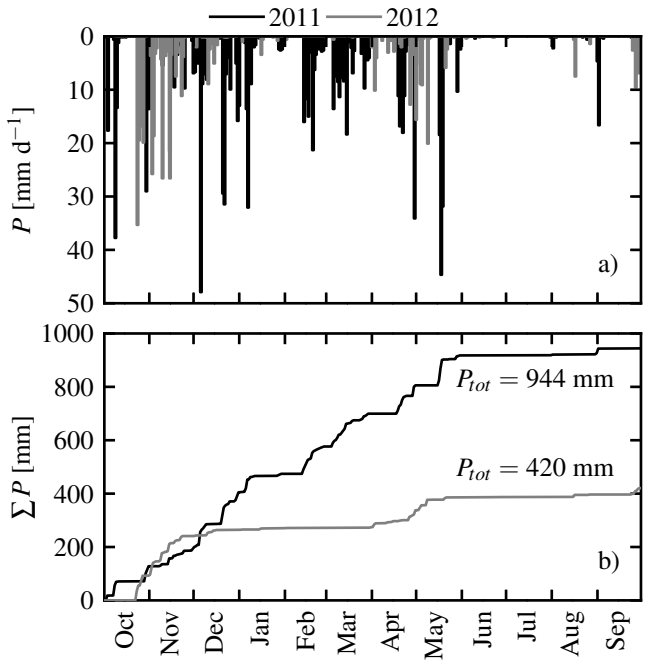

Figure 3.2: a) Daily sum of precipitation P for 2011 (black) and 2012 (grey). b) Cumulative precipitation P for 2011 (black) and 2012 (grey) based on half hourly data.

cooling on leaf temperature could be attributed to the high aerodynamic conductance g_a in this open canopy, enabling a comparably high energy transport by sensible heat.

Evapotranspiration measured at the understorey tower ET_u peaked in March to April 2011 before the beginning of the summer die back of the understorey vegetation, which is rather typical in savannah-type ecosystems (e.g. Paco et al., 2009). ET_o was reduced, though, by 38 % in 2012 compared to 2011. The peak was slightly delayed under drought conditions in 2012, in contrast to ecosystem ET_o. The late onset of autumn precipitation P in October and additionally the missing recharge of upper soil moisture in winter (Fig. 3.5a) had an immediate impact on ET_u inhibiting plant growth and herbaceous transpiration (see Sect. 3.3.3). ET_o, on the other hand, was influenced from March onwards only. The precipitation events occurring in April and March 2012 (Fig. 3.2a) were not able to increase ET_u up to the level of 2011 even though the atmospheric demand was slightly higher in 2012 (Fig. 3.3c). This can be explained on the one hand by very low soil moistures up to 20 [cm] depth in October and from March onwards (Fig. 3.5a), which prevented soil evaporation, and on the other hand, by the strong reduction in plant cover leading to a reduced contribution of herbaceous plant transpiration to ET_u (see Sect. 3.3.3).

Precipitation effectiveness ET_o/P indicates the amount of total precipitation P used for actual ecosystem evapotranspiration ET_o. $ET_o/P = 86\,\%$ in 2011, which

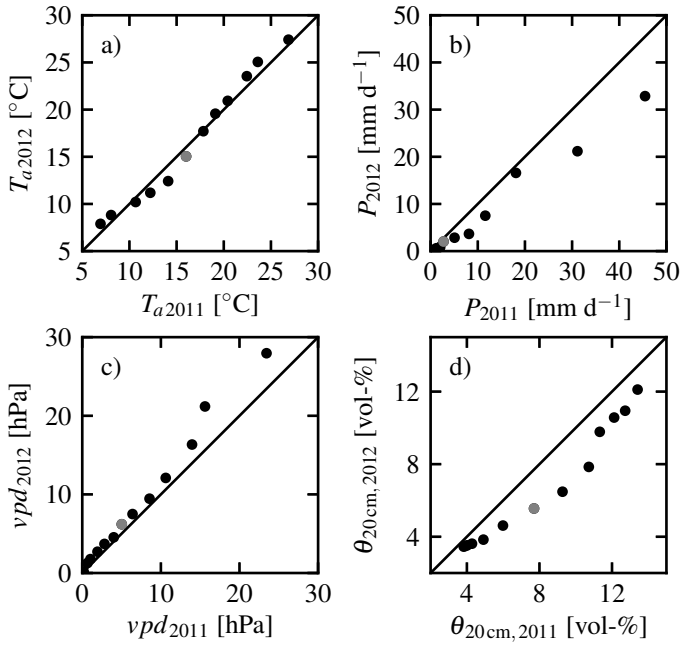

Figure 3.3: Quantile-Quantile plot of important climate and environmental parameters for the years 2011 and 2012 based on daily averages. Black dots represent the 0.01, 0.05, 0.1, 0.2, 0.3, 0.4, 0.6, 0.7, 0.8, 0.9, 0.95, and 0.99 quantiles of the respective distribution. Grey dots represent the 0.5 quantile. a) Air temperature T_a, b) precipitation P, and c) vapour pressure deficit of the air vpd, each measured at 20 [m] height above ground. d) Soil moisture in the first 20 [cm] $\theta_{20\,\mathrm{cm}}$ (root zone of understorey vegetation).

is high but comparable to other studies (Sala and Tenhunen, 1996; Piñol et al., 1991). However, the strong reduction of ecosystem evapotranspiration $\mathrm{ET_o}$ of 26 % in 2012 was vastly exceeded by the reduction in precipitation P of 54 %. This confirms recent results from Besson et al. (2014) showing a certain resilience of *Q. suber* tree transpiration to annual water shortages. This led to $\mathrm{ET_o}/P$ of 122 % in 2012, which is to our knowledge, the highest value reported for *montado* ecosystems so far. Hence more water evaporated from the soil and was transpired by the trees than was brought into the ecosystem by precipitation. This was possible due to the deep soil or ground water access of the trees maintaining a relatively high transpiration rate throughout the summer. But it left also no water for ground water replenishment or runoff generation (cf. Sala and Tenhunen, 1996).

Ecosytem productivity was markedly changed in 2012 due to the strong alterations in the water balance, which will be discussed in the following.

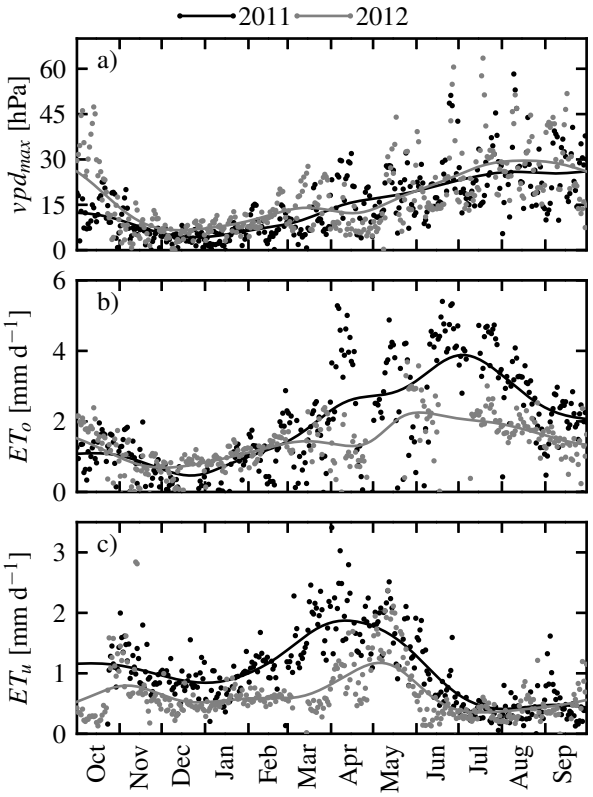

Figure 3.4: a) Maximum daily vapour pressure deficit vpd_{max}, b) daily sum of ecosystem evapotranspiration ET_o and c) daily sum of understorey transpiration + soil evaporation ET_u for 2011 (black) and 2012 (grey). Lines mark kernel regressions.

3.3.3 Understorey growth inhibition

The local understorey vegetation consists of native annual grasses and herbs (Jongen et al., 2013b; Dubbert et al., 2014b). The species are adapted to regular summer droughts by seed formation in spring before the onset of the summer droughts. They survive the dry periods as seeds and germinate again at the onset of autumn precipitation. Species abundance during spring depends thus on the amount of previous winter precipitation (Figueroa and Davy, 1991). The timing of the first autumn rains and rewetting of the soils is thereby of great importance for germination success, number of individuals and plant productivity (Jongen et al., 2013c; de Dios Miranda et al., 2009).

The understorey showed a typical annual cycle of gross primary productivity GPP_u in 2011 (Fig. 3.6c) for savannah-type understorey vegetation with the growth onset at the end of October (Ma et al., 2007). Carbon uptake peaked in February to March and ended with the complete die back at the end of May. GPP_u was strongly reduced by 53 % in 2012 compared to 2011. A small GPP_u peak occurred along with

precipitation P in April and May (Fig. 3.2). The reduction of GPP_u can be explained by the very low soil moisture $\theta_{20\,cm}$ during October 2011 (Fig. 3.5a) due to the late onset of autumn precipitation P inhibiting seed germination. $\theta_{20\,cm}$ was lower during the entire year 2012 in comparison to 2011, particularly over the main growth period of the understorey vegetation from January to April. It was up to 52 % lower in March 2012, inhibiting further growth during winter/spring and probably caused higher seedling mortality. Dubbert et al. (2014b) reported a maximum understorey vegetation cover in this ecosystem of about 80 % for 2011 that was reduced to about 25 % during the same period in 2012 (data for 2012 not shown). Similar effects on seedling germination and mortality were shown by others (Peco and Espigares, 1994; Espigares and Peco, 1995, 1993) under artificial rainfall treatments and could be shown here under natural conditions.

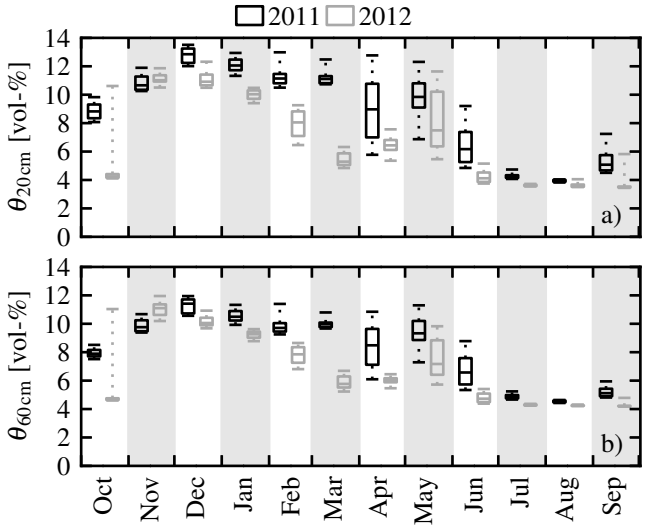

Figure 3.5: Box plot of monthly volumetric soil moisture a) down to 20 [cm] depth $\theta_{20\,cm}$ (root zone of understorey vegetation) and b) down to 60 [cm] depth $\theta_{60\,cm}$ for the years 2011 (black) and 2012 (grey). Central line marks the median, box marks the 0.25 and 0.75 quantiles. Dashed lines mark the 0.05 and 0.95 quantiles. Data within a two day interval after a rain event were excluded.

3.3.4 Ecosystem productivity reduction

Most European, Mediterranean savannah-like ecosystems show a severe drop in gross primary productivity during summer (June to August) framed by a major peak in early spring (April to May) and a minor peak at the onset of autumn rain (Baldocchi et al., 2009).

In our ecosystem, gross primary productivity measured at the overstorey tower GPP_o showed an in this respect atypical annual behaviour with a very late peak during

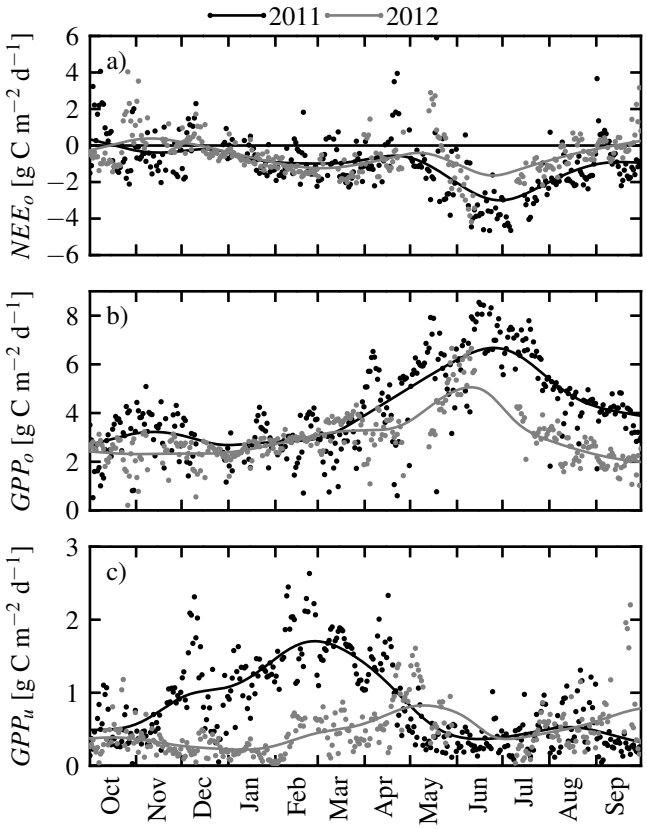

Figure 3.6: a) Ecosystem net carbon exchange NEE_o, b) ecosystem gross primary productivity GPP_o, c) understorey gross primary productivity GPP_u for 2011 (black) and 2012 (grey). Dots mark daily sums, lines are kernel regressions.

June–July (Fig. 3.6b). The amount of carbon gained was also higher compared to other Mediterranean evergreen woodlands in particular during the drought period in summer (Baldocchi et al., 2009; Ma et al., 2007). This annual pattern is rather characteristic for temperate than semi-arid ecosystems. The *Q. suber* trees must have deep soil water or ground water access in "regular" hydrological years, as shown in Sect. 3.3.2. This enabled them to maintain high productivity during the summer period despite high atmospheric water demand and low topsoil soil moisture.

Gross primary productivity GPP_o showed almost the same seasonal timing in 2012 compared to 2011 but was strongly reduced by 28 % (Fig. 3.6b). The major reduction took place in spring and summer (April to September) together with the reduction in evapotranspiration ET_o (Fig. 3.4b) when atmospheric demand was high and the emptied deep soil and ground water reservoirs were unable to supply sufficient water (see Sect. 3.3.2) in 2012 compared to a regular year. This confirms the results of Pereira et al. (2007) who showed that drought effects on sclerophyllous trees became apparent only after the depletion of the deep soil and ground water reserves. Despite

a delayed bud burst in spring, a significant difference in leaf area index LAI could not be observed during the summer period by long-term leaf area index observations of e Silva et al. (2015). Reductions in GPP_o and ET_o can hence be attributed solely to leaf physiological responses discussed in Sect. 3.3.6.

3.3.5 Net ecosystem carbon exchange reduction

The net ecosystem carbon flux NEE_o was strongly reduced by 38 % in the drought year 2012 compared to the wet year 2011 (Fig. 3.6a). The ecosystem was, however, a carbon sink in both years on annual basis even though reductions in precipitation P (Fig. 3.2) and gross primary productivity GPP_o (Fig. 3.6b) were severe in 2012. Pereira et al. (2007) found a similar behaviour in another montado ecosystems in Portugal. It still demonstrates here once more that precipitation is the dominant environmental variable for inter-annual change of NEE in semi-arid ecosystems even in ecosystems with ground water access. The reduction in carbon sink strength took place mainly in summer (May to September) along with the strongest reduction in gross primary productivity GPP_o (Fig. 3.6b) caused by the lack of water availability for the *Q. suber* trees (cf. Sect. 3.3.2). GPP_o exhibited a reduction of 28 % in 2012 compared to 2011 while R_{eco} showed only a reduction of 16 %. R_{eco} is mainly reduced in summer (July to September, data not shown) where soil moisture in the upper soil layer $\theta_{20\,cm}$ is low in both years due to the regular summer drought (Fig. 3.5a) and inter-annual differences are small. NEE_o is therefore much more driven by GPP_o than by R_{eco} in the ecosystem studied here. Reichstein et al. (2002) hypothesized that gross primary productivity GPP_o should be less affected by drought than ecosystem respiration R_{eco} in ecosystems with large subsoil water reservoirs because R_{eco} depends on soil moisture and soil temperature. But it is hot and dry almost every summer in the Mediterranean so that the lack of soil moisture in the upper soil inhibits soil respiration during summer and reduces largely the contribution of R_{eco} to inter-annual variations (e.g. Unger et al., 2009). This could also be the reason for the controversial findings of Valentini et al. (2000) that R_{eco} becomes less important for variations of NEE with decreasing latitude on the Northern Hemisphere. It is, however, clear that vastly different GPP_o and R_{eco} cannot be sustained over long time; R_{eco} base rates have to adapt in the long-term.

3.3.6 Drought impact on tree physiology

Multiple physiological mechanisms of plant responses to drought, excessive irradiance and high temperatures have been recognized on the leaf-level such as reduction of exposed leaf area or leaf shedding (Beyschlag et al., 1986; Sala and Tenhunen, 1996; Tenhunen et al., 1985, 1990; Werner et al., 2001). To avoid hydraulic failure or photodamage, carboxylation efficiency $V_{c,max}$ and/or stomatal conductance g_s can be down-regulated restricting water loss and carbon assimilation and hence increasing photorespiration as a protective electron sink (Farquhar and Sharkey, 1982; Cowan, 1977; Tenhunen et al., 1987; Matthews and Boyer, 1984; Ehleringer and Cook, 1984).

The photosynthesis apparatus can further adapt to altered environmental conditions by changing the rigidity of the membranes altering thus the temperature optimum of, for example, electron transport rates (Kattge and Knorr, 2007; von Caemmerer, 2000; Berry and Björkman, 1980).
There are different levels of complexity on how to describe photosynthesis in the literature. We focus here on Farquhar-type models of photosynthesis (Farquhar et al., 1980). There are three mechanisms that differ strongly between the different models of vegetation-atmosphere exchange: (1) the reactions to soil water stress, (2) the formulations used for the description of stomatal conductance and (3) the reactions to heat stress. How plants react to water stress is probably the least well-described mechanism in photosynthesis models. The different ecosystem and land surface models differ strongly on how they react to soil water stress. The widely used community land model CLM, for example, reduces apparent carboxylation efficiency $V_{\mathrm{c,max}}$ under drought (Oleson et al., 2010), which then indirectly reduces stomatal conductance as well, while the land surface scheme ORCHIDEE down-regulates stomatal conductance directly leaving $V_{\mathrm{c,max}}$ unchanged (Krinner et al., 2005; Verbeeck et al., 2011).
There is also a great variety of descriptions of stomatal conductance (cf. Damour et al., 2010). Most large-scale models apply the formulation of Ball et al. (1987) though, the so called Ball–Berry or sometimes Ball–Woodrow–Berry model (cf. Eq. B.18). Leuning (1995) argued that stomata under controlled conditions react to vapour pressure deficit rather then relative humidity and proposed and alternate form of the Ball–Berry model (cf. Eq. B.17), the so-called Leuning model or sometimes Ball–Berry–Leuning formulation. But the photosynthesis models also differ in their reactions to heat stress. It is still discussed in the physiological literature if heat is only changing thylakoid membrane properties limiting electron transport (von Caemmerer, 2000; June et al., 2004) or if heat is also inhibiting enzyme activities, i.e. also carboxylation rates (Medlyn et al., 2002; Kattge and Knorr, 2007).
Gross primary productivity $\mathrm{GPP_o}$ and evapotranspiration $\mathrm{ET_o}$ were modelled here for the period May to September to investigate drought impact on *Q. suber* tree physiology on the ecosystem scale and further test different model formulations described above. Differences between both years were most prominent during May to September, understorey vegetation had already vanished and soil evaporation was low compared to tree transpiration (Fig. 3.4c).
The following discussion includes (1) whether a down-regulation of only carboxylation efficiency $V_{\mathrm{c,max}}$ or only stomatal sensitivity m is sufficient to describe the ecosystem behaviour in both years. (2) It evaluates the performance of the two prominent stomatal conductance formulations. (3) It compares different representations of photosynthetic temperature dependencies. (4) It discusses possible reasons for down-regulation of stomatal conductance g_{s} and carboxlation $V_{\mathrm{c,max}}$, (5) disentangling the causes for down-regulation of stomatal conductance g_{s}. (6) The unexpected change in optimal temperature T_{opt} between the two years is discussed.
First, $\mathrm{GPP_o}$ and $\mathrm{ET_o}$ were modelled with either allowing the model to adapt each day only $V_{\mathrm{c,max}}$ or only the slope m of the Ball–Berry stomatal conductance formulation

(Ball et al., 1987) (Eq. B.211). The model was not able to reproduce the observations with sufficient performance in both cases, especially in 2012. The goodness of fit to the observed data steadily decreased with ongoing summer drought. GPP_o and ET_o could be successfully modelled if both, $V_{c,max}$ and m were allowed to adapt daily to changing environmental conditions, leading to constantly high Nash–Sutcliffe model efficiencies of $\overline{\varepsilon_{GPP_o}} = 0.81$ and $\overline{\varepsilon_{ET_o}} = 0.89$ for 2011 and $\overline{\varepsilon_{GPP_o}} = 0.80$ and $\overline{\varepsilon_{ET_o}} = 0.76$ for 2012.
Second, the same model calibration experiment was performed with the Leuning model of stomatal conductance (Leuning, 1995) (Eq. B.17). The Leuning model has, however, an additional model parameter D_0 which describes the sensitivity of the stomata to changes in vapour pressure deficit vpd. The Leuning model showed comparable high model performances to the Ball–Berry model in both years. When the Leuning model was used in earlier studies (e.g. Wang and Leuning, 1998), D_0 was fixed to a constant value. This implies that stomatal conductance sensitivity to vpd needs to change always similar to the sensitivity to assimilation. Model performance decreased considerably if D_0 was fixed here. This is because m and D_0 are highly correlated in the Leuning model (cf. Fig. 3.7b and d). This strict coupling is likely incorrect here since daily maximum vpd during the summer drought period was not significantly different between both years (only 1.3 [hPa] increase on average) but a strong decrease in $V_{c,max}$ could be observed (see below). Consequently, a decrease in model performance occurred, when D_0 was set constant. Enabling the *Q. suber* trees to regulate stomatal response to vpd and assimilation A separately was necessary to explain observed GPP_o and ET_o.
The two first points illustrate that the plants needed to regulate their potency of possible carbon assimilation but wanted to increase how swift stomata react to changes. The reduction in maximum carboxylation rate $V_{c,max}$, though, was about 43 % while the increase in the slope m was about 9 % or 29 % whether calculation followed Ball et al. (1987) or Leuning (1995), respectively. The increase in m is not significant when the bootstrapped uncertainty is considered. Still, a significant, overall decrease in stomatal conductance g_s of about 37 % was observed.
Third, the temperature dependency of photosynthetic activity has generally been attributed to two different processes in previous publications. Medlyn et al. (2002) and Kattge and Knorr (2007) described the temperature dependency of both, maximum carboxylation rate $V_{c,max}$ of the Rubisco enzyme and maximum electron transport rate J_{max} by a peaked function, according to Johnson et al. (1942) (Eq. B.13). An increase in enzyme activity with temperature is followed by a decrease above an optimum temperature T_{opt} due to enzyme deactivation (Case 1). Von Caemmerer (2000), among others, attributed possible decrease of activity of the photosynthetic apparatus at high temperatures rather to thylakoid membrane properties only, limiting electron transport, thus changing with leaf temperature. So only J_{max} is down-regulated above an optimum temperature T_{opt} (Eq. B.13), but $V_{c,max}$ increases monotonically with a typical Arrhenius-type function (Eq. B.12, Case 2). This was simplified by June et al. (2004) using a gaussian temperature dependency instead of the original formulation (Eq. B.15, Case 3). Here all cases showed comparable

model performances and no apparent differences in GPP_o and ET_o could be noticed. Thus, neither Case 1 nor Case 2 could be falsified here. Case 1 to case 3, however, show a decreasing demand for parametrization (Case 1: 6, Case 2: 4, and Case 3: 3 parameters). Despite the entropy factors of carboxylation ΔS_V and electron transport ΔS_J (Case 1 and Case 2) and optimum temperature T_{opt} (Case 3), all parameters were fixed to literature values (Table B.1). Case 3, although containing only one parameter for optimization like Case 2, showed a more robust computational performance with fastest optimization by the Nelder–Mead algorithm (Nelder and Mead, 1965) among all cases.

Fourth, multiple reasons for down-regulation of photosynthesis under drought conditions are known, ranging from damage of involved enzymes due to high leaf temperatures, inhibition of the photosynthetic apparatus to avoid excess energy in the leaves, to insufficient availability of nitrogen inside the leaves (Tenhunen et al., 1987; Werner et al., 1999). But protection of the photosynthetic apparatus during environmental stress comes at the cost of reduced carbon sequestration (Tenhunen et al., 1990; Werner et al., 1999; Werner and Correia, 1996). Excessive radiation and high temperatures provide the risk of photoinhibition and photodamage under reduced CO_2 supply due to stomatal closure and low water potentials (Werner et al., 2002). Stomatal conductance g_s was strongly reduced by 37 % in 2012 compared to 2011 (Fig. 3.7f) although differences in daily maximum vpd during the summer drought period were not significant (only 1.3 [hPa] increase on average) between both years (Fig. 3.4a). It is thus very likely that the trees suffered from depleted deep soil or groundwater reservoirs due to the missing recharge by winter precipitation, since upper soil water content values were comparable during summer (Fig. 3.5a and b). This is an evidence that plant water status of *Q. suber* trees is strongly influenced by access to groundwater here and a down-regulation of transpiration occurred to avoid hydraulic failure (David et al., 2007; Oliveira et al., 1992). Although transpirational cooling of leaves should have been reduced due to limited stomatal conductance, the daily maximum leaf temperature $T_{l,max}$ increased by only 1.7 °C in 2012 compared to 2011 (Sect. 3.3.2) so that a temperature-based damage of enzymes relevant for photosynthesis is unlikely. The CO_2 influx into the leaves was, however, heavily reduced under the drought conditions in 2012. Energy utilization is thus limited while incoming photosynthetically active radiation PAR in 2012 was comparably high to 2011 (see Sect. 3.3.1). It is therefore very likely that the main cause for the *Q. suber* trees to down-regulate maximum carboxylation rate $V_{c,max}$ by 43 % (Fig. 3.7a) was to avoid over-excitation and photodamage (Demmig-Adams and Adams, 1992; Long et al., 1994; Werner et al., 2002). However, this effect may have been enforced by a decreased nitrogen availability during the leaf development phase in late spring caused by reduced soil water, and thus nitrogen solubility in 2012 (Fig. 3.5a and b) potentially changing leaf nitrogen status and permanently reducing photosynthetic capacity in 2012 compared to 2011 (Vaz et al., 2010). A possible indication for a permanent reduction of $V_{c,max}$ is that g_s tends to converge to the same value at the end of the drought period in both years (Fig. 3.7f) so that leaf internal CO_2 availability should have approached comparable values as well. $V_{c,max}$ remained,

however, down-regulated permanently. A simultaneous reduction of $V_{c,max}$ by 37 % (Fig. 3.7a) and an increase of m (9 % or 29 % whether g_s was calculated following Ball et al. (1987) or Leuning (1995), Fig. 3.7b and c) was observed. In case of a drought spell like 2012, the *Q. suber* trees responded with both, stomatal limitation as well as down-regulation of assimilation strongly altering entire ecosystem functioning, which was observed in different semi-arid ecosystems before (Reichstein et al., 2003; Egea et al., 2011; Zhou et al., 2013).
Fifth, the use of the Leuning (1995) model with variable D_0 allowed to disentangle the different impacts on g_s. Intra-annually, stomatal conductance showed a much stronger sensitivity to vpd (Fig. 3.7d) than to variations in assimilation (Fig. 3.7e). Between both years, $m/(1 + (\overline{\text{vpd}}/D_0))$ increased only slightly by 10 % as a consequence of a slightly stronger reduction in $V_{c,max}$ than in g_s (43 % and 37 %, respectively). This displays the strong resilience of sclerophyllous tree species like *Q. suber* to drought, maintaining a water use efficiency comparable to regular years (Zhou et al., 2013). The impact of vpd on g_s was, however, weakened in 2012 (reduction of D_0 by 37 %, not significant) since g_s was generally reduced at comparable vpd. m compensated fluctuations in D_0 (Fig. 3.7b and d) to yield the observed robustness to assimilation. The observed high intra-annual robustness indicates that these Mediterranean species are adapted to maintain a stable operational point (Werner and Máguas, 2010).
Sixth, all three model descriptions (Case 1–3) showed a decrease in the optimum temperature of photosynthesis T_{opt} by 4–8 °C from 2011 to 2012 (Fig. 3.7g). Leaf renewal in 2012 occurred under strong drought conditions due to the additional winter drought and under increased temperatures due to the bud burst occurring more than one month later than in 2011 (e Silva et al., 2015). So carbon uptake in 2012 was further weakened due to a higher susceptibility of the photosynthesis apparatus to high temperatures in addition to the already discussed reduction of carboxylation efficiency $V_{c,max}$ by 43 %. Kattge and Knorr (2007) and von Caemmerer (2000), among others, showed for different plant species the opposite trend of increasing T_{opt} with increasing growth temperature. A possible explanation is that not only growth temperature but also nutrient availability and plant water status have changed strongly here affecting thylakoid membrane properties more than growth temperature.
In summary, the *Q. suber* trees responded to the drought year 2012 with a down-regulation of carboxylation efficiency and a decreased optimal temperature of photosynthesis. They counteracted this reduced carbon sequestration with a better responsiveness of the stomata. These plant responses were caused neither by a higher vapour pressure deficit nor by leaf temperatures nor by a depletion of upper soil moisture. But they were most probably triggered by a strong depletion of deep soil or ground water due to the additional winter drought.
The combined model of photosynthesis and stomatal conductance was unable to reproduce the observed carbon assimilation and evapotranspiration if only one reaction was considered, i.e. either in the photosynthetic apparatus or in stomatal conductance. It needed to adapt parameters in both sub-modules, i.e. a strong reduction in carboxylation efficiency and a smaller increase in stomatal sensitivity. Earlier model-data approaches had shown that combined photosynthesis-stomatal

conductance models need to adapt both parts in times of drought but they always predicted decreases in carboxylation efficiency and stomatal sensitivity. However, the modelling performed here could not distinguish between different model formulations found in the literature, i.e. the stomatal conductance formulations of Ball–Berry vs. Leuning and the different formulations of optimal photosynthetic temperatures.

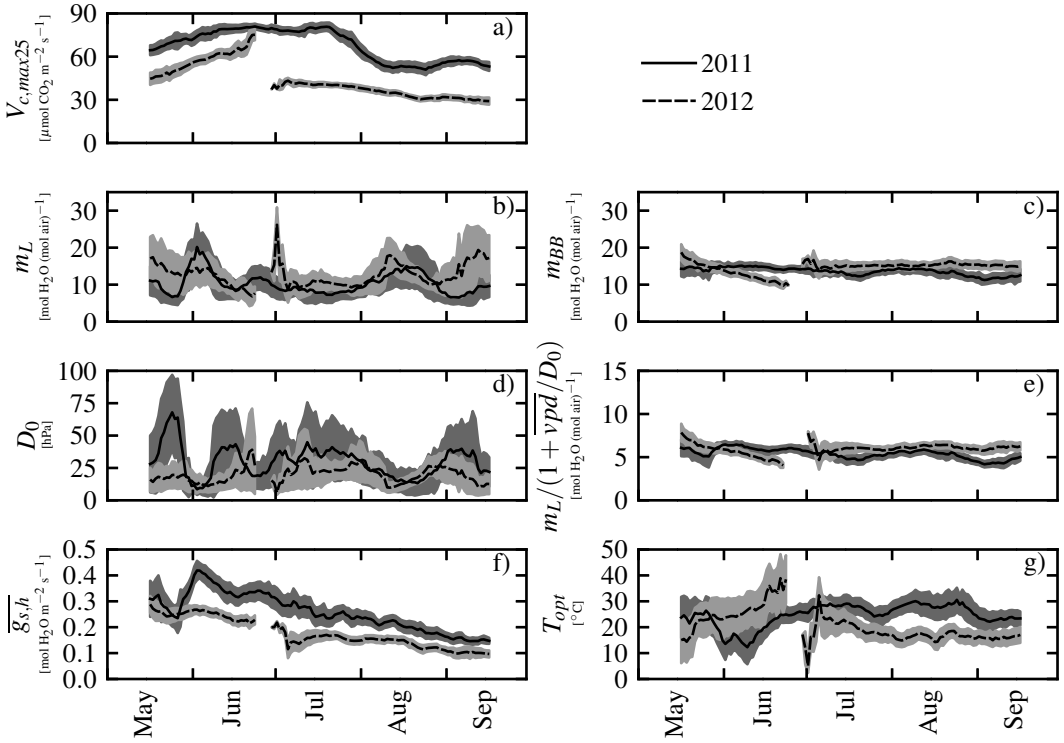

Figure 3.7: Daily values for a) apparent maximum carboxylation rate at 25 °C $V_{\mathrm{c,max25}}$, b) assimilation sensitivity parameter m_L of the Leuning model, c) assimilation sensitivity parameter m_{BB} of the Ball–Berry model, d) vapour pressure deficit sensitivity parameter D_0, e) fraction $m_L/(1+(\overline{\mathrm{vpd}}/D_0))$ relating assimilation A and stomatal conductance g_{s}, f) daily median stomatal conductance for water vapour $\overline{g_{\mathrm{s,h}}}$ during daytime, g) optimal temperature of electron transport T_{opt}. The model is fitted to median daily cycles of gross primary productivity $\mathrm{GPP_o}$ and evapotranspiration $\mathrm{ET_o}$ of the *Q. suber* trees in a 31 day long moving window for the summer period of 2011 (solid line, dark uncertainty band) and 2012 (dashed, light uncertainty band).

3.3.7 Future development

It is expected that the trend of decreasing total annual precipitation and alteration of precipitation patterns on the Iberian Peninsula, namely occurrences of additional

winter/spring droughts, will continue with proceeding climate change (Bussotti et al., 2013; Guerreiro et al., 2013; Hulme et al., 1999). Such severe drought periods might occur at higher frequency (Field et al., 2012; Heimann and Reichstein, 2008; Granier et al., 2007; Miranda et al., 2002) thereby affecting the ecosystem water balance and productivity (Chaves et al., 2002; Fischer et al., 2002). If precipitation patterns similar to 2012 will occur more often then a sustainable depletion of local ground water reservoirs as well as water storage basins might be expected. This will affect strongly local agriculture that relies on ground water for the deep-rooted cork-oak trees and otherwise uses irrigation water from storage basins. The soil seed bank of native understorey plants may also deplete on the long term due to a shorter life cycle and reduced seed formation (Jongen et al., 2013c; Peñuelas et al., 2002, 2004; Gordo and Sanz, 2005). A shift of species composition is likely de Dios Miranda et al. (2009) but could not be observed in this ecosystem in a study by Dubbert et al. (2014b, 2012 data not shown) during the drought year 2012 itself. However, some effects such as tree mortality may only be evident in the long term after multiple, consecutive drought years (David et al., 2004; Bussotti et al., 2013).

3.4 Conclusions

We reported on the ecosystem fluxes of a savannah-type cork oak woodland under extreme hydrological conditions and altered precipitation P pattern. We analysed the effects of drought in the year 2012 compared to the wet year 2011 on evapotranspiration and gross primary productivity of a *montado* ecosystem and its overstorey and understorey components. We additionally analyzed physiological reactions of the *Q. suber* trees.

We conclude the following results: (1) the precipitation effectiveness $\mathrm{ET_o}/P$ increased up to 122 % in the dry year 2012 possible due to the ground water access of *Q. suber* trees leaving no water for ground water replenishing and runoff generation. If trends of decreasing annual P continue, sustainable effects on local ground water reservoirs and storage basins may be expected. (2) The understorey gross primary productivity $\mathrm{GPP_u}$ and the overstorey gross primary productivity $\mathrm{GPP_o}$ were reduced by 53 % and 28 %, respectively, in 2012 compared to 2011 due to a late onset of 2011 autumn rains and an additional severe winter/spring drought. Long term changes in understorey species composition and tree productivity are likely if prolonged summer droughts and additional winter/spring droughts become more frequent. (3) A combined photosynthesis and stomatal conductance model worked best if it was able to adapt the apparent maximum carboxylation rate $V_{\mathrm{c,max}}$ and the stomatal conductance parameters simultaneously. The slope m of the stomatal conductance model had to be increased to compensate partly for the strong decrease in carboxylation rate. The model adjusted also the sensitivity of the stomata D_0 to vapour pressure deficit vpd in the Leuning model because both stomatal parameters, m and D_0 are strongly correlated. The model performance was similar to the Ball–Berry approach. (4) The combined photosynthesis and stomatal conductance model also adjusted the opti-

mum temperature of electron transport T_{opt} to lower values. This decreases carbon sequestration under higher temperatures but makes the photosynthetic apparatus also more vulnerable to heat stress in dry years. (5) The ecosystem was a carbon sink in both years with a 38 % reduced sink strength in the dry year 2012 compared to 2011. Gross primary productivity GPP was thereby a much stronger driver than ecosystem respiration R_{eco} of the inter-annual variations of the carbon sink.

4 Summary

4.1 Summary of the thesis

Chapter 2 gave a description of the employment of vertically and angularly distributed gap probability $P_{gap}(\theta)$ observations and the derivation of vertical leaf area index L and effective leaf area index L_e distributions in an open *Q. suber* forest. The performance of the new digital cover photography method (DCP) was evaluated against the established LAI-2000 method and direct litter collection. Additionally, vertical L distributions were estimated with ground-based observations of crown parameters and a single ground-based L observation.
Height and angularly dependent digital cover photography was successfully applied here for the first time. It could be shown that gap probability $P_{gap}(\theta)$ and effective leaf area index L_e delivered by DCP was very similar to the established LAI-2000. Clumping index Ω is mandatory for deriving a correct leaf area index L from gap probability P_{gap} estimates at any view zenith angle θ accounting for the heterogeneity of natural canopies. Height and angularly dependent leaf clumping index Ω was successfully determined with DCP for the first time. Thus, the effect of leaf clumping on the total leaf area index L of the *Q. suber* canopy yielded a 30% higher L compared to L approximated from LAI-2000 observations. Further, the exclusion of woody tissue from DCP images was successfully conducted here for the first time. Using object-based image analysis, the exclusion yielded on average a 6.9% lower leaf area index L and improved the indirect estimation approach compared to the uncorrected estimation. This was a 'best case' approximation of the error introduced by woody tissue because the algorithm was designed to not overestimate the effect. Consequently, when clumping was included and woody tissue was excluded from DCP, L matched precisely with direct L measurements using litter traps, exceeding the precision of the established LAI-2000 by far. Finally, when height dependent observations are not feasible, an observation strategy could been tested successfully using only ground-based observations of crown parameters to derive reasonable leaf area index L height distributions from a single, ground-based L observation.

As a result of the conducted investigations, for an efficient estimation of leaf area index height profiles of a forest canopy, the following steps were recommended:

- Use below canopy digital cover photography DCP at a view zenith angle $\theta = 57.3°$ because no information on leaf projection function $G(\theta)$ is needed.
- Exclude woody tissue from the images with object-based image analysis.

- Infer total leaf area index L of the canopy explicitly, including leaf clumping.
- Use a digital hypsometer to measure crown top height h_t, crown bottom height h_b, and crown radius r_c from the ground.
- Use the crown parameters and a suitable crown model to extrapolate total leaf area index L along heights above the ground.

Fluxes of the cork oak ecosystem under extreme hydrological conditions and altered precipitation P pattern were analyzed in Chapter 3. The effects of drought in the year 2012 compared to the wet year 2011 on evapotranspiration and gross primary productivity of overstorey and understorey components were analyzed. By using leaf area index L and angularly dependent gap probability $P_{gap}(\theta)$ of Chap. 2, modeling of physiological reactions within *Q. suber* leaves were possible.
It could be shown that the precipitation effectiveness ET/P increased up to 122% in the dry year 2012, possibly due to ground water access of *Q. suber* trees, leaving no water for ground water replenishing and runoff generation. As a consequence, understorey and overstorey gross primary productivity were reduced by 53% and 28%, respectively, in 2012 compared to 2011 due to a late onset of 2011 autumn rains and an additional severe winter/spring drought. When a combined photosynthesis and stomatal conductance model was used to describe the responses of *Q. suber* trees to drought, the best model-data fit could be achieved if the trees were able to adapt apparent maximum carboxylation rate $V_{\mathrm{c,max}}$ and stomatal conductance parameters simultaneously. The slope m of the stomatal conductance model had to be increased to compensate partly for the strong decrease in carboxylation rate. The model adjusted also the sensitivity of the stomata D_0 to vapour pressure deficit *vpd* in the Leuning model because both stomatal parameters, m and D_0 are strongly correlated. The model performance was similar to the Ball-Berry approach. Further, the optimum temperature of electron transport T_{opt} was adjusted to lower values. This decreased carbon sequestration under higher temperatures in addition to the direct drought effect but makes the photosynthetic apparatus also more vulnerable to heat stress in dry years. However, the ecosystem was a carbon sink in both years with a 38% reduced sink strength in the dry year 2012 compared to 2011. Gross primary productivity GPP was thereby a much stronger driver of inter-annual variations of carbon sink strength than ecosystem respiration R_{eco}.

4.2 WATERFLUX project contributions

The field work, measurements, data analysis and results presented in this thesis contributed in various ways to the overall outcome of the WATERFLUX research project.
The interaction between the *Q. suber* overstorey and annual understorey vegetation layers was taken into special focus in Dubbert et al. (2014b), where the effects of facilitation and competition on herbaceous yield, species distribution and carbon

uptake were analysed. Therefore, the effects of trees on microclimate and soil properties, the understorey species composition, aboveground biomass as well as water and carbon fluxes were examined from April to November 2011.
It could be shown that under tree crown cover, a significant reduction in photosynthetic active radiation of 35 mol m^2 d^{-1} and in soil temperature of 5 °C occurred. Simultaneously, species composition and abundance of functional groups became increasingly different with respect to open areas between trees from mid April onwards. During late spring drought adapted native forbs had significantly higher cover and biomass in the open area while cover and biomass of grasses and nitrogen fixing forbs was highest under the trees. Evapotranspiration and net carbon exchange decreased significantly stronger under tree crowns compared to the open area during late spring in conjunction with a faster and earlier senescence of plants under trees. This was most likely caused by interspecific competition for water between trees and herbaceous plants, despite the more favorable microclimate conditions under the trees during the onset of summer drought.
Partitioning of measured water fluxes in soil evaporation and plant transpiration is necessary to further understand the impact of understorey vegetation on ecosystem water balance. For this purpose, stable oxygen isotopes of water provide a valuable tracer. The frequently used Craig and Gordon equation was tested in the WATERFLUX project against continuous field measurements. Therefore, evaporation and its isotopic signature on bare soil plots, as well as evapotranspiration and its corresponding isotopic composition of the herbaceous layer were measured with a cavity ring-down spectrometer connected to an open soil chamber. Thus, the impact of environmental input variables to the Craig and Gordon equation could be quantified. The results in Dubbert et al. (2013) demonstrate that predicting isotopic signature of evaporation using the Craig and Gordon equation leads to good agreement with measurements given that the temperature and ^{18}O isotope profiles of the soil are thoroughly characterized. However, model results are highly sensitive to changes in temperature and isotopic concentration at the evaporative site. This markedly affected the partition results of transpiration and evaporation from the total evapotranspiration flux.
A further elaboration of these findings was conducted in Dubbert et al. (2014a), where the impact of the steady-state assumption of plant transpiration on evapotranspiration partitioning was quantified. For this purpose, the cavity ring-down spectrometer was connected to a branch chamber applied to *Q. suber* trees in order to evaluate the short-term variability of the isotopic composition of transpiration under natural conditions. Significant deviations from isotopic steady-state of transpiration could be observed throughout most of the day, even when leaf water at the evaporating sites was near isotopic steady state. High agreement was found between estimated and modeled isotopic values assuming non-steady-state enrichment of leaf water.
These methodological results could consequently be used in (Dubbert et al., 2014c) to quantify understory vegetation effects on the water balance and productivity of this ecosystem. Evapotranspiration and net ecosystem CO_2 exchange were partitioned and rain infiltration was estimated. The understory vegetation contributed importantly to

total ecosystem evapotranspiration and gross primary production with a maximum of 43 and 51%, respectively. It reached water-use efficiencies similar to the *Q. suber* trees. The understory vegetation inhibited soil evaporation and did not diminish water use efficiency during water-limited times. The understory strongly increased soil water infiltration, specifically following major rain events. Thus, beneficial understory effects are dominant and contribute to the resilience of this *montado* ecosystem.
Finally, the analysis of drought effects on ecosystem carbon and water exchange and change in leaf internal processes of *Q. suber* trees started in this thesis (Chap. 3, Piayda et al. (2014)) was accomplished with a treatment focussing on phenological responses in in the dry year 2012 (e Silva et al., 2015). Results show that annual tree diameter growth was lowered by 63% whereas leaf area index remained nearly unchanged (reduction: 9%). Still, the time of leaf renewal was shifted from mid April to end of May due to the unfavourable conditions in the preceding winter. In contrast to male flower production, fruit setting was severely depressed by water stress with a 54% decrease during the dry year. These results suggest that leaf growth and leaf area maintenance are resilient ecophysiological processes under winter drought and are a priority carbon sink for photoassimilates in contrast to tree diameter growth. Thus, carbon sequestration reductions under low water availabilities in cork oak woodlands should be ascribed to stomatal regulation or photosynthetic limitations as pointed out in Chap. 3 and to a lesser extent to leaf area reductions.

5 Perspectives

In the course of this thesis the new digital cover photography method (DCP) was tested angularly dependent against the established LAI-2000 method. It was shown that DCP, like it was used here, performed excellently handling the major challenges of open canopies, heterogeneous distribution of leaves and woody tissue influence. This encourages to use DCP in other ecosystems with different canopy structure in future research to benefit from the labor-effective application.However, this requires further tests of the reliability of DCP in different ecosystems.
The DCP method comes with the great advantage of using off-the-shelf digital cameras, highly cost efficient compared to special scientific equipment like the LAI-2000. However, the developed algorithm for image separation of this thesis is based on the commercial eCognition image analysis platform (Trimble Germany GmbH). A desirable step for further development would be to port the algorithm to an open source image analysis platform like ImageJ (Schneider et al., 2012) to foster a broader usability.

It is expected that the trend of decreasing total annual precipitation and alteration of precipitation patterns on the Iberian Peninsula, namely occurrences of additional winter/spring droughts, will continue with proceeding climate change (Bussotti et al., 2013; Guerreiro et al., 2013; Hulme et al., 1999). Severe drought periods as shown here might occur at higher frequency (Field et al., 2012; Heimann and Reichstein, 2008; Granier et al., 2007; Miranda et al., 2002) thereby affecting the ecosystem water balance and productivity (Chaves et al., 2002; Fischer et al., 2002). If precipitation patterns similar to 2012 will occur more often, a sustainable depletion of local ground water reservoirs as well as water storage basins might be expected. This will affect strongly local agriculture that relies on ground water for the deep-rooted cork-oak trees and otherwise uses irrigation water from storage basins. The soil seed bank of native understorey plants may also deplete on the long term due to a shorter life cycle and reduced seed formation (Jongen et al., 2013c; Peñuelas et al., 2002, 2004; Gordo and Sanz, 2005). A shift of species composition is likely de Dios Miranda et al. (2009) but could not be observed in this ecosystem during the drought year 2012 itself. However, some effects such as tree mortality may only be evident in the long term after multiple, consecutive drought years (David et al., 2004; Bussotti et al., 2013).
The photosynthesis-stomatal conductance model descriptions tested here could only be applied successfully when the trees were allowed to adapt the photosynthesis apparatus (maximum carboxylation rate) and stomatal conductivity simultaneously as a reaction to drought, confirming previous studies. That clearly points to the

necessity of similar investigations in other ecosystem types and the reevaluation of descriptions used in global climate or land surface models.
Further, the unexpected decrease of optimum temperature of electron transport in the *Q. suber* leaves does not correspond with literature. Previous studies only investigated a possible temperature acclimation of the photosynthesis apparatus with a complete growth cycle under elevated temperatures of annual plants and observed an increase of optimum temperature. Here, only leaf renewal of the evergreen *Q. suber* trees occurred under elevated temperatures. Further investigations are needed to disentangle if the observed decrease of optimum temperature is a possible mathematical artifact of the parameter optimization or if evergreen leaves behave differently from annual leaves.

Acknowledgment

First of all, I would like to thank my supervisor Matthias Cuntz who taught me nearly everything necessary for being a good scientist. Without his patience with me, his constant encouragement and criticism this thesis would never have been possible. He is the best supervisor I ever met in my scientific life.
I would like to thank Christiane Werner for her constant support through all the years making this project happening.
A great thanks goes out to Maren Dubbert, the best PhD companion I can imagine. Her constantly high motivation to keep things going is surpassing.
I would like to thank Corinna Rebmann for her infinite support and education. From beginning to the end I could always rely on her.
Great thanks goes out to the entire UFZ team. First of all to Juliane Mai for her ability to easily teach me difficult things and always having time, but above all for her friendship. To Sabine Attinger for supervising my thesis and supporting me. To Sebastian Gimper for his inventiveness. And of course to all colleagues and friends of the CHS department. And last but not least to Maren Göhler for her friendship.
I would like to thank Olaf Kolle and Martin Hertel for their field support and technical advice and Stephan Unger for giving this project and my thesis a kick-start.
Great thanks goes out to the team of ISA, namely João Santos Pereira, Filipe Costa e Silva, Alexandra Correia, Marjan Jongen and Alexandre Vaz Correia for the successful cooperation and their hospitality. I thank the Ferreira family at Herdade da Machoqueira for the establishment of our field site and the great support.

Personally, I would like to thank my mother for everything and my father making me what I am today. I thank Susi for not letting go.

This study was funded by the Deutsche Forschungsgemeinschaft (WATERFLUX Project: # WE 2681/6-1; # CU 173/2-1) and kindly supported by Helmholtz Impulse and Networking Fund through Helmholtz Interdisciplinary Graduate School for Environmental Research (HIGRADE)

Selbständigkeitserklärung

Ich erkläre, dass ich die vorliegende Arbeit selbständig und unter Verwendung der angegebenen Hilfsmittel, persönlichen Mitteilungen und Quellen angefertigt habe.

Leipzig, den 30. April 2015

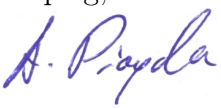

Arndt Gerald Piayda

Bibliography

Aubinet, M., Grelle, A., Ibrom, A., Rannik, Ü., Moncrieff, J., Foken, T., Kowalski, A., Martin, P., Berbigier, P., Bernhofer, C., Clement, R., Elbers, J., Granier, A., Grünwald, T., Morgenstern, K., Pilegaard, K., Rebmann, C., Snijders, W., Valentini, R., Vesala, T., 1999. Estimates of the annual net carbon and water exchange of forests: The euroflux methodology. In: Fitter, A., Raffaelli, D. (Eds.), Advances in Ecological Research. Vol. 30 of Advances in Ecological Research. Academic Press, pp. 113 – 175.
URL http://www.sciencedirect.com/science/article/pii/S0065250408600185

Baldocchi, D., 1997. Measuring and modelling carbon dioxide and water vapour exchange over a temperate broad-leaved forest during the 1995 summer drought. Plant, Cell & Environment 20 (9), 1108–1122.
URL http://dx.doi.org/10.1046/j.1365-3040.1997.d01-147.x

Baldocchi, D. D., Ma, S., Rambal, S., Misson, L., Ourcival, J.-M., Limousin, J.-M., Pereira, J., Papale, D., dec 2009. On the differential advantages of evergreenness and deciduousness in mediterranean oak woodlands: a flux perspective. Ecological Applications 20 (6), 1583–1597.
URL http://dx.doi.org/10.1890/08-2047.1

Ball, J., Woodrow, L. E., Beny, J. A., 1987. A model predicting stomatal conductance and its contribution to the control of photosynthesis under different environmental conditions. In: Biggins, J. (Ed.), Progress in Photosynthesis research. Vol. 4. Nijhoff, Dordrecht, pp. 221–224.

Beadle, C., Talbot, H., Jarvis, P., 1982. Canopy structure and leaf area index in a mature scots pine forest. Forestry 55 (2), 105–123.
URL http://forestry.oxfordjournals.org/content/55/2/105.abstract

Beer, A., 1852. Bestimmung der absorption des rothen lichts in farbigen flüssigkeiten. Annal. Phys. Chem. 86, 78–88.

Beer, C., Reichstein, M., Tomelleri, E., Ciais, P., Jung, M., Carvalhais, N., Rödenbeck, C., Arain, M. A., Baldocchi, D., Bonan, G. B., Bondeau, A., Cescatti, A., Lasslop, G., Lindroth, A., Lomas, M., Luyssaert, S., Margolis, H., Oleson, K. W., Roupsard, O., Veenendaal, E., Viovy, N., Williams, C., Woodward, F. I., Papale, D., 2010. Terrestrial gross carbon dioxide uptake: Global distribution and covariation with

climate. Science 329 (5993), 834–838.
URL http://www.sciencemag.org/content/329/5993/834.abstract

Beerling, D., Quick, W., 1995. A new technique for estimating rates of carboxylation and electron transport in leaves of c3 plants for use in dynamic global vegetation models. Global Change Biology 1 (4), 289–294.
URL http://dx.doi.org/10.1111/j.1365-2486.1995.tb00027.x

Berry, J., Björkman, O., 1980. Photosynthetic response and adaptation to temperature in higher plants. Annual Review of Plant Physiology 31 (1), 491–543.
URL http://www.annualreviews.org/doi/abs/10.1146/annurev.pp.31.060180.002423

Besson, C. K., do Vale, R. L., Rodrigues, M. L., Almeida, P., Herd, A., Grant, O. M., David, T. S., Schmidt, M., Otieno, D., Keenan, T. F., Gouveia, C., Mériaux, C., Chaves, M. M., Pereira, J. S., 2014. Cork oak physiological responses to manipulated water availability in a mediterranean woodland. Agricultural and Forest Meteorology 184, 230–242.
URL http://www.sciencedirect.com/science/article/pii/S0168192313002724

Beyschlag, W., Lange, O., Tenhunen, J. D., 1986. Photosynthesis and water relations of the mediterranean evergreen sclerophyll *Arbutus unedo* l. throughout the year at a site in portugal. i. diurnal courses of carbon dioxide gas exchange and transpiration under natural conditions. Flora 178, 409–444.

Bonan, G. B., 2002. Ecological Climatology: Concepts and Applications. Cambridge University Press, Cambridge.

Bouguer, P., 1729. Essai d'optique sur la gradation de la lumière. Gauthier-Villars et Cie, Paris.

Bugalho, M. N., Caldeira, M. C., Pereira, J. S., Aronson, J., Pausas, J. G., 2011. Mediterranean cork oak savannas require human use to sustain biodiversity and ecosystem services. Frontiers in Ecology and the Environment.
URL http://www.esajournals.org/doi/abs/10.1890/100084

Bunce, J. A., 1989. Growth rate, photosynthesis and respiration in relation to leaf area index. Annals of Botany 63 (4), 459–463.
URL http://aob.oxfordjournals.org/content/63/4/459.abstract

Bussotti, F., Ferrini, F., Pollastrini, M., Fini, A., 2013. The challenge of mediterranean sclerophyllous vegetation under climate change: From acclimation to adaptation. Environmental and Experimental Botany 103 (0).
URL http://www.sciencedirect.com/science/article/pii/S0098847213001421

Chaves, M. M., Pereira, J. S., Maroco, J., Rodrigues, M. L., Ricardo, C. P. P., Osório, M. L., Catvalho, I., Faria, T., Pinheiro, C., 2002. How plants cope with water stress in the field? photosynthesis and growth. Annals of Botany 89 (7), 907–916. URL http://aob.oxfordjournals.org/content/89/7/907.abstract

Chen, J., Black, T., 1992. Foliage area and architecture of plant canopies from sunfleck size distributions. Agricultural and Forest Meteorology 60 (3-4), 249 – 266.
URL http://www.sciencedirect.com/science/article/pii/016819239290040B

Chen, J., Blanken, P., Black, T., Guilbeault, M., Chen, S., 1997a. Radiation regime and canopy architecture in a boreal aspen forest. Agricultural and Forest Meteorology 86 (1-2), 107 – 125.
URL http://www.sciencedirect.com/science/article/pii/S0168192396024021

Chen, J., Cihlar, J., may 1995. Quantifying the effect of canopy architecture on optical measurements of leaf area index using two gap size analysis methods. Geoscience and Remote Sensing, IEEE Transactions on 33 (3), 777 –787.

Chen, J. M., Rich, P. M., Gower, S. T., Norman, J. M., Plummer, S., 1997b. Leaf area index of boreal forests: Theory, techniques, and measurements. Journal of Geophysical Research: Atmospheres 102 (D24), 29429–29443.
URL http://dx.doi.org/10.1029/97JD01107

Ciais, P., Reichstein, M., Viovy, N., Granier, A., Ogee, J., Allard, V., Aubinet, M., Buchmann, N., Bernhofer, C., Carrara, A., Chevallier, F., De Noblet, N., Friend, A. D., Friedlingstein, P., Grunwald, T., Heinesch, B., Keronen, P., Knohl, A., Krinner, G., Loustau, D., Manca, G., Matteucci, G., Miglietta, F., Ourcival, J. M., Papale, D., Pilegaard, K., Rambal, S., Seufert, G., Soussana, J. F., Sanz, M. J., Schulze, E. D., Vesala, T., Valentini, R., Sep. 2005. Europe-wide reduction in primary productivity caused by the heat and drought in 2003. Nature 437 (7058), 529–533.
URL http://dx.doi.org/10.1038/nature03972

Collatz, G. J., Ribas-Carbo, M., Berry, J. A., 1992. Coupled photosynthesis-stomatal conductance model for leaves of c4 plants. Functional Plant Biol. 19 (5), 519–538.
URL http://www.publish.csiro.au/paper/PP9920519

Comeau, P., Heineman, J., Newsome, T., 2006. Evaluation of relationships between understory light and aspen basal area in the british columbia central interior. Forest Ecology and Management 226 (1-3), 80 – 87.
URL http://www.sciencedirect.com/science/article/pii/S0378112706000521

Comeau, P. G., Gendron, F., Letchford, T., 1998. A comparison of several methods for estimating light under a paper birch mixedwood stand. Canadian Journal of Forest Research 28 (12), 1843–1850.
URL http://www.nrcresearchpress.com/doi/abs/10.1139/x98-159

Coops, N. C., Smith, M. L., Jacobsen, K. L., Martin, M., Ollinger, S., 2004. Estimation of plant and leaf area index using three techniques in a mature native eucalypt canopy. Austral Ecology 29 (3), 332–341.
URL http://dx.doi.org/10.1111/j.1442-9993.2004.01370.x

Costa, A. C., Santos, J. A., Pinto, J. G., 2012. Climate change scenarios for precipitation extremes in portugal. Theoretical and Applied Climatology 108 (1-2), 217–234.
URL http://dx.doi.org/10.1007/s00704-011-0528-3

Cowan, I., 1977. Stomatal Behaviour and Environment. Academic Press.
URL http://books.google.com.au/books?id=GYhvNQAACAAJ

Craig, H., Gordon, L. I., 1965. Deuterium and oxygen 18 variations in the ocean and marine atmosphere. In: Tongiogi, E. (Ed.), Stable Isotopes in Oceanographic Studies and Paleotemperatures. Italy, pp. 9–130.

Cutini, A., Matteucci, G., Mugnozza, G. S., 1998. Estimation of leaf area index with the li-cor lai 2000 in deciduous forests. Forest Ecology and Management 105 (1-3), 55 – 65.
URL http://www.sciencedirect.com/science/article/B6T6X-3TW8YV6-5/2/91ceffbc3c2e6fcb6ea14b1626ea9c54

Damour, G., Simonneau, T., Cochard, H., Urban, L., 2010. An overview of models of stomatal conductance at the leaf level. Plant, Cell & Environment 33 (9), 1419–1438.
URL http://dx.doi.org/10.1111/j.1365-3040.2010.02181.x

David, T., Ferreira, M., Cohen, S., Pereira, J., David, J., 2004. Constraints on transpiration from an evergreen oak tree in southern portugal. Agricultural and Forest Meteorology 122 (3–4), 193 – 205.
URL http://www.sciencedirect.com/science/article/pii/S0168192303002351

David, T. S., Henriques, M. O., Kurz-Besson, C., Nunes, J., Valente, F., Vaz, M., Pereira, J. S., Siegwolf, R., Chaves, M. M., Gazarini, L. C., David, J. S., 2007. Water-use strategies in two co-occurring mediterranean evergreen oaks: surviving the summer drought. Tree Physiology 27 (6), 793–803.
URL http://treephys.oxfordjournals.org/content/27/6/793.abstract

de Dios Miranda, J., Padilla, F. M., Pugnaire, F. I., 2009. Response of a mediterranean semiarid community to changing patterns of water supply. Perspectives in

Plant Ecology, Evolution and Systematics 11 (4), 255 – 266.
URL http://www.sciencedirect.com/science/article/pii/S1433831909000201

De Pury, D. G. G., Farquhar, G. D., 1997. Simple scaling of photosynthesis from leaves to canopies without the errors of big-leaf models. Plant, Cell & Environment 20 (5), 537–557.
URL http://dx.doi.org/10.1111/j.1365-3040.1997.00094.x

Deblonde, G., Penner, M., Royer, A., 1994. Measuring leaf area index with the li-cor lai-2000 in pine stands. Ecology 75 (5), pp. 1507–1511.
URL http://www.jstor.org/stable/1937474

Demmig-Adams, B., Adams, W. W., 1992. Photoprotection and other responses of plants to high light stress. Annual review of plant biology 43 (1), 599–626.

Dubbert, M., Cuntz, M., Piayda, A., Maguás, C., Werner, C., 2013. Partitioning evapotranspiration – testing the craig and gordon model with field measurements of oxygen isotope ratios of evaporative fluxes. Journal of Hydrology 496 (0), 142 – 153.
URL http://www.sciencedirect.com/science/article/pii/S0022169413004083

Dubbert, M., Cuntz, M., Piayda, A., Werner, C., 2014a. Oxygen isotope signatures of transpired water vapor: the role of isotopic non-steady-state transpiration under natural conditions. New Phytologist 203 (4), 1242–1252.
URL http://dx.doi.org/10.1111/nph.12878

Dubbert, M., Mosena, A., Piayda, A., Cuntz, M., Correia, A. C., Pereira, J. S., Werner, C., 2014b. Influence of tree cover on herbaceous layer development and carbon and water fluxes in a portuguese cork-oak woodland. Acta Oecologica 59 (0), 35 – 45.
URL http://www.sciencedirect.com/science/article/pii/S1146609X14000654

Dubbert, M., Piayda, A., Cuntz, M., Correia, A. C., Costa e Silva, F., Pereira, J. S., Werner, C., 2014c. Stable oxygen isotope and flux partitioning demonstrates understory of an oak savanna contributes up to half of ecosystem carbon and water exchange. Frontiers in Plant Science 5 (530).
URL http://www.frontiersin.org/functional_plant_ecology/10.3389/fpls.2014.00530/abstract

Duckstein, L., 1981. Multiobjective optimization in structural design: The model choice problem. In: Atrek, E. (Ed.), New Directions in Optimum Structural Design. John Wiley.

e Silva, F. C., Correia, A. C., Piayda, A., Dubbert, M., Rebmann, C., Cuntz, M., Werner, C., David, J. S., ao Santos Pereira, J., 2015. Effects of an extremely dry winter on net ecosystem carbon exchange and tree phenology at a cork oak woodland. Agricultural and Forest Meteorology 204 (0), 48 – 57.
URL http://www.sciencedirect.com/science/article/pii/S0168192315000283

Efron, B., Tibshirani, R. J., 1993. An Introduction tp the Bootstrap. Chapman & Hall.

Egea, G., Verhoef, A., Vidale, P. L., 2011. Towards an improved and more flexible representation of water stress in coupled photosynthesis–stomatal conductance models. Agricultural and Forest Meteorology 151 (10), 1370 – 1384.
URL http://www.sciencedirect.com/science/article/pii/S0168192311001778

Ehleringer, J. R., Cook, C. S., 1984. Photosynthesis in encelia farinosa gray in response to decreasing leaf water potential. Plant Physiology 75 (3), 688–693.
URL http://www.plantphysiol.org/content/75/3/688.abstract

Espigares, T., Peco, B., 1993. Mediterranean pasture dynamics: The role of germination. Journal of Vegetation Science 4 (2), pp. 189–194.
URL http://www.jstor.org/stable/3236104

Espigares, T., Peco, B., 1995. Mediterranean annual pasture dynamics: Impact of autumn drought. Journal of Ecology 83 (1), pp. 135–142.
URL http://www.jstor.org/stable/2261157

Eugster, W., Senn, W., Jun. 1995. A cospectral correction model for measurement of turbulent no2 flux. Boundary-Layer Meteorology 74 (4), 321–340.
URL http://dx.doi.org/10.1007/BF00712375

Farquhar, G., Caemmerer, S., Berry, J., 1980. A biochemical model of photosynthetic CO2 assimilation in leaves of C3 species. Planta 149 (1), 78–90.
URL http://dx.doi.org/10.1007/BF00386231

Farquhar, G. D., Sharkey, T. D., 1982. Stomatal conductance and photosynthesis. Annual Review of Plant Physiology 33 (1), 317–345.
URL http://dx.doi.org/10.1146/annurev.pp.33.060182.001533

Fassnacht, K. S., Gower, S. T., Norman, J. M., McMurtric, R. E., 1994. A comparison of optical and direct methods for estimating foliage surface area index in forests. Agricultural and Forest Meteorology 71 (1-2), 183 – 207.
URL http://www.sciencedirect.com/science/article/pii/0168192394901074

Field, C., Barros, V., Stocker, T., Qin, D., Dokken, D., Ebi, K., Mastrandrea, M., Mach, K., Plattner, G.-K., Allen, S., Tignor, M., Midgley, P. (Eds.), 2012. Managing the Risks of Extreme Events and Disasters to Advance Climate Change Adaptation. IPCC Special Reports. Cambridge University Press, Cambridge.
URL https://www.ipcc.ch/pdf/special-reports/srex/SREX_Full_Report.pdf

Figueroa, M. E., Davy, A. J., 1991. Response of mediterranean grassland species to changing rainfall. Journal of Ecology 79 (4), pp. 925–941.
URL http://www.jstor.org/stable/2261089

Fischer, G., van Velthuizen, H., Shah, M., Nachtergaele, F. (Eds.), 2002. Global Agro-ecological Assessment for Agriculture in the 21st Century: Methodology and Results. International Institute for Applied Systems Analysis.

Foken, T., 2008. The energy balance closure problem: An overview. Ecological Applications 18 (6), 1351–1367.
URL http://dx.doi.org/10.1890/06-0922.1

Foken, T., Wichura, B., 1996. Tools for quality assessment of surface-based flux measurements. Agricultural and Forest Meteorology 78 (1-2), 83 – 105.
URL http://www.sciencedirect.com/science/article/B6V8W-3WBY0VB-6/2/4a27aed016261f7c76f78eea80368d1f

García-Barrón, L., Morales, J., Sousa, A., 2013. Characterisation of the intra-annual rainfall and its evolution (1837-2010) in the southwest of the Iberian Peninsula. Theoretical and Applied Climatology, 1–13.
URL http://dx.doi.org/10.1007/s00704-013-0855-7

Goel, N. S., Strebel, D. E., 1984. Simple beta distribution representation of leaf orientation in vegetation canopies. Agron. J. 76 (5), 800–802.
URL https://www.agronomy.org/publications/aj/abstracts/76/5/800

Gordo, O., Sanz, J. J., 2005. Phenology and climate change: a long-term study in a mediterranean locality. Oecologia 146 (3), 484–495.
URL http://dx.doi.org/10.1007/s00442-005-0240-z

Grace, J., José, J. S., Meir, P., Miranda, H. S., Montes, R. A., 2006. Productivity and carbon fluxes of tropical savannas. Journal of Biogeography 33 (3), 387–400.
URL http://dx.doi.org/10.1111/j.1365-2699.2005.01448.x

Granier, A., Reichstein, M., Bréda, N., Janssens, I., Falge, E., Ciais, P., Grünwald, T., Aubinet, M., Berbigier, P., Bernhofer, C., Buchmann, N., Facini, O., Grassi, G., Heinesch, B., Ilvesniemi, H., Keronen, P., Knohl, A., Köstner, B., Lagergren, F., Lindroth, A., Longdoz, B., Loustau, D., Mateus, J., Montagnani, L., Nys, C., Moors, E., Papale, D., Peiffer, M., Pilegaard, K., Pita, G., Pumpanen, J., Rambal, S., Rebmann, C., Rodrigues, A., Seufert, G., Tenhunen, J., Vesala, T., Wang, Q.,

2007. Evidence for soil water control on carbon and water dynamics in european forests during the extremely dry year: 2003. Agricultural and Forest Meteorology 143 (1–2), 123 – 145.
URL http://www.sciencedirect.com/science/article/pii/S0168192306003911

Grant, O. M., Tronina, Ł., Ramalho, J. C., Kurz Besson, C., Lobo-do-Vale, R., Santos Pereira, J., Jones, H. G., Chaves, M. M., 2010. The impact of drought on leaf physiology of quercus suber l. trees: comparison of an extreme drought event with chronic rainfall reduction. Journal of Experimental Botany 61 (15), 4361–4371.
URL http://jxb.oxfordjournals.org/content/61/15/4361.abstract

Guerreiro, S. B., Kilsby, C. G., Serinaldi, F., 2013. Analysis of time variation of rainfall in transnational basins in iberia: abrupt changes or trends? International Journal of Climatology.
URL http://dx.doi.org/10.1002/joc.3669

Härdle, W., Müller, M., 1997. Multivariate and semiparametric kernel regression. Discussion Papers, Interdisciplinary Research Project 373: Quantification and Simulation of Economic Processes 1997,26, Berlin, urn:nbn:de:kobv:11-10064120.
URL http://hdl.handle.net/10419/66292

Haverd, V., Lovell, J., Cuntz, M., Jupp, D., Newnham, G., Sea, W., 2012. The canopy semi-analytic pgap and radiative transfer (canspart) model: Formulation and application. Agricultural and Forest Meteorology 160 (0), 14 – 35.
URL http://www.sciencedirect.com/science/article/pii/S0168192312000494

Heimann, M., Reichstein, M., Jan. 2008. Terrestrial ecosystem carbon dynamics and climate feedbacks. Nature 451 (7176), 289–292.
URL http://dx.doi.org/10.1038/nature06591

Hollinger, D. Y., Kelliher, F. M., Byers, J. N., Hunt, J. E., McSeveny, T. M., Weir, P. L., 1994. Carbon dioxide exchange between an undisturbed old-growth temperate forest and the atmosphere. Ecology 75 (1), pp. 134–150.
URL http://www.jstor.org/stable/1939390

Hulme, M., Mitchell, J., Ingram, W., Lowe, J., Johns, T., New, M., Viner, D., 1999. Climate change scenarios for global impacts studies. Global Environmental Change 9, Supplement 1 (0), S3 – S19.
URL http://www.sciencedirect.com/science/article/pii/S0959378099000151

Hutchison, B. A., Matt, D. R., McMillen, R. T., Gross, L. J., Tajchman, S. J., Norman, J. M., 1986. The architecture of a deciduous forest canopy in eastern

tennessee, u.s.a. Journal of Ecology 74 (3), pp. 635–646.
URL http://www.jstor.org/stable/2260387

Huxman, T. E., Wilcox, B. P., Breshears, D. D., Scott, R. L., Snyder, K. A., Small, E. E., Hultine, K., Pockman, W. T., Jackson, R. B., Feb. 2005. Ecohydrological implications of woody plant encroachment. Ecology 86 (2), 308–319.
URL http://dx.doi.org/10.1890/03-0583

Ibrom, A., Dellwik, E., Larsen, S. E., Pilegaard, K., 2007. On the use of the webb-pearman-leuning theory for closed-path eddy correlation measurements. Tellus B 59 (5), 937–946.
URL http://dx.doi.org/10.1111/j.1600-0889.2007.00311.x

Jacquemoud, S., Bacour, C., Poilvé, H., Frangi, J.-P., 2000. Comparison of four radiative transfer models to simulate plant canopies reflectance: Direct and inverse mode. Remote Sensing of Environment 74 (3), 471 – 481.
URL http://www.sciencedirect.com/science/article/pii/S0034425700001395

Johnson, F. H., Eyring, H., Williams, R. W., 1942. The nature of enzyme inhibitions in bacterial luminescence: Sulfanilamide, urethane, temperature and pressure. Journal of Cellular and Comparative Physiology 20 (3), 247–268.
URL http://dx.doi.org/10.1002/jcp.1030200302

Jonckheere, I., Fleck, S., Nackaerts, K., Muys, B., Coppin, P., Weiss, M., Baret, F., 2004. Review of methods for in situ leaf area index determination: Part i. theories, sensors and hemispherical photography. Agricultural and Forest Meteorology 121 (1-2), 19 – 35.
URL http://www.sciencedirect.com/science/article/pii/S0168192303001643

Jongen, M., Lecomte, X., Unger, S., Fangueiro, D., Pereira, J. a. S., 2013a. Precipitation variability does not affect soil respiration and nitrogen dynamics in the understorey of a mediterranean oak woodland. Plant and Soil 372 (1-2), 235–251.
URL http://dx.doi.org/10.1007/s11104-013-1728-7

Jongen, M., Lecomte, X., Unger, S., Pintó-Marijuan, M., Pereira, J. S., 2013b. The impact of changes in the timing of precipitation on the herbaceous understorey of mediterranean evergreen oak woodlands. Agricultural and Forest Meteorology 171-172 (0), 163–173.
URL http://www.sciencedirect.com/science/article/pii/S0168192312003577

Jongen, M., Pereira, J. S., Aires, L. M. I., Pio, C. A., 2011. The effects of drought and timing of precipitation on the inter-annual variation in ecosystem-atmosphere exchange in a mediterranean grassland. Agricultural and Forest Meteorology

151 (5), 595 – 606.
URL http://www.sciencedirect.com/science/article/B6V8W-5265YYX-1/2/1be2f9753279ea77ee0ed7acadea46fd

Jongen, M., Unger, S., Fangueiro, D., Cerasoli, S., Silva, J., Pereira, J. S., 2013c. Resilience of montado understorey to experimental precipitation variability fails under severe natural drought. Agriculture, Ecosystems & Environment 178 (0), 18 – 30.
URL http://www.sciencedirect.com/science/article/pii/S0167880913002193

June, T., Evans, J. R., Farquhar, G. D., 2004. A simple new equation for the reversible temperature dependence of photosynthetic electron transport: a study on soybean leaf. Functional Plant Biol. 31 (3), 275–283.
URL http://www.publish.csiro.au/paper/FP03250

Kattge, J., Knorr, W., 2007. Temperature acclimation in a biochemical model of photosynthesis: a reanalysis of data from 36 species. Plant, Cell & Environment 30 (9), 1176–1190.
URL http://dx.doi.org/10.1111/j.1365-3040.2007.01690.x

Kim, J., Guo, Q., Baldocchi, D., Leclerc, M., Xu, L., Schmid, H., 2006. Upscaling fluxes from tower to landscape: Overlaying flux footprints on high-resolution (ikonos) images of vegetation cover. Agricultural and Forest Meteorology 136 (3-4), 132 – 146, advances in Surface-Atmosphere Exchange - A Tribute to Marv Wesely.
URL http://www.sciencedirect.com/science/article/B6V8W-4HWX8KK-1/2/e2c31cc475357b844567c5e307f7f2d9

Knorr, W., 2000. Annual and interannual co2 exchanges of the terrestrial biosphere: process-based simulations and uncertainties. Global Ecology and Biogeography 9 (3), 225–252.
URL http://dx.doi.org/10.1046/j.1365-2699.2000.00159.x

Kobayashi, H., Ryu, Y., Baldocchi, D. D., Welles, J. M., Norman, J. M., 2013. On the correct estimation of gap fraction: How to remove scattered radiation in gap fraction measurements? Agricultural and Forest Meteorology 174-175 (0), 170 – 183.
URL http://www.sciencedirect.com/science/article/pii/S0168192313000415

Kolle, O., Rebmann, C., 2007. Eddysoft documentation of a software package to acquire and process eddy covariance data. Technical Reports 10, Max-Planck-Institut für Biogeochemie, Jena.
URL http://www.bgc-jena.mpg.de/bgc-processes/staff/corinna.rebmann/tech_report10.pdf

Krinner, G., Viovy, N., de Noblet-Ducoudré, N., Ogée, J., Polcher, J., Friedlingstein, P., Ciais, P., Sitch, S., Prentice, I. C., 2005. A dynamic global vegetation model for studies of the coupled atmosphere-biosphere system. Global Biogeochemical Cycles 19 (1), n/a–n/a.
URL http://dx.doi.org/10.1029/2003GB002199

Krishnan, P., Meyers, T. P., Scott, R. L., Kennedy, L., Heuer, M., 2012. Energy exchange and evapotranspiration over two temperate semi-arid grasslands in north america. Agricultural and Forest Meteorology 153 (0), 31–44.
URL http://www.sciencedirect.com/science/article/pii/S0168192311002930

Kucharik, C. J., Norman, J. M., Gower, S. T., 1998. Measurements of branch area and adjusting leaf area index indirect measurements. Agricultural and Forest Meteorology 91 (1-2), 69 – 88.
URL http://www.sciencedirect.com/science/article/pii/S0168192398000641

Kucharik, C. J., Norman, J. M., Murdock, L. M., Gower, S. T., 1997. Characterizing canopy nonrandomness with a multiband vegetation imager (mvi). Journal of Geophysical Research: Atmospheres 102 (D24), 29455–29473.
URL http://dx.doi.org/10.1029/97JD01175

Kurz-Besson, C., Otieno, D., Lobo do Vale, R., Siegwolf, R., Schmidt, M., Herd, A., Nogueira, C., David, T., David, J., Tenhunen, J., Pereira, J., Chaves, M., 2006. Hydraulic lift in cork oak trees in a savannah-type mediterranean ecosystem and its contribution to the local water balance. Plant and Soil 282 (1-2), 361–378.
URL http://dx.doi.org/10.1007/s11104-006-0005-4

Lang, A., Jan. 1986. Leaf-area and average leaf angle from transmission of direct sunlight. Aust. J. Bot. 34 (3), 349–355.
URL http://www.publish.csiro.au/paper/BT9860349

Lasslop, G., Reichstein, M., Papale, D., Richardson, A. D., Arneth, A., Barr, A., Stoy, P., Wohlfahrt, G., 2010. Separation of net ecosystem exchange into assimilation and respiration using a light response curve approach: critical issues and global evaluation. Global Change Biology 16 (1), 187–208.
URL http://dx.doi.org/10.1111/j.1365-2486.2009.02041.x

Leblanc, S. G., Dec 2002. Correction to the plant canopy gap-size analysis theory used by the tracing radiation and architecture of canopies instrument. Appl. Opt. 41 (36), 7667–7670.
URL http://ao.osa.org/abstract.cfm?URI=ao-41-36-7667

Leblanc, S. G., Chen, J. M., Fernandes, R., Deering, D. W., Conley, A., 2005. Methodology comparison for canopy structure parameters extraction from digital

hemispherical photography in boreal forests. Agricultural and Forest Meteorology 129 (3-4), 187 – 207.
URL http://www.sciencedirect.com/science/article/pii/S0168192305000298

Leuning, R., 1995. A critical appraisal of a combined stomatal-photosynthesis model for C3 plants. Plant, Cell & Environment 18 (4), 339–355.
URL http://dx.doi.org/10.1111/j.1365-3040.1995.tb00370.x

Leuning, R., 2007. The correct form of the webb, pearman and leuning equation for eddy fluxes of trace gases in steady and non-steady state, horizontally homogeneous flows. Boundary-Layer Meteorology 123, 263–267.
URL http://dx.doi.org/10.1007/s10546-006-9138-5

LI-COR, 1992. LAI-2000 Plant Canopy Analyzer. Lincoln, NE, USA.

Long, S., Humphries, S., Falkowski, P. G., 1994. Photoinhibition of photosynthesis in nature. Annual review of plant biology 45 (1), 633–662.

Ma, S., Baldocchi, D. D., Xu, L., Hehn, T., 2007. Inter-annual variability in carbon dioxide exchange of an oak/grass savanna and open grassland in california. Agricultural and Forest Meteorology 147 (3–4), 157 – 171.
URL http://www.sciencedirect.com/science/article/pii/S016819230700189X

Macfarlane, C., Arndt, S. K., Livesley, S. J., Edgar, A. C., White, D. A., Adams, M. A., Eamus, D., 2007a. Estimation of leaf area index in eucalypt forest with vertical foliage, using cover and fullframe fisheye photography. Forest Ecology and Management 242 (2-3), 756 – 763.
URL http://www.sciencedirect.com/science/article/B6T6X-4NBRYFY-1/2/e00714e3b089cdc896e0528c7ca3a6e3

Macfarlane, C., Grigg, A., Evangelista, C., 2007b. Estimating forest leaf area using cover and fullframe fisheye photography: Thinking inside the circle. Agricultural and Forest Meteorology 146 (1-2), 1–12.
URL http://www.sciencedirect.com/science?_ob=ArticleURL&_udi=B6V8W-4NXGS61-1&_user=100086&_coverDate=09%2F11%2F2007&_rdoc=1&_fmt=high&_orig=search&_origin=search&_sort=d&_docanchor=&view=c&_searchStrId=1468699538&_rerunOrigin=google&_acct=C000007538&_version=1&_urlVersion=0&_userid=100086&md5=0a1705605f6f14962a091b2f1795e212&searchtype=a

Macfarlane, C., Hoffman, M., Eamus, D., Kerp, N., Higginson, S., McMurtrie, R., Adams, M., 2007c. Estimation of leaf area index in eucalypt forest using digital photography. Agricultural and Forest Meteorology 143 (3-4), 176 – 188.
URL http://www.sciencedirect.com/science/article/B6V8W-4MG1NPV-3/2/8e98a94d96398e78eec59cec248cd41f

Matthews, M. A., Boyer, J. S., 1984. Acclimation of photosynthesis to low leaf water potentials. Plant Physiology 74 (1), 161–166.
URL http://www.plantphysiol.org/content/74/1/161.abstract

Mauder, M., Cuntz, M., Drüe, C., Graf, A., Rebmann, C., Schmid, H. P., Schmidt, M., Steinbrecher, R., 2013. A strategy for quality and uncertainty assessment of long-term eddy-covariance measurements. Agricultural and Forest Meteorology 169 (0), 122 – 135.
URL http://www.sciencedirect.com/science/article/pii/S0168192312002808

Mauder, M., Foken, T., May 2011. Documentation and Instruction Manual of the Eddy-Covariance Software Package TK3. Universität Bayreuth Abt. Mikrometeorologie.
URL http://nbn-resolving.de/urn/resolver.pl?urn:nbn:de:bvb:703-opus-8665

Medlyn, B. E., Dreyer, E., Ellsworth, D., Forstreuter, M., Harley, P. C., Kirschbaum, M. U. F., Le Roux, X., Montpied, P., Strassemeyer, J., Walcroft, A., Wang, K., Loustau, D., 2002. Temperature response of parameters of a biochemically based model of photosynthesis. ii. a review of experimental data. Plant, Cell & Environment 25 (9), 1167–1179.
URL http://dx.doi.org/10.1046/j.1365-3040.2002.00891.x

Meir, P., Grace, J., Miranda, A. C., 2000. Photographic method to measure the vertical distribution of leaf area density in forests. Agricultural and Forest Meteorology 102 (2-3), 105 – 111.
URL http://www.sciencedirect.com/science/article/pii/S0168192300001222

Miller, J., Jan. 1967. A formula for average foliage density. Aust. J. Bot. 15 (1), 141–144.
URL http://www.publish.csiro.au/paper/BT9670141

Miller, J. B., 3 1986. The foliage density equation revisited. The ANZIAM Journal 27, 387–401.
URL http://dx.doi.org/10.1017/S0334270000005038

Miranda, P., Coelho, F., Tomé, A.R. and, V. M., Carvalho, A., Pires, C., Pires, H., Pires, V. C., Ramalho, C., 2002. Climate Change in Portugal: Scenarios, Impacts and Adaptation Measures (SIAM Project). Gradiva, Ch. 20th century Portuguese Climate and Climate Scenarios, pp. 23–83.

Monsi, M., Saeki, T., 1953. über den lichtfaktor in den pflanzengesellschaften und seine bedeutung fur die stoffproduktion. Japanese Journal of Botany 14 (1), 22–52.

Monsi, M., Saeki, T., 2005. On the factor light in plant communities and its importance for matter production. Annals of Botany 95 (3), 549–567.
URL http://aob.oxfordjournals.org/content/95/3/549.short

Monteith, J., 1965. Evaporation and environment. Symposia of the Society for Experimental Biology 19.

Monteith, J. L., 1959. The reflection of short-wave radiation by vegetation. Quarterly Journal of the Royal Meteorological Society 85 (366), 386–392.
URL http://dx.doi.org/10.1002/qj.49708536607

Mourato, S., Moreira, M., Corte-Real, J., 2010. Interannual variability of precipitation distribution patterns in southern portugal. International Journal of Climatology 30 (12), 1784–1794.
URL http://dx.doi.org/10.1002/joc.2021

Nelder, J. A., Mead, R., 1965. A simplex method for function minimization. The Computer Journal 7 (4), 308–313.
URL http://comjnl.oxfordjournals.org/content/7/4/308.abstract

Nilson, T., 1971. A theoretical analysis of the frequency of gaps in plant stands. Agricultural Meteorology 8 (0), 25 – 38.
URL http://www.sciencedirect.com/science/article/pii/0002157171900926

Norman, J. M., Welles, J. M., 1983. Radiative transfer in an array of canopies. Agron. J. 75 (3), 481–488.
URL https://dl.sciencesocieties.org/publications/aj/abstracts/75/3/481

Oleson, K. W., Lawrence, D. M., Bonan, G. B., Flanner, M. G., Kluzek, E., Lawrence, P. J., Levis, S., Swenson, S. C., Thornton, P. E., 2010. Technical description of version 4.0 of the community land model (CLM)leu. Tech. rep., NATIONAL CENTER FOR ATMOSPHERIC RESEARCH.

Oliveira, G., Correia, O., Martins-Loução, M., Catarino, F., 1992. Water relations of cork-oak (quercus suber l.) under natural conditions. In: Romane, F., Terradas, J. (Eds.), Quercus ilex L. ecosystems: function, dynamics and management. Vol. 13 of Advances in vegetation science. Springer Netherlands, pp. 199–208.
URL http://dx.doi.org/10.1007/978-94-017-2836-2_21

Paco, T. A., David, T. S., Henriques, M. O., Pereira, J. S., Valente, F., Banza, J., Pereira, F. L., Pinto, C., David, J. S., 2009. Evapotranspiration from a mediterranean evergreen oak savannah: The role of trees and pasture. Journal of Hydrology 369, 98 – 106.
URL http://www.sciencedirect.com/science/article/pii/S0022169409001036

Papale, D., Reichstein, M., Aubinet, M., Canfora, E., Bernhofer, C., Kutsch, W., Longdoz, B., Rambal, S., Valentini, R., Vesala, T., Yakir, D., 2006. Towards a standardized processing of net ecosystem exchange measured with eddy covariance technique: algorithms and uncertainty estimation. Biogeosciences 3 (4), 571–583.
URL http://www.biogeosciences.net/3/571/2006/

Paredes, D., Trigo, R. M., Garcia-Herrera, R., Trigo, I. F., Feb. 2006. Understanding precipitation changes in iberia in early spring: Weather typing and storm-tracking approaches. J. Hydrometeor 7 (1), 101–113.
URL http://dx.doi.org/10.1175/JHM472.1

Parker, G. G., O'Neill, J. P., Higman, D., 1989. Vertical profile and canopy organization in a mixed deciduous forest. Vegetatio 85 (1-2), 1–11.
URL http://dx.doi.org/10.1007/BF00042250

Peñuelas, J., Filella, I., Comas, P., 2002. Changed plant and animal life cycles from 1952 to 2000 in the mediterranean region. Global Change Biology 8 (6), 531–544.
URL http://dx.doi.org/10.1046/j.1365-2486.2002.00489.x

Peñuelas, J., Filella, I., Zhang, X., Llorens, L., Ogaya, R., Lloret, F., Comas, P., Estiarte, M., Terradas, J., 2004. Complex spatiotemporal phenological shifts as a response to rainfall changes. New Phytologist 161 (3), 837–846.
URL http://dx.doi.org/10.1111/j.1469-8137.2004.01003.x

Peco, B., Espigares, T., 1994. Floristic fluctuations in annual pastures: the role of competition at the regeneration stage. Journal of Vegetation Science 5 (4), 457–462.
URL http://dx.doi.org/10.2307/3235971

Pereira, J. S., Mateus, J. A., Aires, L. M., Pita, G., Pio, C., David, J. S., Andrade, V., Banza, J., David, T. S., Paço, T. A., Rodrigues, A., Sep. 2007. Net ecosystem carbon exchange in three contrasting mediterranean ecosystems - the effect of drought. Biogeosciences 4 (5), 791–802.
URL http://hal.archives-ouvertes.fr/hal-00297720

Pérez-Ramos, I. M., Rodríguez-Calcerrada, J., Ourcival, J. M., Rambal, S., 2013. Quercus ilex recruitment in a drier world: A multi-stage demographic approach. Perspectives in Plant Ecology, Evolution and Systematics 15 (2), 106 – 117.
URL http://www.sciencedirect.com/science/article/pii/S1433831912000741

Piñol, J., Lledó, M. J., Escarré, A., 1991. Hydrological balance of two mediterranean forested catchments (prades, northeast spain). Hydrological Sciences Journal 36 (2), 95–107.
URL http://www.tandfonline.com/doi/abs/10.1080/02626669109492492

Piayda, A., Dubbert, M., Rebmann, C., Kolle, O., Costa e Silva, F., Correia, A., Pereira, J. S., Werner, C., Cuntz, M., 2014. Drought impact on carbon and water

cycling in a mediterranean quercus suber l. woodland during the extreme drought event in 2012. Biogeosciences Discussions 11 (7), 10365–10417.
URL http://www.biogeosciences-discuss.net/11/10365/2014/

Piayda, A., Dubbert, M., Werner, C., Vaz Correia, A., Pereira, J. S., Cuntz, M., 2015. Influence of woody tissue and leaf clumping on vertically resolved leaf area index and angular gap probability estimates. Forest Ecology and Management 340, 103 – 113.
URL http://www.sciencedirect.com/science/article/pii/S0378112714007336

Pisek, J., Lang, M., Nilson, T., Korhonen, L., Karu, H., 2011. Comparison of methods for measuring gap size distribution and canopy nonrandomness at järvselja rami (radiation transfer model intercomparison) test sites. Agricultural and Forest Meteorology 151 (3), 365 – 377.
URL http://www.sciencedirect.com/science/article/B6V8W-51R5139-2/2/95afb6e9e3831e080a6dab2015fa4f93

Rebmann, C., Kolle, O., Heinesch, B., Queck, R., Ibrom, A., Aubinet, M., 2012. Eddy Covariance: A Practical Guide to Measurement and Data Analysis. Springer, Dordrecht, Ch. Data Acquisition and Flux Calculations, pp. 59 – 84.

Reichstein, M., Falge, E., Baldocchi, D., Papale, D., Aubinet, M., Berbigier, P., Bernhofer, C., Buchmann, N., Gilmanov, T., Granier, A., Grünwald, T., Havránková, K., Ilvesniemi, H., Janous, D., Knohl, A., Laurila, T., Lohila, A., Loustau, D., Matteucci, G., Meyers, T., Miglietta, F., Ourcival, J.-M., Pumpanen, J., Rambal, S., Rotenberg, E., Sanz, M., Tenhunen, J., Seufert, G., Vaccari, F., Vesala, T., Yakir, D., Valentini, R., 2005. On the separation of net ecosystem exchange into assimilation and ecosystem respiration: review and improved algorithm. Global Change Biology 11 (9), 1424–1439.
URL http://dx.doi.org/10.1111/j.1365-2486.2005.001002.x

Reichstein, M., Tenhunen, J., Roupsard, O., Ourcival, J.-M., Rambal, S., Miglietta, F., Peressotti, A., Pecchiari, M., Tirone, G., Valentini, R., 2003. Inverse modeling of seasonal drought effects on canopy CO2/H2O exchange in three mediterranean ecosystems. Journal of Geophysical Research: Atmospheres 108 (D23).
URL http://dx.doi.org/10.1029/2003JD003430

Reichstein, M., Tenhunen, J. D., Roupsard, O., Ourcival, J.-m., Rambal, S., Miglietta, F., Peressotti, A., Pecchiari, M., Tirone, G., Valentini, R., 2002. Severe drought effects on ecosystem CO2 and H2O fluxes at three mediterranean evergreen sites: revision of current hypotheses? Global Change Biology 8 (10), 999–1017.
URL http://dx.doi.org/10.1046/j.1365-2486.2002.00530.x

Rodrigues, A., Pita, G., Mateus, J., Kurz-Besson, C., Casquilho, M., Cerasoli, S., Gomes, A., Pereira, J., 2011. Eight years of continuous carbon fluxes measurements

in a portuguese eucalypt stand under two main events: Drought and felling. Agricultural and Forest Meteorology.
URL http://www.sciencedirect.com/science/article/B6V8W-51YXM2N-1/2/b328c63ccb65b7b573cd27bf2ae80e05

Rutter, A., Kershaw, K., Robins, P., Morton, A., 1971. A predictive model of rainfall interception in forests, 1. derivation of the model from observations in a plantation of corsican pine. Agricultural Meteorology 9 (0), 367 – 384.
URL http://www.sciencedirect.com/science/article/pii/0002157171900343

Ryu, Y., Nilson, T., Kobayashi, H., Sonnentag, O., Law, B. E., Baldocchi, D. D., 2010a. On the correct estimation of effective leaf area index: Does it reveal information on clumping effects? Agricultural and Forest Meteorology 150 (3), 463 – 472.
URL http://www.sciencedirect.com/science/article/B6V8W-4Y9V85W-1/2/51f9509e5087cb453c548a6d47a49ed7

Ryu, Y., Sonnentag, O., Nilson, T., Vargas, R., Kobayashi, H., Wenk, R., Baldocchi, D. D., 2010b. How to quantify tree leaf area index in an open savanna ecosystem: A multi-instrument and multi-model approach. Agricultural and Forest Meteorology 150 (1), 63 – 76.
URL http://www.sciencedirect.com/science/article/B6V8W-4X6V9TS-1/2/30f59f0046ad185d78abea44c15d4ae9

Ryu, Y., Verfaillie, J., Macfarlane, C., Kobayashi, H., Sonnentag, O., Vargas, R., Ma, S., Baldocchi, D. D., 2012. Continuous observation of tree leaf area index at ecosystem scale using upward-pointing digital cameras. Remote Sensing of Environment 126 (0), 116 – 125.
URL http://www.sciencedirect.com/science/article/pii/S003442571200346X

Sala, A., Tenhunen, J., 1996. Simulations of canopy net photosynthesis and transpiration in quercus ilex l. under the influence of seasonal drought. Agricultural and Forest Meteorology 78 (3–4), 203 – 222.
URL http://www.sciencedirect.com/science/article/pii/0168192395022503

Santos, J., Corte-real, J., Leite, S., 2007. Atmospheric large-scale dynamics during the 2004/2005 winter drought in portugal. International Journal of Climatology 27 (5), 571 586.
URL http://dx.doi.org/10.1002/joc.1425

Santos, J. A., Woollings, T., Pinto, J. G., Jun. 2013. Are the winters 2010 and 2012 archetypes exhibiting extreme opposite behavior of the north atlantic jet stream?

Mon. Wea. Rev. 141 (10), 3626–3640.
URL http://dx.doi.org/10.1175/MWR-D-13-00024.1

Schindelin, J., Arganda-Carreras, I., Frise, E., Kaynig, V., Longair, M., Pietzsch, T., Preibisch, S., Rueden, C., Saalfeld, S., Schmid, B., Tinevez, J.-Y., White, D. J., Hartenstein, V., Eliceiri, K., Tomancak, P., Cardona, A., Jul. 2012. Fiji: an open-source platform for biological-image analysis. Nat Meth 9 (7), 676–682.
URL http://dx.doi.org/10.1038/nmeth.2019

Schneider, C. A., Rasband, W. S., Eliceiri, K. W., Jul. 2012. Nih image to imagej: 25 years of image analysis. Nat Meth 9 (7), 671–675.
URL http://dx.doi.org/10.1038/nmeth.2089

Schotanus, P., Nieuwstadt, F., Bruin, H., May 1983. Temperature measurement with a sonic anemometer and its application to heat and moisture fluxes. Boundary-Layer Meteorology 26 (1), 81–93.
URL http://dx.doi.org/10.1007/BF00164332

Sellers, P. J., Dorman, J. L., May 1987. Testing the simple biosphere model (sib) using point micrometeorological and biophysical data. J. Climate Appl. Meteor. 26 (5), 622–651.
URL http://dx.doi.org/10.1175/1520-0450(1987)026<0622:TTSBMU>2.0.CO;2

Sinclair, T. R., Murphy, C. E., Knoerr, K. R., 1976. Development and evaluation of simplified models for simulating canopy photosynthesis and transpiration. Journal of Applied Ecology 13 (3), pp. 813–829.
URL http://www.jstor.org/stable/2402257

Stenberg, P., Linder, S., Smolander, H., Flower-Ellis, J., 1994. Performance of the lai-2000 plant canopy analyzer in estimating leaf area index of some scots pine stands. Tree Physiology 14 (7-8-9), 981–995.
URL http://treephys.oxfordjournals.org/content/14/7-8-9/981.abstract

Strachan, I. B., McCaughey, J. H., 1996. Spatial and vertical leaf area index of a deciduous forest resolved using the lai-2000 plant canopy analyzer. Forest Science 42 (2), 176–181.
URL http://www.ingentaconnect.com/content/saf/fs/1996/00000042/00000002/art00008

Tenhunen, J., Lange, O., Gebel, J., Beyschlag, W., Weber, J., 1984. Changes in photosynthetic capacity, carboxylation efficiency, and co2 compensation point associated with midday stomatal closure and midday depression of net co2 exchange of leaves of quercus suber. Planta 162 (3), 193–203.
URL http://dx.doi.org/10.1007/BF00397440

Tenhunen, J., Lange, O., Harley, P., Beyschlag, W., Meyer, A., 1985. Limitations due to water stress on leaf net photosynthesis of quercus coccifera in the portuguese evergreen scrub. Oecologia 67 (1), 23–30.
URL http://dx.doi.org/10.1007/BF00378446

Tenhunen, J., Serra, A., Harley, P., Dougherty, R., Reynolds, J., 1990. Factors influencing carbon fixation and water use by mediterranean sclerophyll shrubs during summer drought. Oecologia 82 (3), 381–393.
URL http://dx.doi.org/10.1007/BF00317487

Tenhunen, J. D., Pearcy, R. W., Lange, O. L., 1987. Stomatal function. Stanford University press, Ch. Diurnal variations in leaf conductance and gas exchange in natural environments.

Thomas, C., Foken, T., 2002. Re-evaluation of integral turbulence characteristics and their parameterisations. 15th Conference on Boundary Layer and Turbulence.

Trigo, R. M., Añel, J., Barriopedro, D., García-Herrera, R., Gimeno, L., Nieto, R., Castillo, R., Allen, M. R., Massey, N., 2013. The record winter drought of 2011-12 in the iberian peninsula. In: Explaining Extreme Events of 2012 from a Climate Perspective. Vol. 95. Bull. Amer. Meteor. Soc., pp. S41 – S45.

Trimble (Ed.), 2012. eCognition Developer 8.7.1 Reference Book. Trimble Germany GmbH.

Twine, T., Kustas, W., Norman, J., Cook, D., Houser, P., Meyers, T., Prueger, J., Starks, P., Wesely, M., 2000. Correcting eddy-covariance flux underestimates over a grassland. Agricultural and Forest Meteorology 103 (3), 279 – 300.
URL http://www.sciencedirect.com/science/article/pii/S0168192300001234

Unger, S., Máguas, C., Pereira, J. S., Aires, L. M., David, T. S., Werner, C., 2009. Partitioning carbon fluxes in a mediterranean oak forest to disentangle changes in ecosystem sink strength during drought. Agricultural and Forest Meteorology 149 (6-7), 949 – 961.
URL http://www.sciencedirect.com/science/article/B6V8W-4VB5565-1/2/eda3bd8b216bec46e4d856e815c8d479

Valentini, R., Matteucci, G., Dolman, A. J., Schulze, E.-D., Rebmann, C., Moors, E. J., Granier, A., Gross, P., Jensen, N. O., Pilegaard, K., Lindroth, A., Grelle, A., Bernhofer, C., Grünwald, T., Aubinet, M., Ceulemans, R., Kowalski, A. S., Vesala, T., Rannik, U., Berbigier, P., Loustau, D., Gudmundsson, J., Thorgeirsson, H., Ibrom, A., Morgenstern, K., Clement, R., Moncrieff, J., Montagnani, L., Minerbi, S., Jarvis, P. G., Apr. 2000. Respiration as the main determinant of carbon balance in european forests. Nature 404 (6780), 861–865.
URL http://dx.doi.org/10.1038/35009084

Vargas, R., Sonnentag, O., Abramowitz, G., Carrara, A., Chen, J., Ciais, P., Correia, A., Keenan, T., Kobayashi, H., Ourcival, J.-M., Papale, D., Pearson, D., Pereira, J., Piao, S., Rambal, S., Baldocchi, D., 2013. Drought influences the accuracy of simulated ecosystem fluxes: A model-data meta-analysis for mediterranean oak woodlands. Ecosystems, 1–16.
URL http://dx.doi.org/10.1007/s10021-013-9648-1

Vaz, M., Pereira, J., Gazarini, L., David, T., David, J., Rodrigues, A., Maroco, J., Chaves, M., 2010. Drought-induced photosynthetic inhibition and autumn recovery in two mediterranean oak species (quercus ilex and quercus suber). Tree Physiology 30 (8), 946–956.
URL http://treephys.oxfordjournals.org/content/30/8/946.abstract

Verbeeck, H., Peylin, P., Bacour, C., Bonal, D., Steppe, K., Ciais, P., 2011. Seasonal patterns of co2 fluxes in amazon forests: Fusion of eddy covariance data and the orchidee model. Journal of Geophysical Research: Biogeosciences 116 (G2).
URL http://dx.doi.org/10.1029/2010JG001544

von Caemmerer, S., 2000. Biochemical Models of Leaf Photosynthesis. CSIRO Publishing.

Wang, W.-M., Li, Z.-L., Su, H.-B., 2007. Comparison of leaf angle distribution functions: Effects on extinction coefficient and fraction of sunlit foliage. Agricultural and Forest Meteorology 143 (1-2), 106 – 122.
URL http://www.sciencedirect.com/science/article/pii/S016819230600390X

Wang, Y.-P., Leuning, R., 1998. A two-leaf model for canopy conductance, photosynthesis and partitioning of available energy i:: Model description and comparison with a multi-layered model. Agricultural and Forest Meteorology 91 (1–2), 89 – 111.
URL http://www.sciencedirect.com/science/article/pii/S0168192398000616

Wang, Y. S., Miller, D. R., Welles, J. M., Heisler, G. M., 1992. Spatial variability of canopy foliage in an oak forest estimated with fisheye sensors. Forest Science 38 (4), 854–865.
URL http://www.ingentaconnect.com/content/saf/fs/1992/00000038/00000004/art00010

Warren Wilson, J., 1959. Analysis of the spatial distribution of foliage by two-dimensional point quadrats. New Phytologist 58 (1), 92–99.
URL http://dx.doi.org/10.1111/j.1469-8137.1959.tb05340.x

Warren Wilson, J., 1960. Inclined point quadrats. New Phytologist 59 (1), 1–7.
URL http://dx.doi.org/10.1111/j.1469-8137.1960.tb06195.x

Warren Wilson, J., 1965. Stand structure and light penetration. i. analysis by point quadrats. Journal of Applied Ecology 2 (2), pp. 383–390.
URL http://www.jstor.org/stable/2401487

Warren Wilson, J., 1967. Stand structure and light penetration. iii. sunlit foliage area. Journal of Applied Ecology 4 (1), pp. 159–165.
URL http://www.jstor.org/stable/2401415

Watson, D. J., 1947. Comparative physiological studies on the growth of field crops: I. variation in net assimilation rate and leaf area between species and varieties, and within and between years. Annals of Botany 11 (1), 41–76.
URL http://aob.oxfordjournals.org/content/11/1/41.short

Webb, E. K., Pearman, G. I., Leuning, R., 1980. Correction of flux measurements for density effects due to heat and water vapour transfer. Quarterly Journal of the Royal Meteorological Society 106 (447), 85–100.
URL http://dx.doi.org/10.1002/qj.49710644707

Werner, C., Correia, O., 1996. Photoinhibition in cork-oak leaves under stress: influence of the bark-stripping on the chlorophyll fluorescence emission in *Quercus suber* l. Trees 10 (5), 288–292.
URL http://dx.doi.org/10.1007/BF02340774

Werner, C., Correia, O., Beyschlag, W., 1999. Two different strategies of mediterranean macchia plants to avoid photoinhibitory damage by excessive radiation levels during summer drought. Acta Oecologica 20 (1), 15–23.
URL http://www.sciencedirect.com/science/article/pii/S1146609X99800113

Werner, C., Correia, O., Beyschlag, W., Jan. 2002. Characteristic patterns of chronic and dynamic photoinhibition of different functional groups in a mediterranean ecosystem. Functional Plant Biol. 29 (8), 999–1011.
URL http://www.publish.csiro.au/paper/PP01143

Werner, C., Máguas, C., 2010. Carbon isotope discrimination as a tracer of functional traits in a mediterranean macchia plant community. Funct. Plant Biol. 37 (5), 467–477.
URL http://dx.doi.org/10.1071/FP09081

Werner, C., Ryel, R. J., Correia, O., Beyschlag, W., 2001. Effects of photoinhibition on whole-plant carbon gain assessed with a photosynthesis model. Plant, Cell & Environment 24 (1), 27–40.
URL http://dx.doi.org/10.1046/j.1365-3040.2001.00651.x

Whitford, K., Colquhoun, I., Lang, A., Harper, B., 1995. Measuring leaf area index in a sparse eucalypt forest: a comparison of estimates from direct measurement, hemispherical photography, sunlight transmittance and allometric regression.

Agricultural and Forest Meteorology 74 (3-4), 237 – 249.
URL http://www.sciencedirect.com/science/article/pii/0168192394021890

Wilczak, J., Oncley, S., Stage, S., Apr. 2001. Sonic anemometer tilt correction algorithms. Boundary-Layer Meteorology 99 (1), 127–150.
URL http://dx.doi.org/10.1023/A:1018966204465

Wit, C. d., 1965. Photosynthesis of leaf canopies. Tech. rep., Wageningen.
URL http://edepot.wur.nl/187115

Zhou, S., Duursma, R. A., Medlyn, B. E., Kelly, J. W., Prentice, I. C., 2013. How should we model plant responses to drought? an analysis of stomatal and non-stomatal responses to water stress. Agricultural and Forest Meteorology (0).
URL http://www.sciencedirect.com/science/article/pii/S0168192313001263

A Leaf area index and gap probability

A.1 Nomenclature

A	[pxl]	total number of pixels in each image
$f(\alpha)$	[−]	leaf angle distribution function
ff	[−]	foliage cover
fc	[−]	crown cover
$G(\theta)$	[−]	leaf projection function
gl	[pxl]	number of pixels in gaps between crowns
gt	[pxl]	number of pixels in all gaps (gaps between crowns + gaps within crowns envelopes)
h	[m]	height above ground
h_t	[m]	height of the crown top
h_b	[m]	height of the crown bottom
$K(\theta)$	[−]	contact frequency
L	$[\mathrm{m}^2_{\mathrm{leaf}}/\mathrm{m}^2_{\mathrm{ground}}]$	leaf are index
$\sum L$	$[\mathrm{m}^2_{\mathrm{leaf}}/\mathrm{m}^2_{\mathrm{ground}}]$	cumulative leaf are index
εL	[%]	relative bias of leaf are index
L_e	$[\mathrm{m}^2_{\mathrm{leaf}}/\mathrm{m}^2_{\mathrm{ground}}]$	effective leaf are index
$\sum L_e$	$[\mathrm{m}^2_{\mathrm{leaf}}/\mathrm{m}^2_{\mathrm{ground}}]$	cumulative effective leaf are index
$P_{gap}(\theta)$	[−]	gap probability
$\varepsilon P_{gap}(\theta)$	[%]	relative bias of gap probability
r_c	[m]	crown radius
$S_e(h)$	[−]	ellipsoidal crown shape model
$S_{e\,9/10}(h)$	[−]	asymmetric ellipsoidal crown shape model
$S_t(h)$	[−]	triangular crown model
θ	[°]	view zenith angle
α	[°]	angle of the leaf's normal to the zenith
θ_v	[°]	view angle span
W	$[\mathrm{m}^2_{\mathrm{wood}}/\mathrm{m}^2_{\mathrm{ground}}]$	wood area index
$\Omega(\theta)$	[−]	clumping index

A.2 Image object classification criteria

The colour criteria used for the classification of gap objects are brightness $\overline{bri}$, blue difference $\overline{bd}$:

$$\overline{bd} = \overline{B} - (\frac{\overline{G} + \overline{R}}{2}) \tag{A.1}$$

and blue ratio $\overline{br}$:

$$\overline{br} = \frac{3\overline{B}}{\overline{B} + \overline{G} + \overline{R}} \tag{A.2}$$

They are combined in a threshold criteria as:

$$gap = \begin{cases} (\overline{br} > 0.95) \wedge (\overline{bri} > 127) & \text{or} \\ (\overline{bri} > 230) & \text{or} \\ (\overline{br} > 1.5) & \text{or} \\ (\overline{bd} > 10) \wedge (\overline{bri} > 230) \wedge (0.95 < \overline{br} < 1.8) & \end{cases} \tag{A.3}$$

Within a radius of 50 pixels around each object classified as gap, the average difference to neighbouring gap and unclassified objects of brightness ($\overline{bri_{dif\ gap}}$ and $\overline{bri_{dif\ unc}}$) and blue ratio ($\overline{br_{dif\ gap}}$ and $\overline{br_{dif\ unc}}$) are calculated for the refinement of the gap edges. All gap objects missing the following threshold are declared as unclassified:

$$unc = \begin{cases} (\overline{bri_{dif\ unc}} < 100) \wedge (\overline{bri_{dif\ gap}} < -30) \wedge (\overline{bri_{dif\ gap}} > 40) & \text{or} \\ (\overline{bri_{dif\ unc}} < 70) \wedge (\overline{br_{dif\ gap}} < -0.15) & \end{cases} \tag{A.4}$$

This threshold is iteratively applied until no further changes in classifications occurs. Image objects were classified as woody tissue with thresholds based on the shape features area/width, length/width, curvature/length, border length/area, roundness, ellipse ratio, elliptic fit, and rectangular fit (feature description can be found in Trimble (2012)) as well as rgb sum $\sum \overline{RGB}$:

$$\sum \overline{RGB} = \overline{B} + \overline{G} + \overline{R} \tag{A.5}$$

and green ratio $\overline{gr}$:

$$\overline{gr} = \frac{3\overline{G}}{\overline{B} + \overline{G} + \overline{R}} \tag{A.6}$$

The thresholds values for the woody tissue detection are dependent on object size classes, therefore numerous and not shown here.

B Drought impact on carbon and water cycling

B.1 Nomenclature

A	$[[\mathrm{mol\,m^{-2}\,s^{-1}}]]$	carbon assimilation
b	$[[\mathrm{mol\,H_2O\,m^{-2}s^{-1}}]]$	Leuning model parameter (offset)
D_0	[hPa]	Leuning model parameter (vpd sensitivity)
$\mathrm{ET_o}$	$[[\mathrm{mm\,d^{-1}}]]$	evapotranspiration measured at the overstorey tower
$\mathrm{ET_u}$	$[[\mathrm{mm\,d^{-1}}]]$	evapotranspiration measured at the understorey tower
$\mathrm{ET_o}/P$	[%]	precipitation effectiveness
$\overline{\varepsilon_{\mathrm{GPP_o}}}$	[–]	average Nash–Suttcliff model efficiency for $\mathrm{GPP_o}$
$\overline{\varepsilon_{\mathrm{ET_o}}}$	[–]	average Nash–Suttcliff model efficiency for $\mathrm{ET_o}$
f_s	[–]	fraction of sunlit leaves
GPP	$[[\mathrm{g\,C\,m^{-2}\,d^{-1}}]]$	gross primary productivity
$\mathrm{GPP_o}$	$[[\mathrm{g\,C\,m^{-2}\,d^{-1}}]]$	gross primary productivity measured at the overstorey tower
$\mathrm{GPP_u}$	$[[\mathrm{g\,C\,m^{-2}\,d^{-1}}]]$	gross primary productivity measured at the understorey tower
$g_\mathrm{s,h}$	$[[\mathrm{mol\,H_2O\,m^{-2}\,s^{-1}}]]$	stomatal conductance for water vapour
$g_\mathrm{s,c}$	$[[\mathrm{mol\,CO_2\,m^{-2}s^{-1}}]]$	stomatal conductance for carbon
LAI	$[[\mathrm{m^2_{leaf}\,m^{-2}_{ground}}]]$	leaf area index
m	$[[\mathrm{mol\,H_2O\,mol\,air^{-1}}]]$	Leuning model parameter (slope)
NEE	$[[\mathrm{g\,C\,m^{-2}\,d^{-1}}]]$	net ecosystem carbon exchange
$\mathrm{NEE_o}$	$[[\mathrm{g\,C\,m^{-2}\,d^{-1}}]]$	net ecosystem carbon exchange measured at the overstorey tower
$\mathrm{NEE_u}$	$[[\mathrm{g\,C\,m^{-2}\,d^{-1}}]]$	understorey + soil net carbon exchange
P	[mm]	precipitation
p	[hPa]	atmospheric pressure
PAR	$[[\mu\mathrm{mol\,m^{-2}\,s^{-1}}]]$	photosynthetically active radiation
P_gap	[–]	tree canopy gap probability
R_eco	$[[\mathrm{g\,C\,m^{-2}\,d^{-1}}]]$	ecosystem respiration
rH	[%]	relative air humidity
$\mathrm{rH_s}$	[%]	relative air humidity at the leaf surface
θ	[%]	soil moisture
T	$[[\mathrm{mm\,d^{-1}}]]$	transpiration
T_a	[°C]	air temperature
T_l	[°C]	leaf tempearture
$T_\mathrm{l,max}$	[°C]	maximum daily leaf tempearture
T_opt	[°C]	optimum temperature of electron transport

T_s	[°C]	soil temperature
$V_\mathrm{c,max}$	$[[\mu\mathrm{mol\,m^{-2}\,s^{-1}}]]$	apperent maximum carboxylation rate
vpd	[hPa]	air vapour pressure deficit
$\mathrm{vpd}_\mathrm{max}$	[hPa]	maximum daily air vapour pressure deficit

B.2 Photosynthesis-stomatal conductance model

The entire canopy was separated in a sunlit and shaded part with the fraction of sunlit leaves as:

$$f_\mathrm{s} = \frac{1 - \exp\left(-K\mathrm{LAI}\right)}{K\mathrm{LAI}} \tag{B.7}$$

where LAI $[[\mathrm{m^2_{leaf}\,m^{-2}_{ground}}]]$ is leaf area index and $K = G\left(\beta\right) / \cos\left(\beta\right)$ with G being the angular dependent leaf projection function and β [°] being the sun zenith angle. The shaded fraction of the canopy equals $(1 - f_\mathrm{s})$. Carbon assimilation A $[[\mathrm{mol(CO_2)\,m^{-2}\,s^{-1}}]]$ was modeled for each fraction with the Farquhar et al. (1980) model in the form of Knorr (2000) and enhanced by a smooth minimum function smin:

$$A = \mathrm{smin}\left\{J_\mathrm{C}; J_\mathrm{E}; \eta\right\} - R_d \tag{B.8}$$

with the carboxylation-limited rate J_C $[[\mathrm{mol(CO_2)\,m^{-2}\,s^{-1}}]]$, the electron transport-limited rate J_E $[[\mathrm{mol(CO_2)\,m^{-2}\,s^{-1}}]]$ and mitochondrial respiration R_d $[[\mathrm{mol(CO_2)\,m^{-2}\,s^{-1}}]]$. The smoothing parameter η was set to 0.9. The Rubisco-limited rate J_C was described by:

$$J_\mathrm{C} = V_\mathrm{c,max}\frac{C_\mathrm{i} - \Gamma_\star}{C_\mathrm{i} + K_\mathrm{C}\left(1 + \left(\frac{O_i}{K_\mathrm{O}}\right)\right)} \tag{B.9}$$

with maximum carboxylation rate $V_\mathrm{c,max}$ $[[\mathrm{mol(CO_2)\,m^{-2}\,s^{-1}}]]$, CO_2 concentration inside the stomatal cavity C_i $[[\mathrm{mol(CO_2)\,mol(air)^{-1}}]]$, CO_2 compensation point $\Gamma_\star$ $[[\mathrm{mol(CO_2)\,mol(air)^{-1}}]]$ (set to leaf temperature $T_\mathrm{l} \times 1.7 \times 10^{-6}$), Michaelis–Menten constants for CO_2 K_C $[[\mathrm{mol(CO_2)\,mol(air)^{-1}}]]$ and O_2 K_O $[[\mathrm{mol(O_2)\,mol(air)^{-1}}]]$, respectively. O_i $[[\mathrm{mol(O_2)\,mol(air)^{-1}}]]$ is the stomatal cavity O_2 concentration taken as 21 %. The RuBP-limited CO_2 assimilation rate J_E was described by:

$$J_\mathrm{E} = J\frac{C_\mathrm{i} - \Gamma_\star}{4\left(C_\mathrm{i} + 2\Gamma_\star\right)} \tag{B.10}$$

with the rate of electron transport J $[[\mathrm{mol\,m^{-2}\,s^{-1}}]]$ as:

$$J = J_\mathrm{max}\frac{\alpha\mathrm{PAR}}{\sqrt{J^2_\mathrm{max} + \alpha^2\mathrm{PAR}^2}} \tag{B.11}$$

with maximum electron transport rate J_max $[[\mathrm{mol(CO_2)\,m^{-2}\,s^{-1}}]]$, quantum yield of electron transport α and incident photosynthetically active photon flux density PAR

[[mol(quanta) m^{-2} s^{-1}]]. The sunlit fraction of leaves f_s receives direct as well as diffuse incoming radiation where the shaded fraction of leaves $(1 - f_s)$ only receives diffuse radiation. The temperature dependencies of K_C, K_O and R_d were modelled using Arrhenius functions:

$$f(T_l) = K_{25} \exp\left(\frac{E_K(T_l - 25)}{298R(T_l + 273)}\right) \tag{B.12}$$

with the base rates $K_{C_{25}}$ [[mol(CO_2) mol(air)$^{-1}$]], $K_{O_{25}}$ [[mol(O_2) mol(air)$^{-1}$]], Rd_{25} [[mol(CO_2) m^{-2} s^{-1}]] at 25 °C and activation energies E_C, E_O, E_{Rd} [[J mol^{-1}]], respectively. T_l [°C] is leaf temperature and R [[J mol^{-1} K^{-1}]] is universal gas constant. Temperature dependencies of $V_{c,max}$ and J_{max} were treated by three test cases with decreasing complexity and computational demand. Case 1 according to Medlyn et al. (2002) and Kattge and Knorr (2007): $V_{c,max}$ and J_{max} were both modelled using a modification of the Arrhenius function (Eq. B.12) showing a peak at optimum temperature followed by a decline with increasing T_l:

$$f(T_l) = K_{max25} \exp\left(\frac{E_K(T_l - 25)}{298R(T_l + 273)}\right) \frac{1 + \exp\left(\frac{298\Delta S_K - Hd_K}{298R}\right)}{1 + \exp\left(\frac{(T_l+273)\Delta S_K - Hd_K}{(T_l+273)R}\right)} \tag{B.13}$$

with base rates $V_{c,max25}$ and J_{max25} at 25 °C, respectively. ΔS_V and ΔS_J [[J mol^{-1} K^{-1}]] are the entropy factors and Hd_V and Hd_J [[J mol^{-1}]] are the deactivation energies of $V_{c,max}$ and J_{max}, respectively. Case 2 according to von Caemmerer (2000): only the temperature dependency of J_{max} was modelled with the peaked function (Eq. B.13), but $V_{c,max}$ was modelled with the simple Arrhenius function (Eq. B.12). Case 3 according to June et al. (2004): $V_{c,max}$ was modelled with the simple Arrhenius function but J_{max} was modelled with a simple gaussian temperature dependency:

$$\begin{aligned} J_{max} &= J_{opt} \exp\left(-\frac{(T_l - T_{opt})^2}{\Omega^2}\right) \\ &= J_{max25} \exp\left(\frac{(25 - T_{opt})^2 - (T_l - T_{opt})^2}{\Omega^2}\right) \end{aligned} \tag{B.14}$$

with optimum temperature T_{opt} [°C] and the empirical parameter $\Omega = 18$ °C.
Leaf surface CO_2 concentration C_s [[mol(CO_2) mol(air)$^{-1}$]] and H_2O concentration W_s [[mol(H_2O) mol(air)$^{-1}$]] were calculated via:

$$C_s = C_a - A\left(\frac{1}{g_a} + \frac{1.3}{g_b}\right) \tag{B.15}$$

$$W_s = W_a - ET_{mod}\left(\frac{1}{g_a} + \frac{1}{g_b}\right) \tag{B.16}$$

with the atmospheric CO_2 concentration C_a [[mol(CO_2) mol(air)$^{-1}$]], aerodynamic conductance g_a [[mol(air) m^{-2} s^{-1}]], leaf boundary layer conductance g_b [[mol(air) m^{-2} s^{-1}]],

atmospheric H_2O concentration W_a [[mol(H_2O) mol(air)$^{-1}$]], modelled transpiration ET_{mod} [[mol(H_2O) m^{-2} s^{-1}]] and stomatal conductance for water vapour $g_{s,h}$ [[mol(H_2O) m^{-2} s^{-1}]]. g_a was measured (see section 3.2.2) and g_b was estimated with the approach of Bonan (2002) via $g_b = 200\sqrt{d/u}$ where d is the measured leaf size and u is the observed wind speed.
Stomatal conductance for water vapour $g_{s,h}$ was calculated with the formulation of Leuning (1995):

$$g_{s,h} = m \frac{A}{(C_s - \Gamma_\star)\left(1 + \frac{W_i - W_s}{D_0}\right)} + b \tag{B.17}$$

with the slope m [[mol(H_2O) mol(air)$^{-1}$]], the sensitivity parameter of vapour pressure deficit D_0 [[mol(H_2O) mol(air)$^{-1}$]] and the offset b [[mol(H_2O) m^{-2} s^{-1}]]. The description of Ball et al. (1987) was also tested:

$$g_{s,h} = m \frac{A\, rH_s}{C_s} + b \tag{B.18}$$

with relative humidity at the leaf surface rH_s [–]. Total conductance for CO_2 $g_{c,c}$ and H_2O $g_{c,h}$ were then derived by:

$$g_{c,c} = \frac{1}{\left(\frac{1.56}{g_{s,h}} + \frac{1}{g_a} + \frac{1.3}{g_b}\right)} \tag{B.19}$$

$$g_{c,h} = \frac{1}{\left(\frac{1}{g_{s,h}} + \frac{1}{g_a} + \frac{1}{g_b}\right)} \tag{B.20}$$

CO_2 concentration in the stomatal cavity was thus calculated by:

$$C_i = C_a - \frac{A}{g_{c,c}} \tag{B.21}$$

and modelled transpiration ET_{mod} [[mol(H_2O) m^{-2} s^{-1}]] and gross primary productivity GPP_{mod} [[mol(CO_2) m^{-2} s^{-1}]] for both, the sunlit and shaded fraction of the canopy, could be derived by:

$$ET_{mod} = g_{c,h}\,(W_i - W_a) \tag{B.22}$$

$$GPP_{mod} = g_{c,c}\,(C_a - C_i) + R_d \tag{B.23}$$

The optimum temperature T_{opt} of maximum electron transport rate J_{max} was calculated in Cases 1 and 2 according to von Caemmerer (2000):

$$T_{opt} = \frac{Hd_J}{\Delta S_J - R \log\left(\frac{E_{J_{max}}}{Hd_J - E_{J_{max}}}\right)} - 273.15 \tag{B.24}$$

The entire calculation was iterated with initial values for $\mathrm{ET}_{\mathrm{mod}} = 0$, $g_{\mathrm{s,h}} = 1$ and $C_{\mathrm{i}} = 0.8\,C_{\mathrm{a}}$, until a conversion of C_{i} was achieved for every time step. The modeled was $\mathrm{ET}_{\mathrm{mod}}$ and $\mathrm{GPP}_{\mathrm{mod}}$ of the sunlit and shaded part of the canopy were averaged using f_{s} and fitted against measured ET and GPP under variation of $V_{\mathrm{c,max25}}$, ΔS_J, m and D_0. Constant relationships of $J_{\mathrm{max25}} = 1.67\,V_{\mathrm{c,max25}}$ and $\mathrm{Rd}_{25} = 0.011\,V_{\mathrm{c,max25}}$ were assumed (Medlyn et al., 2002; Kattge and Knorr, 2007). All other parameters used can be found in Table B.1.

Table B.1: Parameters used in the photosynthesis-stomatal conductance model. The offset parameter b was estimated first with an optimization on the entire data set and then set constant in following model runs.

parameter	value	unit	source
α	0.28	$[-]$	(Beerling and Quick, 1995)
b	4300×10^{-6}	$[\mathrm{mol(H_2O)\,m^{-2}\,s^{-1}}]$	site average
E_{C}	59 356	$[\mathrm{J\,mol^{-1}}]$	(Farquhar et al., 1980)
$E_{J_{\mathrm{max}}}$	35 870	$[\mathrm{J\,mol^{-1}}]$	(Medlyn et al., 2002)
E_{O}	35 948	$[\mathrm{J\,mol^{-1}}]$	(Farquhar et al., 1980)
E_{Rd}	50 967	$[\mathrm{J\,mol^{-1}}]$	(Collatz et al., 1992)
$E_{V_{\mathrm{c,max}}}$	58 520	$[\mathrm{J\,mol^{-1}}]$	(Farquhar et al., 1980)
Hd_J	220 000	$[\mathrm{J\,mol^{-1}}]$	(von Caemmerer, 2000)
Hd_V	200 000	$[\mathrm{J\,mol^{-1}}]$	(Medlyn et al., 2002)
$K_{\mathrm{C}_{25}}$	460×10^{-6}	$[\mathrm{mol(CO_2)\,mol(air)^{-1}}]$	(Farquhar et al., 1980)
$K_{\mathrm{O}_{25}}$	0.33	$[\mathrm{mol(O_2)\,mol(air)^{-1}}]$	(Farquhar et al., 1980)
O_i	0.21	$[\mathrm{mol(O_2)\,mol(air)^{-1}}]$	(Farquhar et al., 1980)
Ω	18	$[^{\circ}\mathrm{C}]$	(June et al., 2004)

C Publications

C.1 Overview

In the following, the publications out of this thesis and from the study released or submitted so far are given below chronologically. The contributions of the authors are listed accordingly:

- Dubbert, M., Cuntz, M., **Piayda, A.**, Maguás, C., Werner, C., 2013. Partitioning evapotranspiration – Testing the Craig and Gordon model with field measurements of oxygen isotope ratios of evaporative fluxes. Journal of Hydrology 496, 142 - 153.

Autors	Contributions
Dubbert, M.	development of experimental design, accomplishment of field work, modeling and laboratory analyses, preparation of the manuscript
Cuntz, M.	discussions on the results, help with model development, suggestions to improve the manuscript
Piayda, A.	suggestions to improve the manuscript, help with field work
Maguás, C.	laboratory analyses
Werner, C.	discussions on experimental design and results, suggestions to improve the manuscript

- Dubbert, M., Cuntz, M., **Piayda, A.**, Werner, C., 2014. Oxygen isotope signatures of transpired water vapor: the role of isotopic non-steady-state transpiration under natural conditions. New Phytologist 203, 1242 - 1252.

Autors	Contributions
Dubbert, M.	development of experimental design, accomplishment of field work, modeling and laboratory analyses, preparation of the manuscript
Piayda, A.	suggestions to improve the manuscript, help with field work
Cuntz, C.	discussions on results, help with model development, suggestions to improve the manuscript
Werner, C.	discussions on experimental design and results, suggestions to improve the manuscript

- Dubbert, M., Mosena, A., **Piayda, A.**, Cuntz, M., Correia, A., Pereira, J. S., Werner, C., 2014. Influence of tree cover on herbaceous layer development and carbon and water fluxes in a Portuguese cork-oak woodland. Acta Oecologica 59, 35 - 45.

Autors	Contributions
Dubbert, M.	development of experimental design, accomplishment of field work and laboratory analyses, preparation of the manuscript
Mosena, A.	accomplishment of field work and laboratory analyses, preparation of the manuscript (Material & Methods, parts of results)
Piayda, A.	help with field work, discussions on the results, comments on the manuscript
Cuntz, M.	suggestions to improve the manuscript
Correia, A.	suggestions to improve the manuscript
Pereira, J. S.	suggestions to improve the manuscript
Werner, C.	discussion on experimental design and results, suggestions to improve the manuscript

- **Piayda, A.**, Dubbert, M., Rebmann, C., Kolle, O., Costa e Silva, F., Correia, A., Pereira, J. S., Werner, C., Cuntz, M., 2014. Drought impact on carbon and water cycling in a Mediterranean *Quercus suber* L. woodland during the extreme drought event in 2012. Biogeosciences 11, 7159 - 7178.

Autors	Contributions
Piayda, A.	development of experimental design, field work and modeling, preparation of the manuscript
Dubbert, M.	help with field work, discussions on results, help with manuscript preparation
Rebmann, C.	discussions on results, help with field site establishment
Kolle, O.	help with field site establishment
Costa e Silva, F.	help with field work, suggestions to improve the manuscript
Correia, A.	help with field work, suggestions to improve the manuscript
Pereira, J. S.	suggestions to improve the manuscript
Werner, C.	discussion on results, suggestions to improve the manuscript
Cuntz, M.	model development, discussion on results, comments on the manuscript

- Dubbert, M., **Piayda, A.**, Cuntz, M., Correia, A. C., Costa e Silva, F., Pereira, J. S., Werner, C., 2014. Stable oxygen isotope and flux partitioning demonstrates understory of an oak savanna contributes up to half of ecosystem carbon and water exchange. Frontiers in Plant Science 5.

Autors	Contributions
Dubbert, M.	development of experimental design, field work, modeling and laboratory analyses, preparation of the manuscript
Piayda, A.	help with field work, suggestions to improve the manuscript
Correia, A.	suggestions to improve the manuscript
Costa e Silva, F.	suggestions to improve the manuscript
Pereira, J. S.	suggestions to improve the manuscript
Cuntz, M.	suggestions to improve the manuscript, help with model development
Werner, C.	discussion on experimental design and results, suggestions to improve the manuscript

- **Piayda, A.**, Dubbert, M., Werner, C., Vaz Correia, A., Pereira, J. S., Cuntz, M., 2015. Influence of woody tissue and leaf clumping on vertically resolved leaf area index and angular gap probability estimates. Forest Ecology and Management 340, 103 - 113.

Autors	Contributions
Piayda, A.	development of experimental design, accomplishment of field work, preparation of the manuscript
Dubbert, M.	accomplishment of field work, discussions on results, suggestions to improve the manuscript
Werner, C.	discussions on results, suggestions to improve the manuscript
Vaz Correia, A.	help with field work
Pereira, J. S.	suggestions to improve the manuscript
Cuntz, M.	discussions on experimental design and the results, suggestions to improve the manuscript

- Costa e Silva, F., Correia, A. C., **Piayda, A.**, Dubbert, M., Rebmann, C., Cuntz, M., Werner, C., David, J. S., Pereira, J. S., 2015. Effects of an extremely dry winter on net ecosystem carbon exchange and tree phenology at a cork oak woodland. Agricultural and Forest Meteorology 204, 48-57.

Autors	Contributions
Costa e Silva, F.	accomplishment of experimental design and field work, preparation of the manuscript
Correia, A.	field work, discussions on the results, suggestions to improve the manuscript
Piayda, A.	treatment of Eddy-covariance data, discussion on results, suggestions to improve the manuscript
Dubbert, M.	accomplishment environmental and water potential measurements, discussion on results, help with manuscript preparation
Rebmann, C.	discussions on results, help with field site establishment
Cuntz, C.	suggestions to improve the manuscript
Werner, C.	discussions on results, suggestions to improve the manuscript
David, J. S.	suggestions to improve the manuscript
Pereira, J. S.	discussions on experimental design and the results, suggestions to improve the manuscript